# RATIONAL DESIGN AND SYNTHESIS OF DRUG DELIVERY PLATFORMS FOR TREATING DISEASES ASSOCIATED WITH INTESTINAL INFLAMMATION

A Dissertation
Presented to
The Academic Faculty

by

David “Scott” Wilson

In Partial Fulfillment
of the Requirements for the Degree
Doctor of Philosophy in Bioengineering in the
Department of Chemical and Biomolecular Engineering

Georgia Institute of Technology
December 2011

# RATIONAL DESIGN AND SYNTHESIS OF DRUG DELIVERY PLATFORMS FOR TREATING DISEASES ASSOCIATED WITH INTESTINAL INFLAMMATION

Approved by:


Dr. Niren Murthy, Advisor
Department of Biomedical Engineering
*Georgia Institute of Technology*

Dr. Didier Merlin
Department of Internal Medicine
*Emory University*

Dr. Julie Champion
School of Chemical and
Biomolecular Engineering
*Georgia Institute of Technology*

Dr. Mark R. Prausnitz
School of Chemical and
Biomolecular Engineering
*Georgia Institute of Technology*

Dr. Andrés García
School of Mechanical Engineering
*Georgia Institute of Technology*

Dr. Lakeisha Taite
Department of Biomedical Engineering
*Georgia Institute of Technology*


Date Approved: December, 2011

## Acknowledgments

First, I would like to thank Dr. Murthy for his direction and mentorship during my time at Georgia Tech. Dr. Murthy's passion for research was contagious and helped motivate me throughout my time as a graduate student. Dr. Murthy helped me develop as a scientist by providing me with direction and at the same time gave me the freedom to explore my own scientific curiosities. I am very fortunate and grateful that I had the opportunity to work in his lab and learn from his example. I will be forever grateful for the opportunity Dr. Murthy has given me.

I thank Dr. Didier Merlin for his contribution to this work and my development. The work presented here would not have been possible without his contribution. Dr. Merlin's excitement for and commitment to the project was equal to our own, and made working with him and in his lab a pleasure. Dr. Merlin allowed me to work in his lab as if it was my own, and this allowed me to expand my horizons, learn new techniques, and was a critical part of my development as a graduate student. I cannot thank Dr. Merlin enough for all of his help.

It is with a heavy heart that I would like to recognize and thank Dr. Shanthi Sitaraman for her contribution to these projects. This past year, Dr. Sitaraman lost her long and courageous battle with cancer. Throughout her battle, she continued to work and provide unwavering support to her students and postdocs. Her diagnosis predates our collaboration, and I am honored and humbled that she took the time to contribute to this work. Her life and her work have and will continue to be a source of inspiration.

While at Georgia Tech I had the opportunity to participate in the GAANN program, which is directed by Dr. Mark Prausnitz. In addition to serving on my committee, I would like to thank Dr. Prausnitz for all of his work as the director of the GAANN fellowship program. I enjoyed both the class, and the opportunity to meet with you and the seminar speakers during the round table discussions.

In addition to serving on my committee, I thank Dr. Andrés García, for allowing me to participate in the Georgia Tech Training Program in Cellular and Tissue Engineering, and for serving as an informal advisor to me during my time here at Georgia Tech. Dr. García puts an amazing amount of time and effort into directing the program, and I would like to thank him for doing so. It gave me the opportunity to expand my knowledge of tissue engineering research, commune with fellow students, realize I was not meant to work in industry (7:00 am are you kidding?), and an extra hour to trade banter with Dr. García, which I will never pass up (25-10☺). Most importantly, Dr. García's advice and words of encouragement have been an integral part of my personal and professional development. When I was a kid, I wanted to be a fireman, but now, when I grow up I want to be Dr. García.

In would also like to thank Dr. Lakeisha Taite and Dr. Julie Champion for taking the time to serve on my committee, and your excellent comments during my update. I have enjoyed speaking with you both at conferences and before seminars.

Members of the Murthy Lab, both past and present, have been a constant source of support, commiseration, laughter, and fun. I would like to thank "Big Daddy" Stephen Yang and Michael Heffernan, two of the best lab members anyone could have, for always being willing to answer my endless list of stupid questions, showing me the

ropes, and paving the way for the grad students that have followed in the Murthy lab. Both Stephen and Michael are very intelligent, patient, kind, all around great people, and people I try and emulate in and out of the lab. I owe a special debt of gratitude to Dr. Siraj Khaja, without whom I never would have made it through graduate school. Siraj taught me most everything I know about doing and loving organic chemistry. I cannot count the number of times Siraj would take time out of his day, and often night, to help me with a problem, give me a pep-talk, and teach me about life, surviving graduate school, and the rules of test match cricket. Speaking of working at night, I also need to thank Dr. Dongwon Lee for his support, late night lab philosophy sessions, and introducing me to the culinary delights of Korean Cooking. In addition to being an extremely nice person, Dr. Sungmun Lee deserves special thanks for teaching me, and everyone else in our lab, how to do cell culture and experiments not performed in round bottom flasks. Without Sungmun, our lab would still be wondering why our cells were so small, moved, and made the media look funky. Dr. Madhuri Dasari has also been a source of chemistry knowledge and perhaps the nicest person I have ever met. I thank Jay Sy for his support and teaching me the value of networking and career development. During my time at Tech, I had the opportunity to mentor one of the brightest people I have ever met, Sydney Shaffer. Her joie de vivre and wide-eyed fascination with science made every day I worked with her a joy. I am honored I could be an infinitesimal part of her stardom. I thank Dongin Kim for his friendship and always being up for hitting the buffet circuit around town. I think most of the restaurants in town would like to thank us for going on diets. I thank Dr. Xinghai Ning for his friendship and help in the lab. His mentorship and unparalleled skill has made me a better chemist and opened my eyes to

new possibilities. Thanks to Xinghai, I will never let a piece of glassware go unwashed. I would like to thank Dr. Khallilah Reddie for bringing some culture into the lab. I have enjoyed our conversations about all things book, NPR, and cross-cultural. I promise I will finish *The Elegance of the Hedgehog* as soon as I defend. I thank Warren Gray for trying to get me out of the lab and his ability to brighten a room with his effervescence. I would also like to thank John Perng, Jason Lee, Abhinav Acharya, and Kousik Kundu for their help and support.

All of the members of Dr. Didier Merlin and Dr. Shanthi Sitaraman's labs played a pivotal role in this work. I need to thank my French brother from another mother, Dr. Guillaume Dalmasso. I cannot underscore how important Guillaume's mentorship and friendship were, and continue to be, to my success as a graduate student. Neither one of the projects presented here could have been completed if it were not for his help and his belief in these projects. Guillaume's talent is otherworldly, and the joy he puts into his work made going to Emory the best part of my week. I am forever in his debt for his contribution to this work. I thank Hang Nguyen for all of the PBS I stole from her and her help in the second part of this thesis. Although Guillaume and Hang are very much missed, I would like to thank Yutao Yan for picking up where they left off and his hard work and dedication. I thank Dr. Lixin Wang for her contribution to the project Hammed Laroui and Palavi Garg for their help and friendship.

In addition to those who directly contributed to this work, there are dozens of others in the Georgia Tech community that I need to thank. I would like thank Steve Woodard for training me on all of the core facility equipment. Even though he is probably the busiest person in our department, he always had time to help whenever I

needed it. I would like to thank Colly Mitchell for organizing the Petit Scholars Program, and Janice Russell for all of her help with the funding for the Training Grant. Ms. Russell did an amazing job making sure I was paid on time and had access to my funding.

I want to extend a special thanks to Dr. Todd McDevitt, who served as the director of the Petit Scholars Program and as an informal advisor to me during my time at Georgia Tech. Dr. McDevitt's friendship and guidance have been an invaluable source of support, direction, and confidence. The way he conducts his research and his service to the Georgia Tech Community are a testament to his person and something to which I aspire. If I cannot be Dr. García when I grow up, I hope I can be Dr. McDevitt. I need to thank Meg McDevitt, for her friendship, looking out for me, and her advice, as well.

My scientific journey started many years ago as an undergraduate. I must thank the man who is responsible for lighting the fire of research in me that still burns today. I thank Dr. Lloyd L. Lee for recognizing talents in me that theretofore had gone unnoticed. Dr. Lee is the most erudite and well studied scientist I have ever met, and I owe him more than I would ever be able to repay.

I would also like to thank a group of poets, prophets, muses, and ne'er-do-wells for their friendship and support, which is either too salacious to recount or not covered by the statue of limitations: My best friend Stephen Lee, the "Doda Tonde" Sudhir Kasturi, Rachel Wood, Kevin Gallagher, Dave Dumbauld, Katie Rommel, Jacob Lucrezi, Peng Meng Kou, Todd Rogers, Janette Wise, Hajira Ahmad, Ed Park, and Richard Lawson.

Last, I would like to dedicate this work to my family, whose love and unconditional support made this possible.

# Table of Contents

# List of Figures

# List of Abbreviations

| | |
|---|---|
| 4% CCNP: | CAPE nanoparticles loaded with 4 weight % CPT-11 |
| 12% CCNP: | CAPE nanoparticles loaded with 12 weight % CPT-11 |
| AOM: | azoxymethane |
| Bcl-xL: | B-cell lymphoma-extra large |
| CAC: | colitis associated cancer |
| CAPE: | caffeic acid phenethyl ester |
| CCNP: | caffeic acid phenethyl ester nanoparticles loaded with Irinotecan |
| CNP: | caffeic acid phenethyl ester nanoparticles |
| CNP-780: | caffeic acid phenethyl ester nanoparticles loaded with IR-780 |
| CPT-11: | Irinotecan |
| CRC: | colorectal cancer |
| DCM: | dichloromethane |
| DMF: | dimethylformamide |
| DOTAP: | 1,2-dioleoyl-3-trimethylammonium-propane |
| DSL: | dynamic light scattering |
| DSS | dextran sodium sulfate |
| FACS: | Fluorescence-activated cell sorting |
| GPC: | gel permutation chromatography |
| h: | hour(s) |
| HMPA: | hexamethylphosphoramide |
| IKK: | IκB kinase |
| min: | minute |
| ml: | milliliter |
| MPO: | myeloperoxidase |
| MRA: | Michael reaction acceptor |
| mRNA: | messenger ribonucleic acid |
| NF-κB: | nuclear factor-κB |
| PBS: | phosphate buffered saline |
| PCAPE: | poly-CAPE |

| | |
|---|---|
| qPCR: | quantitative (real-time) polymerase chain reaction |
| RNAi: | RNA interference |
| ROS: | reactive oxygen species |
| rt: | room temperature |
| siRNA: | small-interfering ribonucleic acid |
| TNFα: | tumor necrosis factor-α |
| THF: | tetrahydrofuran |
| UC: | ulcerative colits |
| US: | United States |
| wt: | weight |

## Summary

It is estimated that over 500,000 million people worldwide suffer from disease associated with intestinal inflammation, including gastric cancer, inflammatory bowel disease, *h. pylori* infections, and numerous vial and bacterial infections. Although potentially effective therapeutics exist for many of these pathologies, delivery challenges thwart their clinical viability. For example, due to their specificity and efficacy, RNA interference (RNAi)-based therapeutics have been heralded as next generation therapeutics that are anticipated to revolutionize the treatment of inflammatory and infectious diseases. However, their rapid systemic clearance of RNAs and their potential off target toxicities have kept these therapies from transitioning from the laboratory to the bathroom shelf. In addition to potentiating new therapies for diseases associated with intestinal inflammation, novel delivery strategies could also improve the efficacy, while reducing the toxicity, of drugs currently in use. Chemotherapeutics currently used to treat colitis-associated cancer are extremely toxic and actually induce drug resistance by activating prosurvival pathways in tumors. For this reason, delivery strategies that localize chemotherapeutics to CAC tumors and block drug resistance would dramatically enhance the treatment of CAC.

The objective of this work was to develop drug delivery platforms that could target immunomodulator therapeutics to diseased intestinal tissues and thus improve the treatment of diseases associated with intestinal inflammation. To meet this objective we developed an oral delivery vehicle for siRNA and an NF-κB inhibiting nanoparticle that reduces drug-resistance. A summary of the development of these two delivery platforms is presented below.

Small interfering RNA (siRNA) represents a promising treatment strategy for numerous gastrointestinal (GI) diseases associated with chronic intestinal inflammation; however, the oral delivery of siRNA to inflamed intestinal tissues remains a major challenge. In this chapter, we present a delivery vehicle for siRNA, termed thioketal nanoparticles (TKNs), that can orally deliver siRNA to sites of intestinal inflammation, and thus inhibit gene expression in diseased intestinal tissue. TKNs are formulated from a new polymer, poly-(1,4-phenyleneacetone dimethylene thioketal) (PPADT), that degrades selectively in response to reactive oxygen species (ROS). Therefore, when delivered orally, TKNs target the release of encapsulated agents to the elevated levels of ROS specific to sites of intestinal inflammation[1-3]. Using a murine model of ulcerative colitis (UC), we demonstrate that orally administered TKNs loaded with TNFα-siRNA (TNFα-TKNs) diminish TNFα messenger RNA (mRNA) levels in the colon and protect mice from intestinal inflammation. Given the prevalence of intestinal inflammation in GI diseases[2], and the therapeutic potential of siRNA[4], we anticipate numerous applications of the TKNs for treating GI diseases.

Activation of nuclear factor-κB (NF-κB) results in the expression of numerous prosurvival genes that block apoptosis, thus mitigating the efficacy of chemotherapeutics. Paradoxically, all conventional therapeutics for cancer activate NF-κB, and in doing so initiate drug resistance. Although adjuvant strategies that block NF-κB activation could potentiate the activity of chemotherapeutics in drug resistant tumors, clinical evidence suggests that current adjuvant strategies also increase apoptosis in non-malignant cells. In this chapter, we present a nanoparticle, formulated from a polymeric NF-κB-inhibiting prodrug, that can target the chemotherapeutic irinotecan

(CPT-11) to solid tumors, and thus abrogate CPT-11-mediated drug resistance and inhibit tumor growth. In order to maximize the amount of NF-κB inhibitor delivered to tumors, we synthesized a novel polymeric prodrug, termed PCAPE, that releases the NF-κB inhibitor caffeic acid phenethyl ester (CAPE) as its major degradation product. Using a murine model of colitis-associated cancer, we demonstrated that when administered systemically, CPT-11-loaded PCAPE-nanoparticles (CCNPs) are three time more effective than a cocktail of the free drugs at reducing both tumor multiplicity and tumor size. Given the central role played by NF-κB activation in drug resistance and inflammatory diseases, we anticipate numerous applications for CNPs.

# Chapter 1: Introduction

Controlled inflammation is an essential part of numerous salubrious physiological processes such as wound healing[5], cancer surveillance[6], and defense from invading pathogens. However, aberrant inflammation, caused by the deregulated expression and activation of proinflammatory mediators, is a central factor in the onset and persistence of numerous gastrointestinal (GI) diseases, including inflammatory bowel disease[7,8] (IBD), gastric cancers[6,9], *h. pylori* infection[10], and viral infections[11]. Thus, delivery platforms that could target immune suppressive agents to diseased intestinal tissues would improve the treatment of numerous diseases associated with intestinal inflammation. For example, unabated expression of the proinflammatory cytokine tumor necroses factor-α (TNFα) is an initiating and exacerbating phenomenon in the pathophysiology of IBD[5]. In this clinical setting, nanoparticles formulated from a biomaterial that degrades selectively in the presence of reactive oxygen species (ROS), which are produced excessively in inflamed intestinal tissues, could ferry anti-TNFα small interfering-RNAs through the GI tract then release them in response to the elevated ROS levels specific to inflamed intestinal tissues[12-15].

Localized delivery of immunosuppressive agents could also improve the treatment of colitis associated cancer (CAC)[16-18]. Despite the initial response to treatment, most CAC tumors treated with chemotherapeutics develop drug resistance and experience tumor regrowth and metastasis[19-21]. Recent studies indicate that chemotherapeutics activate the proinflammatory transcription factor-κB (NF-κB), which up regulates the expression of numerous prosurvival genes, thereby mitigating their efficacy[22-26]. For this reason, a delivery vehicle that could target both an NF-κB inhibitor and chemotherapeutic to tumors could abrogate drug resistance, thus potentiating the tumor to chemotherapy induced apoptosis.

Our *long-term goal* is to develop drug delivery platforms that target therapeutics to diseased intestinal tissues. The objective of this proposal was to develop biomaterials that have the chemical and physical properties needed to either target orally delivered siRNA to inflamed intestinal tissues or inhibit chemotherapy-induced drug resistance in CAC tumors. *The central hypotheses of this proposal were that: 1. Nanoparticles formulated from a thioketal-containing polymer that degrades selectively in the presence of ROS would have the stability to protect siRNA from the harsh environment of the GI system, but the sensitivity needed to target siRNA to inflamed intestinal tissues; and 2. Nanoparticles formulated from a polymeric NF-κB inhibitor can co-localize the delivery of an NF-κB inhibitor and chemotherapeutic to CAC tumors, and thus improve the therapy of CAC by blocking NF-κB-mediated drug resistance.*

The overall objective was accomplished by testing our central hypothesis in the following specific aims:

***Specific Aim I: Design and synthesis of ROS-sensitive polymers for the oral delivery of siRNA to treat intestinal inflammation.*** We hypothesized that polymers formulated from ROS-sensitive thioketal linkages would resist hydrolysis and enzymatic cleavage, but degrade selectively in the presence of the elevated ROS levels specific to inflamed tissues. In this study, siRNA against TNFα, a known protagonist of IBD, was encapsulated in nanoparticles formulated from polythioketals (TKNs) and delivered orally via daily gavage to mice with an experimental form of IBD. After 7 days, mice were sacrificed and colon samples analyzed for mucosal TNF-α mRNA, extracellular TNF-α levels, and disease progression. A head-to-head comparison with relevant controls and siRNA-loaded PLGA nanoparticles was performed to assess the unique ability of TKNs to protect siRNA in the GI tract and manipulate gene expression *in vivo*.

**Specific Aim II: Treating CAC via NF-κB inhibiting nanoparticles that co-loclize the delivery of a chemotherapeutic and NF-KB inhibitor to tumors, and thereby prevent chemotherapy-induced drug resistance.**

We hypothesize that the NF-κB inhibitor caffeic acid phenethyl ester (CAPE) can potentiate the anti-tumor effect of the chemotherapeutic Irinotecan (CPT-11) by inhibiting the activation of NF-κB. The ability of the NF-κB inhibitor CAPE to improve the efficacy of CPT-11 on HT-29 cancer cells was investigated and a mechanism for improved efficacy suggested. Polymers that incorporate the NF-κB inhibitor CAPE into their backbone were synthesized and characterized. CPT-11-loaded nanoparticles formulated from CAPE containing polymers were generated and characterized. The efficacy of the CPT-11-loaded CAPE nanoparticles versus appropriate controls was assessed in a preclinical study of CAC.

# Chapter 2: Project Significance

Inflammatory bowel disease (IBD), including ulcerative colitis (UC) and Crohn's Disease, is an idiopathic autoimmune disorder that affects millions of people worldwide and is characterized by chronic uncontrolled inflammation of the intestinal mucosa[27,28]. Although IBD causes less than 1000 mortalities per year in the United States (US), it is a tremendous burden on the medical infrastructure and the economy. In the US alone, IBD accounts for nearly 1.1 million ambulatory care visits per year and costs 1.6 billion dollars a year to treat[29]. Furthermore, since IBD affects people in the prime of their life, IBD results in 3.6 billion dollars of lost productivity per year[30]. For this reason, strategies to treat IBD would decrease health care expenditures and increase medical access for patients suffering from more critical diseases.

Currently, IBD is an incurable condition, for which treatment options are limited[30]. First-round therapeutics include corticosteroids, however, approximately 30% of IBD cases are steroid resistant[31]. Additionally, corticosteroids have many potentially life threatening side effects, including obesity, psychosis, and heart failure[32,33]. In the last decade, biological therapeutics, such as monoclonal antibodies for the proinflammatory cytokine TNFα and TNFα receptor antagonists, have significantly improved the treatment of IBD[34]. While these biologics are more effective than corticosteroids, they too have potentially deadly side effects[35]. The use of TNFα targeting therapies has been associated with an increased risk of cancer, tuberculosis, and heart failure[36]. Furthermore, these therapeutics must be delivered via injection.

Here, we describe a new class of ROS-sensitive biomaterials, termed polythioketals, that have the properties needed to orally deliver siRNA and target inflamed mucosal tissue. Polythioketals have the stability needed to survive the extreme pHs of the gastrointestinal (GI) tract and resist cellular proteolysis, but degrade in the

presence of ROS[37]. These unique properties endow orally delivered siRNA-loaded polythioketal nanoparticles (TKNs) with the ability to transport anti-TNFα siRNA (TNFα-siRNA) through the acidic environment of the stomach, release it in inflamed mucosal tissues, and inhibit TNF-α gene expression in the GI tract. Due to their stability, oral availability, and ability to target inflammation, TKNs have several advantages over existing delivery vehicles for siRNA[38]. TKNs loaded with TNF-siRNA can be formulated via a single emulsion solvent evaporation procedure that produces particles that can be lyophilized and stored as a dry powder, unlike liposomal delivery vehicles. Furthermore, since polythioketals are delivered orally, we expect improved patient compliance over injectable and suppository based siRNA delivery vehicles[39]. Finally, by localizing TNFα-siRNA to sites of intestinal inflammation, TKNs reduce the potential toxicity caused by the system suppression of TNFα[40].

Although the total number of cancer related mortalities has declined over the past ten years, the worldwide mortality rate of colorectal cancer has increased steadily over that same period of time[41,42]. Today, more than 1 million new cases of colorectal cancer (CRC) are diagnosed each year worldwide [41]. CRC is the third most common cancer and the fourth most common cause of cancer related mortality in the world[43]. Although advances in early detection and chemotherapy have decreased the number of CRC mortalities in the United States (US), CRC remains the third most common cause of cancer related death in the US [43]. Current first-round therapies for CRC include surgery and radiotherapy; however, 32% of patients receiving these interventions experience a relapse within 12 months[42]. These resurrected tumors are usually addressed with toxic chemotherapeutics that can have devastating side effects, and paradoxically activate the critical factors within the tumor that are responsible for drug resistance[44]. The rising rate of CRC mortalities, the toxicity of current second-round therapeutics, and the prevalence of reoccurrence, underscore the need for new therapeutic strategies to treat CRC.

Accumulating clinical and genetic evidence indicates that CRC's proclivity for avoiding the effects of chemotherapeutics is a result of NF-κB activation [45]. NF-κB is a transcriptional activator that has been extensively studied for its role as a central regulator of the inflammatory response[46]. Recently, it has become clear that NF-κB plays a pivotal role in drug resistance by elevating the expression of numerous genes that promote survival, proliferation, and metastasis [47]. Consequently, NF-κB activation is an excellent predictor of tumor prognosis as well as resistance to chemotherapy and radiotherapy [25].

Despite the overwhelming evidence indicating that blocking NF-κB inhibits drug resistance and thus improves the efficacy of chemotherapeutics, there has yet to be a successful clinical trial on this approach[23,48]. A major obstacle block the development of such therapeutic strategies is the increased toxicity of NF-κB inhibition in non-malignant cells that are normally targeted by chemotherapeutics[49]. Here, we present the development of a novel drug delivery platform that can target CAC tumors, inhibit drug-resistance by blocking NF-κB activation, while simultaneously delivering a chemotherapeutic. The ability of this technology to target an NF-κB inhibitor and chemotherapeutic to solid tumors should decrease the toxicity of the combined therapies.

# Chapter 3: Review of relevant literature

## 3.1. Specific Aim I

### 3.1.1. Oxidative Stress is central to inflammatory bowel disease

The central focus of Specific Aim I is on the targeting of siRNA to inflamed mucosal tissue under oxidative stress via an ROS-sensitive delivery vehicle. Although the exact role of ROS in the etiology of UC remains uncertain, abnormally high levels of ROS are produced in the colons of patients with UC[50]. This abnormally high level of ROS is produced from activated neutrophils that congregate in inflamed mucosal tissues[51]. The overproduction of ROS by these activated neutrophils is so severe that it damages gap junctions between mucosal epithelial cells leading to bacterial infiltration and infection, which ultimately results in leukocyte infiltration and increased oxidative stress [52]. These high levels of oxidative stress in patients with UC provide a molecular signature for inflammation and can be targeted with ROS-sensitive biomaterials.

### 3.1.2. ROS-cleavable polymers

Materials that can target siRNA to mucosal tissues under oxidative stress by oral delivery must be composed of ROS-sensitive linkages that are stable to both acidic and photolytic cleavage. A linkage that meets these criteria is the thioketal. Thioketals have been used extensively in organic synthesis as oxidation sensitive protecting groups for carbonyl compounds[53].

As protecting groups, thioketals are particularly useful because they are stable to acid and base catalyzed hydrolysis. Thioketal protecting groups are formed by performing a Lewis Acid-catalyzed condensation reaction between a carbonyl compound and ethane-1,2-diol. Thioketals can also be found in the structure of some pharmaceutical compounds and are known to cleave under biologically relevant levels of ROS[54]. In the past 8 years, traditional acetals, or ketals, have been incorporated into the

backbones of biodegradable polymers using the acetyl exchange reaction between various diols and 2,2-dimethoxypropane [55-57]. This synthetic strategy produces traditional polyketal polymers with molecular weights ranging from 4000–6000 Da. Polythioketal polymers have been used to formulate microparticles that encapsulate both hydrophobic small molecules and proteins[58,59]. We anticipated that the flexibility of the acetal exchange reaction can be used to synthesize homo- and copolymers that contain the ROS-sensitive thioketal linkage in their backbones.

### 3.1.3. TNF-α is a protagonist in the development and persistence of UC

The experiments in this proposal will develop an oral siRNA delivery vehicle based upon an ROS-sensitive biomaterial. In the experiments proposed below, anti-TNF-α siRNA will be delivered to inflamed mucosal tissue as a treatment for ulcerative colitis (UC). Although the exact pathogenesis of UC is not well understood, TNF-α has been shown to play an integral role in the development of the disease [60,61]. Several studies have demonstrated that fresh colonic mucosal biopsies of UC patients show increased levels of TNF-α expression[62,63]. Pharmacologic studies have also demonstrated the importance of TNF-α in the pathophysiology of UC. Small molecule inhibitors of TNF-α are efficacious in mouse models of UC[64]. Multiple clinical trials have demonstrated the efficacy of monoclonal antibodies against TNF-α in the treatment of UC[65,66]. Although these antibodies are highly effective, nearly 25% of patients taking the monoclonal antibody Infliximab® experienced at least one serious adverse event, including pneumonia, cancer, and acute inflammations[66].

## 3.2. Specific Aim II

### 3.2.1. Intestinal inflammation, NF-κB, and CRC

Rudolf Virchow made the first observation of the symbiotic relationship between inflammation and cancer in 1863 when he observed that human tumors are often festooned with leukocytes[6]. In the last decade, the ying-yang relationship between inflammation and cancer has been well established by genetic, pharmacological, and epidemiological data[67-71]. Nearly 20% of all cancers arise in association with infection or chronic inflammation, and nearly all of those that are not, contain elevated levels of inflammatory mediators[38]. Colitis-associated cancer (CAC) represents the archetype for the link between inflammation and cancer, given its high frequency in patients with IBD, the protective role of nonsteroidal anti-inflammatory drugs[67], and CAC's association with inflammatory gene expression[72]. Recently, scientists have begun to elucidate the mechanisms by which immune cells, cytokines, ROS, and reactive nitrogen species contribute to the three phases of tumor development, namely initiation, promotion, and progression[73].

The transcription factor NF-κB is well established as a central regulator of numerous proinflammatory genes such as cytokines, cytokine receptors, and cell adhesion molecules[69]. More recently, NF-κB activation has been implicated as being involved with multiple aspects of tumorigenesis, including the control of genes that control survival, angiogenesis, proliferation, adhesion, and metastasis[41,74-76] (Figure 3.1). Studies performed on mice suffering from experimental CAC, demonstrated that NF-κB activation was necessary for both tumorigenesis as well as tumor growth[74]. Clinical studies performed on patients suffering from ulcerative colitis have demonstrated that NF-κB activation in the colon is an excellent predictor of the probability of CAC development[76].

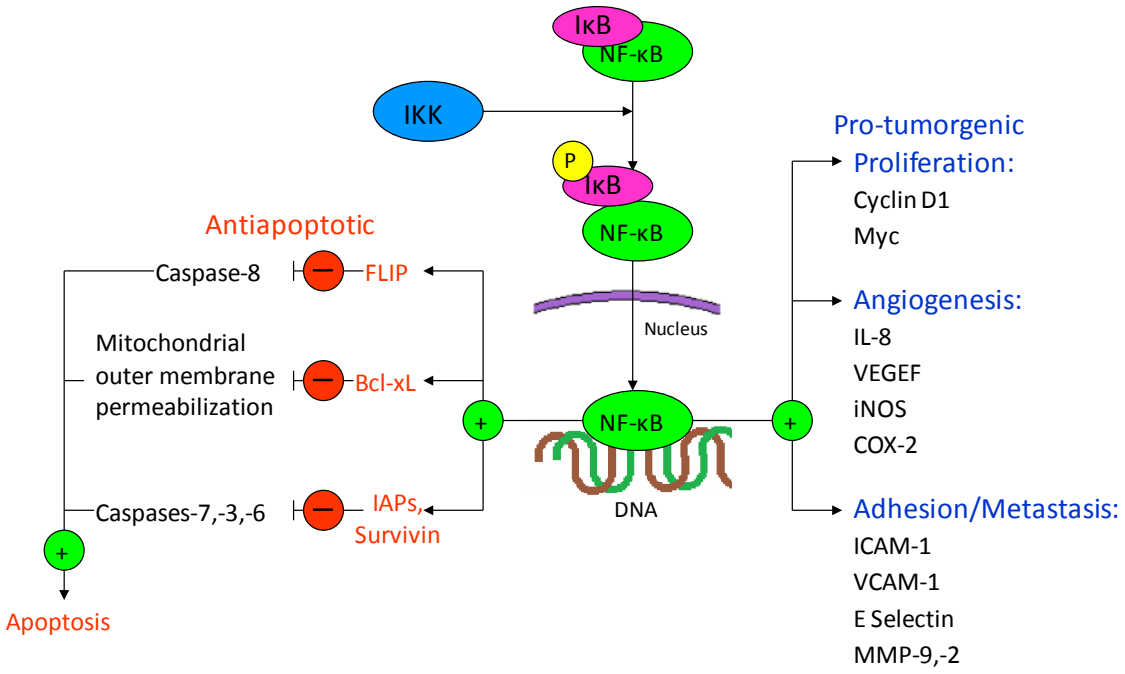


**Figure 3.1. Ilistration of NF-κB activation pathway and the protumorigenic and prosurvival genes initiated by its activation.** Upon phosphorylation by the IKK complex IκB is degraded, liberating NF-κB and allowing it to translocate to the nucleus.

In addition to cancer development, NF-κB activation is the primary mechanism by which cells avoid treatment by chemotherapeutics[77-79]. In its inactive form, NF-κB is sequestered in the cytoplasm by a family of NF-κB binding proteins called IκB (Figure 3.1). In response to activating stimuli, including cytokines and DNA-damaging agents, IκB is phosphorylated by the IκB kinase complex (IKK), which leads to IκB ubiquitination and subsequent degradation by the proteosome[80]. The degradation of IκB liberates NF-κB allowing it to translocate to the nucleus, where it increases the expression of a variety of prosurvival genes, including Bcl-xL, IAP, FLIP and survivin[81-84]. These genes block the effects of chemotherapeutics and generate a drug resistant state in the cell[26].

3.2.2. Irinotecan: Mechanism of action, NF-κB activation

Since its introduction in 1996 Irinotecan (CPT-11) has improved the prognosis of patients suffering from CAC and metastatic CRC[85,86]. CPT-11 is an analog of camptothecin, characterized by the presence of a bulky piperidino side-chain that is

cleaved by host enzymes to give 7-ethyl-10-hydroxy-camptothecin (SN-38), which is 100-fold more potent than CPT-11[87]. Irinotecan has been used clinically to treat CRC, esophageal cancer, gastric cancers, lung cancer, leukemia, and various gliomas[88]. Irinotecan causes S-phase specific cell death by targeting cellular topoisomerase I (Topo I)-DNA complexes. Topoisomerase I binds to double-stranded DNA and cleaves the phosphate backbone of one of the DNA strands to reduce the twisting and supercoiling that occur in selected regions of DNA during DNA transcription, replication, and repair[89]. Irinotecan interacts with the Topo I-DNA complex after DNA-strand cleavage to form a covalent Topo I-DNA reaction intermediate[90]. Although nonlethal by itself, the enzyme-DNA complex generated by Irinotecan halts the advancement of the replication fork, and in doing so generates a double-stranded DNA-break on the leading strand of the newly synthesized DNA. This double-stranded break terminates DNA replication and causes the death of the dividing cell.

Although double-stranded DNA damage is lethal and causes cell-cycle arrest, the DNA damage caused by CPT-11 activates cytoplasmic signaling cascades that liberate active NF-κB from its inhibitor protein, IκBα, through an IKK-dependent pathway that does not require extracellular signaling via the classical or alternative pathways[21]. In this way, CPT-11 initiates the tumor cells' central defense mechanism against chemotherapy, inducing drug resistance. Numerous clinical and experimental studies have verified the link between CPT-11 and induced drug resistance in CRC[91,92]. CRC tumor biopsies taken from patients before and after first-round treatment with CPT-11 showed elevated levels of NF-κB activation after CPT-11 treatment[48]. CPT-11 has also been shown to increases NF-κB activation in a dose and time dependent manner in numerous colon cancer cell lines including LoVo[93], HCT-15[23], HCT 116[84], Caco-2[23], colon26[24], and the CPT-11 resistant cell line HT-29[26]. Additionally, tumor xenografts formed from HT-29, HCT-116, or colon26 cells showed elevated levels of NF-κB

activation post treatment with CPT-11[23,24,26]. In order to demonstrate the drug resistance inducing power CPT-11, Lagadec et al. showed that at a dose of 30 mg $kg^{-1}$, CPT-11 increases the activation of NF-κB and the expression of the down-stream anti-apoptotic genes Bcl-xl, c-IAP1, and Survivin in HT-29 xenografts tumors in mice[26]. These clinical and experimental results suggest that reducing NF-κB activation in concert with CPT-11 treatment may help prevent CPT-11-mediated drug resistance, and in doing so increase CPT-11 efficacy.

The first preclinical experiments demonstrating the synergy between NF-κB inhibition and CPT-11 in a colon cancer xenograft were performed with an adenoviral delivery vector[94]. In this work, mice bearing LoVo xenografts were treated once a week for three weeks with both CPT-11(33 mg $kg^{-1}$ $week^{-1}$, 21 days) and an adenovirus expressing a super-repressor IκBα that cannot be phosphorylated by IKK and thus inhibits NF-κB activation. Mice treated with both CPT-11 and the adenovirus experienced no increase in tumor size over the 21 days of treatment, whereas mice treated with only CPT-11 or the adenovirus experienced tumor growth equivalent to the untreated animals. Given the clinical issues with adenovirus delivery of genes, Kokura et al. demonstrated a significant decrease in tumor size as well as lung metastasis when mice bearing colon26 tumors were treated with the radical scavenger edaravone and CPT-11 (30 mg $kg^{-1}$ $day^{-1}$, 18 days) compared to mice receiving only edaravone or CPT-11[24]. This decrease in tumor size with the combination therapy was attributed to edaravone's ability to inhibit NF-κB in colon26 cells via the scavenging of ROS. Although edaravone is only approved for use in Japan, these results verified the adjuvant effect of inhibiting NF-κB via a pharmacological agent in the treatment of colon cancer tumors with CPT-11 and the ability to inhibit NF-κB activation in tumors with a radical scavenger. Recently, studies that used the IKK inhibitor AS602868 (25 or 100 mg $kg^{-1}$ $week^{-1}$, 10 weeks) in combination with CPT-11 in the treatment of HT29

xenograft tumors in mice demonstrated improved efficacy of the combined therapy versus the individual drugs[85].

Despite convincing preclinical and *in vitro* results that demonstrate the synergy of NF-κB inhibition and CPT-11 in the treatment of colon cancer, there has yet to be a successful clinical trial on the combination of an NF-κB inhibitor with CPT-11. NF-κB inhibitors must be non-toxic to normal cells, minimally immunosuppressive, and have few side effects. Given that NF-κB activation serves as the central anti-apoptotic mechanism for all cells, and not just cancer cells, NF-κB inhibitors could increase the toxicity of CPT-11 to the liver, immune system, and heart[95-101].

### 3.2.3. Caffeic Acid Phenethyl Ester (CAPE): NF-κB inhibitor

Despite the convincing preclinical and in vitro results that demonstrate the synergy of NF-κB inhibition and CPT-11 in the treatment of colon cancer, there has yet to be a successful clinical trial using the combination of an NF-κB inhibitor with CPT-11. Clinically viable NF-κB inhibitors must be non-toxic to normal cells, minimally immunosuppressive, and have few side effects[102]. Given their low levels of toxicity and minimal side effects, food derived flavonoids that inhibit NF-κB are promising adjuvants for the treatment of colon cancer. Among the natural flavonoids that inhibit NF-κB, the most hopeful candidate for treating cancer is caffeic acid phenethyl ester (CAPE). CAPE, which is an active component of propolis from honeybee hives, is a well-documented inhibitor of NFκB[103] that has anti-inflammatory and anti-carcinogenic properties, and has been used to treat animal models of ulcerative colitis[104-107], ischemic injury[108-135], pulmonary fibrosis[136], myocardial infarct, and numerous cancer tumors[137-154].

Although the exact molecular mechanisms have yet to be fully elucidated, CAPE's inhibition of NF-κB stems from its ability to reduce IKK activity and thereby inhibit IκBα's phosphorylation, subsequent degradation, and release of NF-κB. Given

that, CAPE's polyphenolic catechol group is a powerful ROS scavenger and the ability of radical scavengers to inhibit IKK activation, the NF-kB inhibition induce by CAPE had been attributed to its prowess as an antioxidant. A recent structure-activity study with non-ROS scavenging and ROS-scavenging CAPE analogues indicates that CAPE's Michael reaction acceptor (MRA) and ethyl-aromatic ring play a role in its ability to inhibit NF-κB[155]. In this study, both catechol and cinnaminic acid phenethyl ester, which has an MRA but no catechol group, were able to inhibit TNFα-induced NF-κB activation in HT-116 cells, whereas phenpropionic acid phenethyl ester, which has neither a catechol nor a MRA, did not.

Various studies have demonstrated the NF-κB inhibiting potential of CAPE in numerous cancer cell lines including prostate cancer PC-3[156], breast cancer MCF-7[138], malignant peripheral nerve sheath tumors, astrocytoma GRT-MG[157], myeloid leukemia U-937[158], human B-lymphoma[159], and colon cancer HT-29, 26-L5[160,161], CT-26 and HT-116 cells. McEleny et al investigated the effect of CAPE on reducing NF-κB activation by paclitaxel in PC-3 cells. Their work concluded that at 25 µg/ml CAPE reduced paclitaxel NF-κB activation by 50% and that this reduction was sufficient to reduce the downstream activation of prosurvival genes including cIAP-1, cIAP-2, and XIAP. Although CAPE has yet to be used as an adjuvant in treating tumors, CAPE has been effectively used as a standalone therapeutic and inhibits the growth of 6 glioma[162] (1.0 mg $kg^{-1}$ $day^{-1}$) , cholangiocarcinoma MZ-CH1-1[163](10 mg $kg^{-1}$ $day^{-1}$), and colon cancer CT-26 (10 mg $kg^{-1}$ $day^{-1}$) xenograft tumors grown in mice. In studies performed on MZ-CH1-1 xenografts[149], the level of NF-κB inhibition induced by CAPE was sufficient to reduce the expression of anti-apoptotic genes Bax, Bcl-2 in the tumor and thus increase apoptosis in the tumor.

# Chapter 4: Thioketal Nanoparticles Orally Delivery siRNA, Target Intestinal Inflammation and Suppress Proinflammatory Gene Expression*

## 4.1. Abstract

Gene silencing via orally delivered small interfering RNA (siRNA) represents a promising treatment strategy for numerous gastrointestinal (GI) diseases associated with chronic intestinal inflammation; however, the oral delivery of siRNA to inflamed intestinal tissues remains a major challenge. In this chapter, we present a delivery vehicle for siRNA, termed thioketal nanoparticles (TKNs), that can orally deliver siRNA to sites of intestinal inflammation, and thus inhibit gene expression in diseased intestinal tissue. TKNs are formulated from a new polymer, poly-(1,4-phenyleneacetone dimethylene thioketal) (PPADT), that degrades selectively in response to reactive oxygen species (ROS). Therefore, when delivered orally, TKNs target the release of encapsulated agents to the elevated levels of ROS specific to sites of intestinal inflammation[1-3]. Using a murine model of ulcerative colitis (UC), we demonstrate that orally administered TKNs loaded with TNFα-siRNA (TNFα-TKNs) diminish TNFα messenger RNA (mRNA) levels in the colon and protect mice from intestinal inflammation. Given the prevalence of intestinal inflammation in GI diseases[2], and the therapeutic potential of siRNA[4], we anticipate numerous applications of the TKNs for treating GI diseases.

* Adapted and Modified from "Orally delivered thioketal nanoparticles loaded with TNF-α-siRNA target inflammation and inhibit gene expression in the intestines." Wilson DS, Dalmasso G, Wang L, Sitaraman SV, Merlin D, Murthy N., *Nat Materials* 2010.

## 4.2. Introduction

Due to constant insult from luminal bacterial and food antigens, the intestinal mucosa is in a state of orchestrated inflammation, characterized by an intricate balance of proinflammatory and toleragenic mediators[76]. Numerous pathologies including infections[164], neoplastic transition[165], and autoimmune disorders[166] can disrupt the intestinal immune system's regulatory process, resulting in a pathogenic inflammatory event. Although, the exact etiology of each of these diseases is unique, the resulting intestinal inflammatory response is driven primarily by the aberrant production of the proinflammatory cytokine tumor necrosis factor-α (TNFα)[76]. Given the central role of TNFα in orchestrating the intestinal inflammatory response, therapeutic strategies that target TNFα production in the intestines could improve the treatment of virtually every disease associated with intestinal inflammation.

RNA interference (RNAi) strategies directed against TNFα, have a tremendous potential to treat disease associated with intestinal inflammation[167]. Nevertheless, the systemic depletion of TNFα has been shown to compromises the immune system, thus resulting in an elevated risk of infection[168], lymphoma[169], and cardiac dysfunction[170]. Therefore, the immune suppressive power of anti-TNFα RNAi-based therapeutics, such as siRNAs, must be localized to sites of intestinal inflammation. Oral delivery vehicles have direct access to the intestinal mucosa, and thus represent an ideal platform for localizing siRNA to diseased intestinal tissue. Furthermore, by eliminating needles, oral delivery eases administration and eliminates the risk of disease transmission by contaminated needles. Various delivery vehicles have been developed to orally deliver therapeutics to intestinal tissue[171-173], yet none of these strategies have demonstrated the ability to protect siRNA from the harsh environment of the GI tract and silence gene expression in intestinal tissues.

To localize the delivery of siRNA to diseased intestinal tissue, we identified the abnormally high levels of ROS produced at sites of intestinal inflammation as a disease specific triggering mechanism for siRNA release[2]. For example, biopsies taken from patients suffering from UC[1,3,174], colon cancer[175], and *h. pylori* infections[2] have a ten- to hundred-fold increase in mucosal ROS concentrations that are confined to sites of disease development and correlate with disease progression. To target intestinal inflammation we developed TKNs, which release encapsulated agents in response to ROS. TKNs are formulated from PPADT, a new polymer composed of ROS-sensitive thioketal linkages[176] that are stable to acid-, base-, and protease-catalyzed degradation[176,177] (Figure 4.1.a). Therefore, orally delivered TNFα-TKNs remain stable in the GI-tract, thereby protecting siRNA and preventing its release to non-inflamed tissues (Figure 4.1.b, upper panel). In contrast, at sites of intestinal inflammation the elevated ROS levels trigger the degradation of the TNFα-TKNs, thus localizing the release of siRNA to inflamed intestinal tissues (Figure 4.1.b, lower panel).

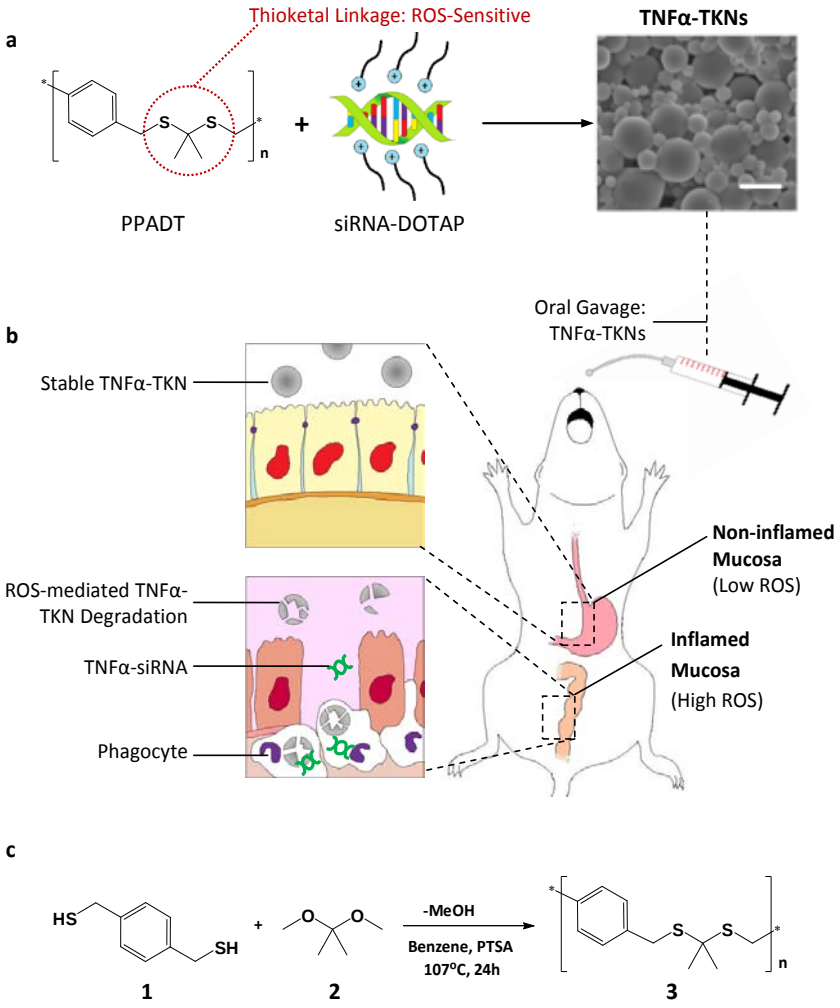


**Figure 4.1. Thioketal nanoparticles are formulated from a new ROS-sensitive polymer and release orally delivered siRNA at sites of intestinal inflammation.** (a) PPADT is a new polymer composed of ROS-sensitive thioketal linkages (circled in red). TNFα-TKNs were prepared by first precomplexing TNFα-siRNA with the cationic lipid 1,2-dioleoyl-3-trimethylammonium-propane. Next, these siRNA-DOTAP complexes were added to an organic solution containing PPADT. A single-emulsion procedure was then used to produce particles with mean diameters of ~600 nm that contain 4.7 μg TNFα siRNA/mg particles. SEM image shows TNFα-TKNs (scale bar represents 1.5 μm). (b) When delivered orally, TNFα-TKNs remain stable in the harsh environment of the GI tract, protecting TNFα-siRNA and preventing its release to non-inflamed mucosal tissues. However, at sights of intestinal inflammation, where infiltrating phagocytes produce unusually high levels of ROS, the TKNs degrade, thus releasing TNFα-siRNA to the site of inflammation. (c) PPADT 3 was synthesized using the acetal exchange reaction.

## 4.3. Methods

Unless otherwise noted, all reagents were used as received from Sigma.

### 4.3.1. PPADT Synthesis and ROS sensitivity assay

Briefly, a two-necked flask was charged with distilled benzene, 1,4-benzenedimethanethiol 1 (1.0 eq) and 2,2-dimethoxypropane 2 (1.0 eq.), then equipped with a metering funnel and distillation head for removal of the methanol by-product. The mixture was then stirred continuously and heated to 95 °C before a catalytic amount of re-crystallized *p*-toluenesulfonic acid (0.003 eq.) in distilled ethyl acetate was added to start the reaction. After 1 h, a solution of 2,2-dimethoxypropane and distilled benzene was added to the metering funnel and the funnel stopcock was set so that a small amount of 2,2-dimethoxypropane (0.08 eq per h) was add drop-wise over a period of 12 h. The reaction was allowed to stir overnight before the resulting polymer was isolated by precipitation in cold hexanes. The polymer was vacuum-dried and analyzed by $^{1}$H-NMR (Burker DMX 400, 400MHz), $^{13}$C NMR, and gel permeation chromatography (Shimadzu). $^{1}$H-NMR: Per repeating unit, (400MHz, $CDCl_3$,) δ ppm 7.28 (4H), 3.85 (4H), 1.60 (9H). $^{13}$C- NMR: (400 MHz, $CDCl_3$) δ ppm 129.54, 77.56, 77.25, 76.93, 35.03, and 31.01. The molecular weight of the resulting polymer was approximately 9 kDa with a polydispersity of 1.8. In order to assess the ROS-sensitivity of PPADT, PPADT was exposed to superoxide according to the procedure described in Reference 173.

### 4.3.2. Preparation of CMFDA- and rhodamine B-loaded TKNs

CMFDA (Invitrogen) and rhodamine B were encapsulated in TKNs via an oil-in-water single-emulsion procedure. Either CMFDA (1.0 mg) or rhodamine B (1.0 mg) were solubilized in dimethyl sulfoxide (DMSO) and added to a solution of PPADT (100 mg) in dichloromethane (DCM) (500 µl). This organic phase was then added to 10 mL of a 5% solution of polyvinyl alcohol (PVA) in pH 7.4 phosphate buffer saline (PBS) and the

biphasic mixture was homogenized (17,500 rpm) for 60 sec. The resulting oil-in-water emulsion was then added to 60 mL of a 1% solution of PVA in PBS and stirred in an open container for 4 h to evaporate the DCM. The resulting particles were isolated by centrifugation and washed three times with PBS to remove any residual PVA. Finally, the particles were frozen at -75°C and lyophilized to obtain a fine powder. Empty TKNs were formulated as described above without any dye. Particles contained either 8.3 μg of CMFDA per mg of particles or 6.9 μg of rhodamine B per mg of particles. For all particle formulations, particle size was determined by dynamic light scattering [DLS (Brookhaven Instruments Corporation)], and visual evidence of particle formation was obtained via a scanning electron microscope [SEM (Hitachi S-800)]

4.3.3. Preparation of siRNA-loaded TKNs and PLGA nanoparticles

Nanoparticles loaded with siRNA were generated by first preparing complexes between the cationic lipid 1,2-dioleoyl-3-trimethylammonium-propane (DOTAP) then using the above single-emulsion protocol to encapsulate these complexes into nanoparticles. The TNFα-siRNA sequence 5'- CAC AAC CAA CUA GUG GUG CUU-3' (Dharmacon) or a scrambled non-specific siRNA sequence or Cy3-tagged scrambled siRNA sequence were complexed with DOTAP (Avanti Polar Lipids Inc.) by adding 400 μl of a 187.5 μM solution of siRNA in nuclease free water to 400 μl of a 9.45 mM DCM/DOTAP solution. To this two-phase solution was added 880 μl of MeOH and the resulting single-phase solution was vortexed for 60 sec. Next, DCM (400 μl) and nuclease free water (400 μl) were added to the siRNA-DOTAP solution, and the solution was centrifuged (1000 g for 10 min) to separate the two phases. Next, the organic phase (aprox. 800 μl) containing the DOTAP-siRNA complexes was collected and added to 50 mg of PPADT or PLGA. This organic siRNA-DOTAP/PPADT mixture was then used to formulate oil-in-water single-emulsion particles as described above. This

protocol produced TNFα-TKNs, Sc-TKNs, Cy3siRNA-TKNs, and TNFα-PLGA that contained 4.7, 4.1, 5.7 and 6.1 μg of siRNA per mg of particles, respectively.

4.3.4. Preparation of TNFα siRNA loaded βGPs

βGPs containing TNFα-siRNA were prepared exactly as described in Reference 12.

4.3.5. ROS-responsive release from TKNs *in vitro*

RAW 264.7 macrophages (ATCC) were cultured in Dulbecco's Modified Eagle's Medium (DMEM) supplemented with 10% fetal bovine serum (FBS) and maintained at 37°C in a humidified 5% $CO_2$ atmosphere. Cells were seeded in 12 well culture plates ($10^7$ cells/well) and incubated with 0.2 mg/ml CMFDA-TKNs. After 3 h, the cells were washed with PBS three times, and then treated with either DMEM/FBS, DMEM/FBS spiked with LPS or DMEM/FBS spiked with LPS and TEMPOL (2.5 mM & 5.0 mM). After 20 h, the media was removed and the cells were washed with PBS and suspended in 1.5 ml of PBS containing 1% FBS and 5 mM EDTA. The cells were then passed through a 45 μm nylon mesh before being analyzed via fluorescence-activated cell sorting (FACS) to assess intracellular dye release. FACS analysis was carried out on DB® FACSVantageSE/DiVa® instrumentation, and the results were analyzed with FlowJow® software.

4.3.6. *in vitro* silencing of TNFα expression via TNFα-TKNs

RAW 264.7 macrophages were cultured as described above, and seeded in 12 well culture plates ($10^7$ cells/well). After 12 h, the cell media was replaced with a solution of DMEM/FBS containing one of the following treatments: TNFα-TKNs, Sc-TKNs, TNFα-TKNs, TNFα-βGPs, or siRNA-DOTAP complexes. For treatments

containing siRNA cells received 23.0 μg siRNA/ml. After 4 h of treatment, the media was removed, the cells were washed with PBS, and then treated with either normal DMEM/FBS or DMEM/FBS spiked with LPS (5 μg/ml). After 24 h, 100 μl of media was collected from each sample and analyzed for TNFα via ELISA according to the manufactures protocol (eBioscience).

4.3.7. Induction of colitis and oral TNFα-siRNA delivery

Animal experiments were performed in female C57BL/6 mice (8wk, 17 – 20 g, Jackson Laboratories). Mice were group housed under a controlled temperature (25 °C), photoperiod (12:12-h light-dark cycle), and allowed unrestricted access to potables and standard mouse chow. They were allowed to acclimate to these conditions for at least seven days before being included in experiments. Colitis was induced by adding 3% (wt./vol) DSS [35,000 Da, (ICN Biochemicals)] to their drinking water. For each of the animal experiments, groups of mice were treated with DSS or regular water for seven days. Mice were observed daily and evaluated for changes in body weight and development of the clinical symptoms of colitis. Starting on day zero, mice receiving DSS were given a daily gavage of PBS (200μl) or a PBS solution (200μl) containing one of the following: TNFα-TKNs, TNFα-PLGA, Sc-TKNs, TNFα-βGPs, or TNFα-DOTAP. Mice receiving siRNA-loaded particles or TNFα-DOTAP were treated with either 2.3 mg/kg or 0.23 mg/kg of TNFα-siRNA or scrambled siRNA per day for five days. Mice were sacrificed after seven days, and histological assessment of colonic inflammation was performed by hematoxylin and eosin (H&E) staining of 5 μm-colonic tissue sections and analyzed by microscopy (20X & 10X). All animal experiments were approved by The Animal Care Committee of Emory University, Atlanta (IACUC ID: 156-2008) and were performed in accordance with the guide for the *Care and Use of Laboratory Animals*, published by the U.S. Public Health Service.

4.2.8. Real time RT-PCR

Total RNA was extracted from mouse colons using TRIzol (Invitrogen). A reverse transcription (RT) reaction was performed on 2 µg of each sample and an oligo-dT primer, using a RETROscript® System (Ambion Inc.). Next, 10 ng of reverse-transcribed cDNA, 400 nM of gene-specific primers, and the iQ SYBR Green Suppermix (Biorad) was amplified at 50°C for 2 min and 95°C for 10 min, followed by 40 cycles of 95°C for 15 s and 60°C for 1 min. The 36B4 expression levels were used as reference, and fold-induction was calculated by the Ct method as follows: $\Delta\Delta CT=(Ct_{Target} - Ct_{36B4})_{DSS+Treatment} - (Ct_{Target} - Ct_{36B4})_{DSS+ PBS}$. Thus producing results normalized against mice receiving DSS and treated with PBS. The final data were then derived from $2^{-\Delta\Delta CT}$. The primers used were designed using the Primer Express Program (Applied Biosystems) and were as follows: TNFα sense 5'-AGG CTG CCC CGA CTA CGT-3' antisense 5'-GAC TTT CTC CTG GTA TGA GAT AGC AAA-3'; IL-1β sense 5'-TCG CTC AGG GTC ACA AGA AA-3' antisense 5'-CAT CAG AGG CAA GGA GGA AAA C-3'; IL-6 sense 5'-ACA AGT CGG AGG CTT AAT TAC ACA T-3' antisense 5'-TTG CCA TTG CAC AAC TCT TTT C-3'; IFN-γ sense 5'-CAG CAA CAG CAA GGC GAA A -3' antisense 5'-CTG GAC CTG TGG GTT GTT GAC -3'.

4.3.9. Myeloperoxidase (MPO) Activity

Neutrophil infiltration into the colon was quantified by measuring MPO activity. Briefly, a portion of the colon was homogenized in 1:20 (w/v) of 50 mM phosphate buffer (pH 6.0) containing 0.5% hexadecyltrimethyl ammonium bromide on ice using a homogenizer (Polytron). The homogenate was then sonicated for 10 s, freeze-thawed three times, and centrifuged at 14,000 rpm for 15 min. The supernatant (14 µl) was then added to 1 mg/ml *o*-dianisidine hydrochloride and 0.0005% hydrogen peroxide, and the

change in absorbance at 460 nm was measured. MPO activity was expressed as units per mg of protein, where one unit was defined as the amount that degrades 1 μmol of hydrogen peroxide per minute at 25°C.

4.3.10. Targeting of Cy3-labed siRNA to inflamed tissues using TKNs

Mice receiving DSS or normal water were given a daily gavage of a PBS solution (200μl) containing empty TKNs or Cy3siRNA-TKNs (50 mg/ ml) (total of four groups with n =3 per group). After seven days, each mouse receiving DSS had lost at least 10% of their body weight and had elevated fecal blood levels consistent with disease development. Organ samples (0.5 g - 0.9 g) were removed, washed with cold PBS, patted dry with a paper towel, and then homogenized in 1 ml of PBS (Polytron). Samples were then centrifuged at 14,000 rpm for 30 min, and Cy3 was quantified in 100 μl of the supernatant using a fluorometer ($\lambda_{ex}/\lambda_{em}$ = 550/570; Shimadzu). To correct for the background fluorescence resulting from the tissue and residual PPADT, the fluorescence measured from organ samples taken from mice receiving empty TKNs was subtracted from the fluorescence measured in samples taken from animals treated with Cy3siRNA-TKNs. Results are expressed as fluorescent units per gram of tissue.

4.3.11. Release of Cy3-tagged siRNA in response to ROS *in vitro*

A 0.4 mg/ml solution of Cy3siRNA-TKNs in PBS was prepared and added to an equal volume of PBS containing either: 2 mM hydroxide radical, 0.2 mM hydroxide radical, 2 mM $KO_2$, or 0.2mM $KO_2$. Hydroxide radical is formed by mixing Fenton's Reagent with $H_2O_2$. Each sample was prepared in triplicate. The samples were then agitated on a rotary shaker at room temperature for either 4 or 12 hours. After 4 or 12 hours, the particles were isolated from the solution via centrifugation. Finally, the

amount of Cy3-siRNA released from particles was measured by analyzing the fluorescence of the supernatant ($\lambda_{ex}/\lambda_{em}$ = 535/590; Tecan).

4.3.12. Measuring CMFDA and rhodamine B loading in TKNs

CMFDA encapsulation was verified by dissolving CMFDA-loaded TKNs in dichloromethane (DCM) and extracting the dye from the organic phase into a 1N NaOH solution. The aqueous phase was then neutralized with 1N HCl and analyzed for fluorescence ($\lambda_{ex}/\lambda_{em}$ = 490/525; Shimadzu). rhodamine B-loading was quantified by dissolving Rho-TKNs particles in DCM then assaying the DCM solutions for fluorescence ($\lambda_{ex}/\lambda_{em}$ = 540/625). To account for the auto-fluorescence of PPADT, empty TKNs solution were prepared as described above and the fluorescence of these solutions was subtracted from the fluorescence measured from the dye-loaded particles.

4.3.13. Measuring siRNA loading in TKNs and PLGA nanoparticles

The amount of siRNA encapsulated in siRNA containing particles was quantified by isolating the encapsulated siRNA and measuring the amount of siRNA retrieved from the particles with the double-stranded RNA binding dye SYBR Green (Invitrogen). Particles containing siRNA were solubilized in DCM and then washed with a 20mM solution of NaCl in nuclease free water to disrupt the siRNA-DOTAP complexes and isolate the encapsulated siRNA. Empty TKNs were also solubilized and washed with a salt solution to determine the background. The aqueous phases were then isolated and analyzed for siRNA concentration using SYBR Green according to the manufacture's protocol.

4.3.14. Measuring rhodamine release rate in intestinal fluids

Rhodamine-loaded PLGA nanoparticles and rhodamine-loaded TKNs were incubated in simulated gastric fluid (pH 1.2, pepsin 0.32% w/v) and simulated intestinal

fluid (pH 7.5, pancreatin 1% w/v) at 37°C on a rotary shaker. On an hourly basis, particles were separated from the supernatant by centrifugation and the concentration of rhodamine released from the particles was determined by fluorescent spectroscopy.

4.3.15. Cytotoxicity of TKNs and PLGA nanoparticles

An MTT [3-(4,5-dimethylthiazol-2-yl)-2,5-diphenyltetrazoliumbromide] reduction assay was used to measure the cytotoxicity of TNFα-TKNs and TNFα-PLGA nanoparticles. Macrophages ($1X10^5$ cells/well, 96-well plate) were incubated with either TNFα-TKNs or TNFα-PLGA at various concentrations (1.0 – 5.0 mg/ml). After 28 hours, 20 µl of MTT solution (5 mg/ml in PBS) was added to each well, and the cells were incubated for 2 h. Next, the MTT solution was removed and the cells washed 2 X before adding 200 µl of dimethyl sulfoxide to each well to dissolve the resulting formazan crystals. After 10 min of incubation, the absorbance at 585nm was measured using an Emax Microplate reader (Molecular Devices, Sunnyvale, CA,USA). Normalized cell viability was calculated by comparing the absorbance of untreated cells to that of particle-treated cells.

## 4.4. Results

4.4.1. PPADT synthesis and ROS sensitivity

PPADT was synthesized from 1,4-benzenedimethanethiol 1 and 2,2-dimethoxypropane 2 via a step-growth polymerization that produces polymers with molecular weights (MN) of approximately 9,000 Da (Figure 4.1.c). To investigate the specificity of PPADT for ROS, we incubated PPADT with either a superoxide solution, 0.5 N HCl solution, or a 0.5 N NaOH solution and then analyzed the resulting product's molecular weight via gel permeation chromatography (GPC). The GPC traces shown in Figure 2a demonstrate that exposing PPADT to superoxide decreases its molecular

weight from almost 9,000 Da to approximately 810 Da in 8 h, whereas incubating PPADT in either an acidic or basic environment had no effect on its molecular weight.

4.4.2. TKNs release encapsulated agents in response to cellular ROS

The unusually high concentrations of ROS localized to sites of intestinal inflammation are generated by activated phagocytes[178]. To determine the capability of the TKNs to release agents in response to a physiologically relevant source of ROS, we compared the amount of intracellular dye released from dye-loaded TKNs in activated (ROS overproducing) versus non-activated phagocytes. Macrophages were treated with TKNs loaded with 5-chloromethylfluorescein diacetate (CMFDA), washed of excess particles, and then activated with lipopolysaccharide (LPS). CMFDA is activated by intracellular proteases; therefore, the cellular fluorescence of cells treated with CMFDA-loaded TKNs (CMFDA-TKNs) will be proportional to the amount of CMFDA released from phagocytosed TKNs. Figure 4.2.b shows that CMFDA-TKNs released CMFDA at an accelerated rate in response to ROS produced by activated macrophages. For example, LPS-activated macrophages showed a greater than seven-fold increase in cellular fluorescence compared to non-activated macrophages. This dramatic increase in cellular fluorescence was mitigated by treating LPS-activated macrophages with the ROS-scavenger TEMPOL (Figure 4.2.b), indicating that the amount of CMFDA released from CMFDA-TKNs is a function of ROS.

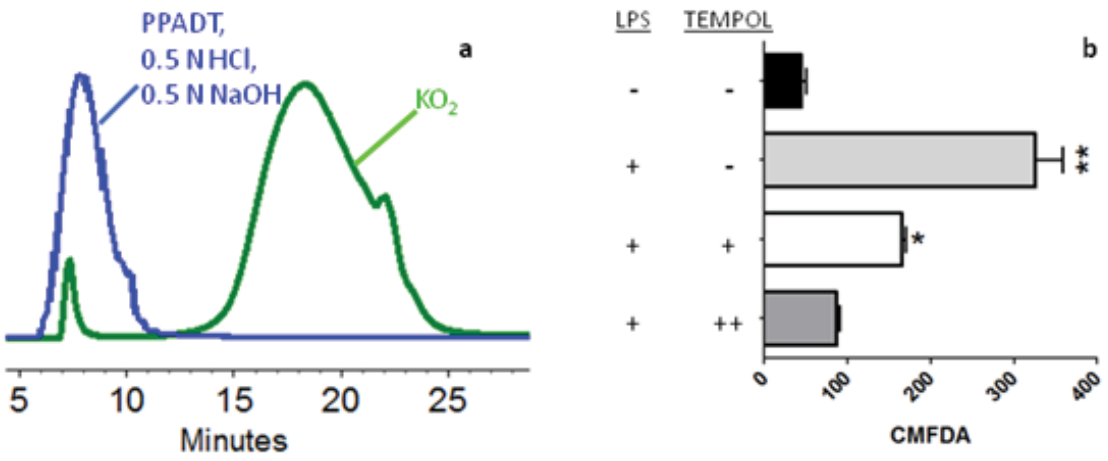


**Figure 4.2. PPADT is an ROS-sensitive polymer and nanoparticles formulated from it release their payloads in response to ROS produced by activated macrophages and inflamed colonic tissue.** (a) GPC traces of PPADT before (blue) and after exposure to $KO_2$ (green). Incubating PPADT in acidic and basic environments (0.5 N HCl & 0.5 N NaOH) had no effect on the molecular weight of PPADT (coincident traces represented with blue line). (b) Intracellular fluorescence of macrophages treated with CMFDA-loaded TKNs. Results expressed as mean fluorescence ± standard error of the mean (s.e.m.) for n = 3 per group. Statistical significance was determined by a one-way ANOVA using Bonferroni's post hoc test (*$p \leq 0.05$, **$p \leq 0.001$).

### 4.4.3. TKNs and not PLGA nanoparticles remain stable in intestinal fluids

To evaluate the stability of both TKNs and particles made from the FDA approved material PLGA in the presence of digestive fluids, we incubated nanoparticles loaded with the dye Rhodmine in simulated gastric and intestinal fluids (GF and IF, respectively) prepared according to the recommendations found in US pharmacopoeia. During the course of the experiments we measured die release into the media. As reflected by the data presented in Figure 4.3.a, which shows the percentages of encapsulated dye released into the medium in 4 h, PLGA nanoparticles released nearly 10 X more rhodamine into the simulated fluids than did the TKNs. After 4 h, the PLGA nanoparticles had released almost 25% and 10% of their contents in intestinal and gastric fluids, respectively. Whereas TKNs released less than 4% of their contents over that same time period.

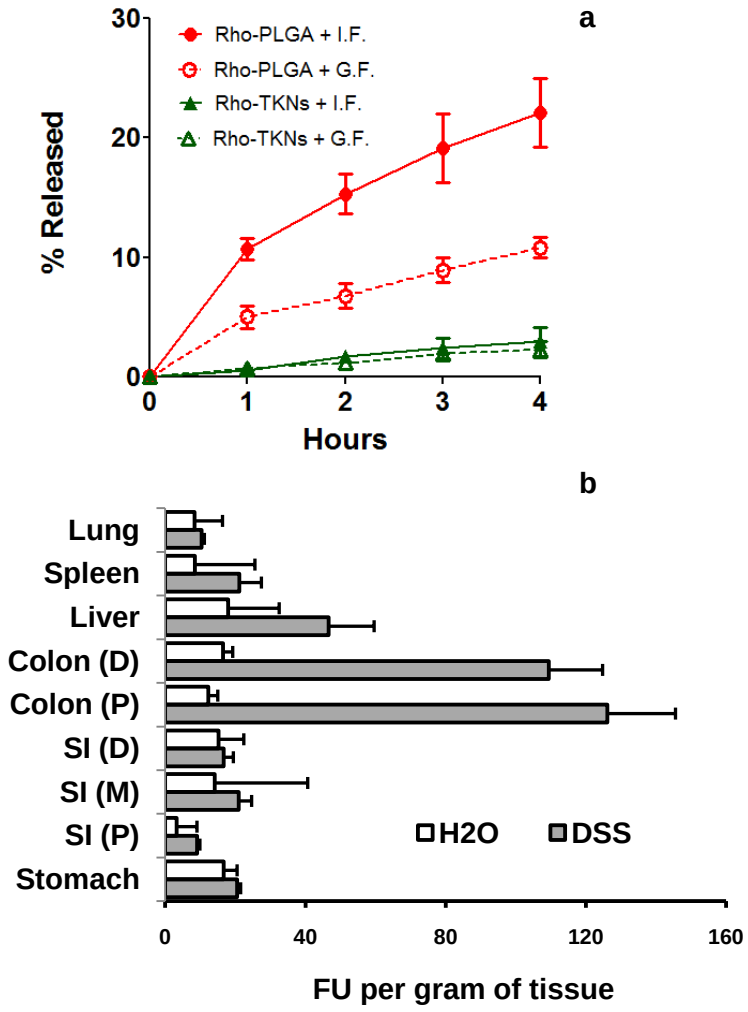


**Figure 4.3. TKNs remain stable in simulated gastric fluids, and when delivered orally, target encapsulated agents to inflamed intestinal.** (a) Release rate of rohdamine from TKNs and PLGA nanoparticles in simulated gastric fluids. Results depicted as mean % of encapsulated dye ± s.d. for n = 3 samples. (b) Biodistribution of Cy3-tagged siRNA in the organs on day seven of mice treated with a daily gavage of Cy3siRNA-TKN s for 6 days (D: distal, M: medial, P: proximal). Fluorescent units (FU) per gram of tissues depicted as the mean ± s.d. for n = 3 mice per group (*p ≤ 0.05).

### 4.4.4. Orally delivered siRNA-loaded TKNs target intestinal inflammation

The stability of the TKNs to simulated GI fluids and their ability to release encapsulated agents, including siRNA in response to ROS, motivated us to determine if orally delivered TKNs could target siRNA to inflamed intestinal tissues. Intestinal inflammation was induced in female C57BL/6 mice by replacing their drinking water on

day zero with a 3% solution of DSS[179]. Starting on day zero, mice receiving either DSS or normal drinking water were given a daily oral gavage of TKNs loaded with a Cy3-tagged scrambled siRNA (Cy3siRNA). On day seven, the biodistribution of siRNA was measured by fluorescence. Our results demonstrate that the TKNs can localize orally delivered siRNA to sites of intestinal inflammation (Figure 4.3.b). For example, Figure 4.3.b shows a greater than 3-fold increase in the amount of Cy3siRNA delivered to the distal and proximal sections of the colons of mice receiving DSS and Cy3siRNA-TKNs as compared to mice receiving normal water and treated with Cy3siRNA-TKNs.

### 4.4.5. TNFα-TKNs reduce TNFα mRNA levels in activated macrophages

Due to the essential role played by TNFα in the onset and persistence of intestinal inflammation[180], we chose to treat mice suffering from DSS-induced colitis with a known TNFα-siRNA sequence[181]. To demonstrate the ability of TNFα-TKNs to silence TNFα expression in the cells responsible for propagating the intestinal inflammatory response, we treated LPS-activated macrophages with TNFα-TKNs or appropriate controls. Figure 4.4.a shows that treating LPS-activated macrophages with TNFα-TKNs resulted in a statistically significant reduction in TNFα production as compared to cells treated with PBS or TKNs loaded with a scrambled siRNA sequence (Sc-TNFα) ($p \leq 0.05$). In addition, we discovered that TNFα-TKNs have an excellent cytotoxicity profile that is similar to nanoparticles formulated from the FDA approved material poly(lactic-co-glycolic acid) (PLGA) (Appendix A). These results show that TNFα-TKNs can protect siRNA from serum, deliver TNFα-siRNA in its active form, and decrease the expression of TNFα in activated phagocytes.

4.4.6. TNFα-TKNs colonic mRNA of proinflammatory cytokines

Based on these results, we hypothesized that orally administered TNFα-TKNs could silence TNFα expression in mice suffering from DSS-induced colitis, and thus inhibit intestinal inflammation. To test our hypothesis, mice receiving DSS were given TNFα-siRNA or scrambled siRNA (2.3 mg siRNA/kg) encapsulated in TKNs via oral gavage once daily for five days. Mice receiving DSS were also treated with free TNFα-siRNA/DOTAP complexes (2.3 mg siRNA/kg/day) (TNFα-DOTAP) or PBS. After seven days, the colonic mRNA levels of TNFα and other pro-inflammatory cytokines activated by TNFα, namely IL-6, IL-1, and IFN-γ, were analyzed by real-time PCR (RT-PCR). As shown in Figure 4.4.b mice treated with TNFα-TKNs (2.3 mg siRNA/kg/day) experienced a dramatic ten-fold decrease in colonic TNFα mRNA ($p \leq 0.001$). Analysis of colonic IL-6, IL-1, and IFN-γ, mRNA levels show that TNFα-TKNs also inhibited the activation of other pro-inflammatory signaling cascades (Appendix A).

In order to determine if the increased stability of the TKNs (Appendix A) improves the efficacy of nanoparticle-mediated oral delivery of siRNA, we also treated mice receiving DSS with a daily gavage of TNFα-siRNA (2.3 mg siRNA/kg) encapsulated in size- and charge-matched PLGA (50:50) nanoparticles (TNFα-PLGA) prepared as described above for TNFα-TKNs. Figure 4.4b shows that mice receiving DSS and treated with TNFα-PLGA did not experience a significant decrease in colonic TNFα-mRNA.

The high level of colonic TNFα suppression achieved by the TNFα-TKNs at a dose of 2.3 mg siRNA/kg/day motivated us to establish a minimum effective dose for TNFα-TKNs. Mice receiving DSS were treated with a ten-fold lower dose of TNFα-TKNs (0.23 mg TNFα-siRNA/kg/day ) via a daily oral gavage for five days. Figure 4.4.c illustrates that at this much lower dose TNFα-TKNs continue to produce a significant decrease in colonic TNFα mRNA ($p \leq 0.05$) in mice receiving DSS. In addition, this

approximately three-fold decrease in TNFα mRNA mitigated the activation of other proinflammatory signaling pathways that have been implicated in the development of UC, namely IL-6, IL-1, and IFN-γ (Figure 4.4.d). To examine if the ROS-responsive properties of the TKNs play a significant role in their ability to treat intestinal inflammation, we compared the efficacy of TNFα-TKNs to (TNFα-siRNA)-loaded β-glucan particles (TNFα-βGPs), which are designed to orally deliver siRNA to specialized cells in the intestines for systemic gene manipulation[171]. Figure 4.4.c shows that mice receiving DSS and treated with TNFα-βGPs (0.23 mg siRNA/kg/day) did not experience a significant decrease in colonic TNFα-mRNA (Appendix Afor characterization of TNFα-βGPs).

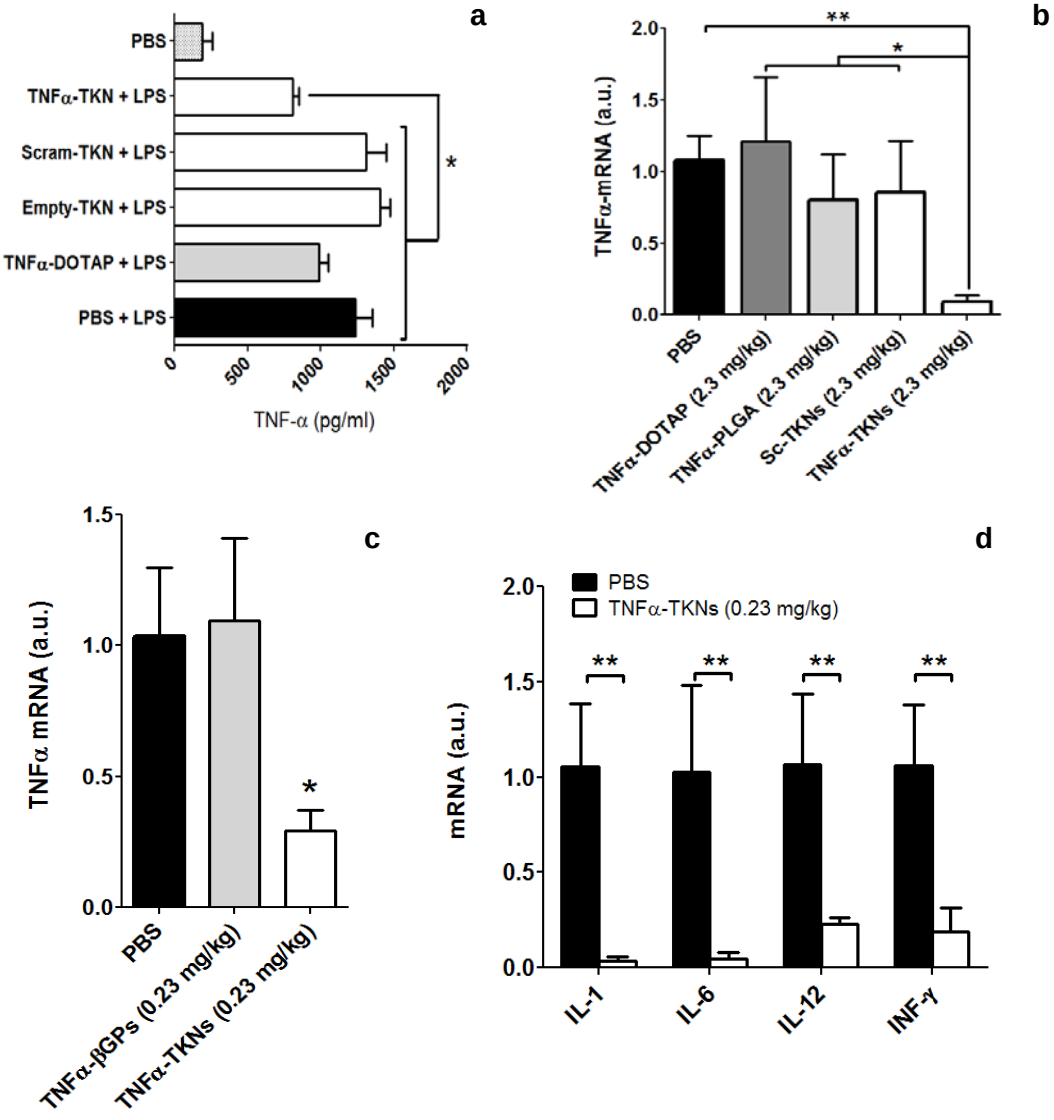


**Figure 4.4. TNFα-TKNs inhibit TNFα expression in vitro and reduce the colonic mRNA levels of proinflammatory cytokines in mice suffering from DSS-induced ulcerative colitis.** (a) Extracellular TNFα mRNA levels as determined by ELISA. Macrophages treated with 23.0 μg TNFα-siRNA/ml via TNFα-TKNs and activated with LPS expressed significantly less TNFα as compared to LPS-activated macrophages treated with PBS. Results depicted as mean pg of TNFα per ml of media ± s.e.m. for n = 3 per treatment group. (b) TNFα mRNA levels in mice receiving DSS and treated scrambled- or TNFα-siRNA with 2.3 mg siRNA/kg/day via either TNFα-TKNs (n = 6), TNFα-PLGA (n = 5), Sc-TKNs (n = 5), siRNA-DOTAP (n = 6). (c) TNFα mRNA levels in mice receiving DSS and treated with 0.23 mg TNFα-siRNA/kg/day via either TNFα-TKNs (n = 10) or TNFα-βGPs (n=10). (d) Colonic cytokine mRNA levels in mice receiving DSS and treated with either PBS or 0.23 mg TNFα-siRNA 0.23/kg/day via TNFα-TKNs (n = 10). Statistical differences in Figures a-d determined by a one-way ANOVA using Bonferroni's post hoc test (*$p \leq 0.05$, **$p \leq 0.001$). Figures b-d determined by a one-way ANOVA using Bonferroni's post hoc test (*$p \leq 0.05$, **$p \leq 0.001$).

4.4.7. TNFα-TKNs reduce the clinical manifestation of Colitis

Finally, we investigated if the reduction in colonic TNFα mRNA generated by TNFα-TKNs was sufficient to allay the clinical manifestations of DSS-induced UC. Our results demonstrate that TNFα-TKNs protected mice from DSS-induced colitis as assessed by histological analysis, colonic myeloperoxidase (MPO)-activity, and weight loss (Appendix A). For example, the colons of mice receiving DSS and treated with TNFα-siRNA (0.23 mg/kg/day) via TNFα-TKNs had intact epitheliums, well defined crypt structures, and relatively low levels of neutrophil invasion (Figure 4.5.d). Additionally, colonic MPO activity in mice receiving DSS and treated with TNFα-TKNs (0.23 mg siRNAkg/day) was markedly reduced (Figure 4.5.g). Finally, as depicted in Figure 4, mice treated with TNFα-siRNA via TNFα-TKNs were significantly heavier after seven days than mice receiving DSS and other treatments. In contrast, mice receiving DSS and treated with TNFα-PLGA, TNFα-βGPs, Sc-TKNs, TNFα-DOTAP, and TNFα-βGPs showed all of the characteristics of DSS-induced inflammation as measured by histology, high levels of MPO activity, and significant weight loss (Figure 4.5 & Appendix A).

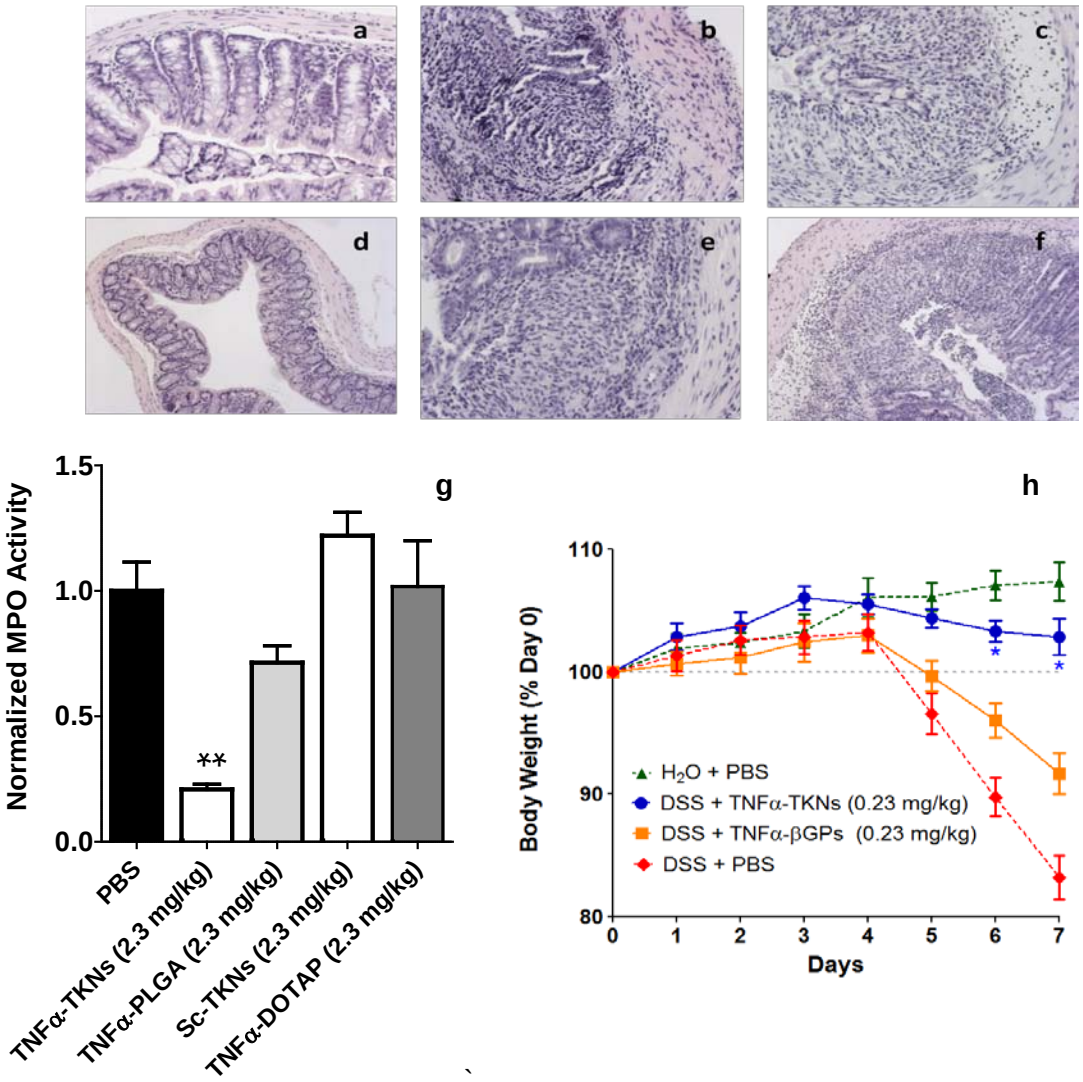


**Figure 4.5. Orally administered TNFα-TKNs protect mice from DSS-induced colitis**. (a) H&E-stained colon section from mice after seven days of receiving normal water and a daily oral gavage of PBS (20X). (b-f) H&E-stained colon sections form DSS-treated mice given a daily gavage of one of the following: (b) PBS, (c) Sc-TKNs (2.3 mg/kg), (d) TNFα-TKNs (0.23 mg/kg), (e) TNFα-PLGA (2.3 mg/kg), or (f) TNFα-βGPs (0.23 mg/kg) (20X). (g) Colonic MPO activity. Results are expressed as mUnits of MPO activity per mg protein and error bars represent ± s.e.m. Statistical significance was calculated using a one-way ANOVA and Bonferroni's post hoc test (**$p \leq 0.05$). (h) Time course of mouse body weight. Mouse body weight was normalized as a percentage of day zero body weight. Body weight depicted as the mean of each treatment group. Error bars represent ± s.e.m. Asterisk represents statistical significance from all other groups and was determined by a one-way ANOVA using Bonferroni's post hoc test (*$p \leq 0.05$).

## 4.5. Discussion

Numerous controlled release devices such as pellets, capsules, tables and sub millimeter sized spheres have been used for decades to ferry therapeutics through the GI system and delivery drugs specifically to the colon[182]. These devices are engineered to target the colon via various mechanisms, including pH changes, bacterial content, and residence time through the GI-system. These mechanisms are organ specific and thus unable to target physical stimuli specific to diseased colons. Furthermore, the macroscopic size of these carriers makes them susceptible to rapid GI clearance due to diarrhea, a common symptom of IBD[182]. Although drug delivery platforms in the sub-nanometer range have proven to have longer residence times in the GI systems of animals suffering from IBD, and are effective at delivering small molecules to treat intestinal inflammation, these nanoparticles systems are composed of polymers containing ester linkages, which are susceptible to enzymatic and hydrolytic cleavage in the gastrointestinal tract[183-185].

In this chapter, we describe a drug delivery platform that is able to target orally delivered siRNA to sites of diseased development via two distinct mechanisms. First, TKNs remain stable in the GI tract, thus preventing delivery to healthy GI tissues. Second, TKNs degrade in the presence of ROS, which can be as much as 100 times greater at sites of intestinal inflammation. Indeed, we have provided evidence that TKNs, and not nanoparticles formulated from ester-containing biomaterials, remain stable in fluids that resemble those of the GI system. Furthermore, ROS-mediated release results and targeting studies demonstrate that, when delivered orally, TKNs localize the delivery of siRNA to inflamed intestinal tissues.

Although it is unknown into which physiological compartment siRNA is released from the TKNs, based on our cell culture results, the pathophysiology of colitis, and the

formulation of TKNs, we hypothesize that both extracellular and intracellular ROS can initiate the release of therapeutically viable siRNA. Given the major source of inflammation-related ROS is produced by activated macrophages and neutrophils in the submucosal region of the colon, ROS-mediated damage to cellular luminal components such as tight junction proteins and membrane lipids is an exacerbating and persistent feature of colitis[12,186]. Furthermore, oxidation events on proteoglycans that compose the intestinal mucosa have also been documented in patients suffering from ulcerative colitis[14]. Based on these results, it is safe to assume that the dissemination of ROS away from the epithelium into the luminal compartment will results in TKNs degradation and subsequent siRNA release at locations distant from the epithelial surface. In an attempt to increase the efficacy of siRNA released into the lumen, prior to encapsulation in nanoparticles, we complexed siRNA oligos with the cationic lipid DOTAP, and then loaded these siRNA-DOTAP complexes into nanoparticles. Complexing siRNA with cationic species, such as DOTAP, enhances siRNA trasfection by increasing siRNA stability[187], internalization[188], mucosal transport[189], and endosomal escape[190,191]. Thus, at sites of intestinal inflammation, these DOTAP complexes are expected to act as a secondary delivery vehicle and thereby improve the efficacy of siRNA released from the TKNs in response to both intracellular and extracellular ROS.

Another major luminal boundary to siRNA delivery is the layer of 155 μM thick mucus that covers the intestinal epithelium. Although appearing homogeneous, the mucus layer covering the epithelium is actually stratified into regions of high-density near the epithelium, with pore sizes of less than 200nm, and a luminal low-density region, with pore sizes of greater than 1 μM[192]. Given that particle that can penetrate the low density region of the mucus are cleared more slowly from the intestines, we engineered siRNA-loaded TKNs to have diameters of ~600 nm. We hypothesized that this nanoparticle size would limit nonspecific uptake by enterocytes[193], yet still allow for

binding to inflamed colonic mucosa[194] and efficient uptake by phagocytes[190,195], which are exposed to the luminal space at sites of severe inflammation [196]. Furthermore, incorporating DOTAP endows nanoparticles with a net positive surface charge (Appendix A), which is known to increase particle uptake by phagocytes[195] and adhesion to the negatively charged intestinal mucosal surface[197].

Due to the low bioavailability of most orally administered drugs, oral administration is generally considered to be less toxic and safer than iv administration. Indeed, during the course of treatment, particles started to appear in the fecal matter of mice receiving formulation containing nanoparticles (data not shown). Reported studies with orally delivered radio labeled polystyrene nanoparticles have shown that less than 13% of orally delivered nanoparticles are actually taken up by intestinal tissues in healthy mice[192]. Although we anticipate this percentage is greater in inflamed intestinal mucosa, we hypothesize that the majority of nanoparticles pass through the animal without delivering siRNA. A discussion of strategies to improve the efficacy of the TKNs is provided in Chapter 6 of this thesis.

In another undocumented finding, after three days of therapy, the cages acquired the faint rotten egg odor that is distinctive of free thiols. Although the polymer is synthesized from di-thiol monomers, the polymerization traps these terminal thiols in thioketal linkages, which eliminates their odor. According to the reported mechanism for thioketal oxidation, PPADT degrades into acetone and the starting monomeric dithiol[198]. Thus, the faint odor of thiols in the animals' excrement is an indirect sign of particle degradation and subsequent clearance of the degradation products from the animals. Although the free thiols produced upon polymer degradation could undergo disulfide exchange with native proteins, disulfides produced in the lumen are more likely to react with free thiols in the luminal environment and be cleared from the body. Conversely, thiols are well-known scavengers of ROS, and thus the degradation products might also

be weakly anti-inflammatory. Further studies will need to be done with radio labeled polymers to determine the clearance rate and exit point of the polymers degradation products and un-degraded particles.

In this work, we performed a head-to-head comparison with another delivery vehicle reported to potentiate the oral delivery of siRNA, namely the β-glucan particles[199]. It is not surprising that the TKNs outperformed the β-glucan particles, which require 4 days of pre-dosing before being effective. Furthermore, β-glucan particles were designed to treat acute systemic inflammation, and thus are ill-suited to treat chronic diseases that are localized to a particular organ such as ulcerative colitis. At the lowest dose examined in this work, 0.23 mg siRNA $kg^{-1}day^{-1}$, TKNs were able abrogate the effects of DSS-induced colitis. These results suggest that orally delivered TKNs perform as well as current systemic delivery systems for siRNA that have been used to treat DSS-induced colitis, which required 2.5 mg siRNA$kg^{-1}48h^{-1}$ to achieve a similar level of colonic gene suppression[167].

Oral administration represents the most convenient and cost-effective means to deliver siRNA to diseased intestinal tissues, and thus has the potential to significantly increase the patient population treated via siRNA-based therapeutics. However, GI fluids, the intestinal mucosa, and cellular barriers to uptake represent significant obstacles for orally delivered siRNA. In this chapter, we present evidence that TKNs have the chemical and physical properties needed to overcome these obstacles and provide a therapeutic level of gene silencing in inflamed intestinal tissues. Indeed, elevated ROS levels are also associated with GI diseases that affect the proximal organs of the GI system, such as Crohn's Disease (small-intestine), stomach cancer, *H. pylori* infections (stomach), and pancolitis (proximal and distal regions of large intestine). Given the non-organ specific delivery mechanism of the TKNs, we anticipate TKNs will

find numerous applications in the treatment of other intestinal diseases linked to inflammation.

# Chapter 5: NF-κB-inhibiting Poly-CAPE nanoparticles Block Drug Resistance and Potentiate the effect of CPT-11

## 5.1. Abstract

Activation of nuclear factor-κB (NF-κB) results in the expression of numerous prosurvival genes that block apoptosis, thus mitigating the efficacy of chemotherapeutics[82]. Paradoxically, conventional therapeutics for cancer activate NF-κB, and in doing so initiate drug resistance[21]. Although adjuvant strategies that block NF-κB activation could potentiate the activity of chemotherapeutics in drug resistant tumors, clinical evidence suggests that current adjuvant strategies also increase apoptosis in non-malignant cells[48]. In this chapter, we present a nanoparticle, formulated from a polymeric NF-κB-inhibiting prodrug, that can target the chemotherapeutic irinotecan (CPT-11) to solid tumors, and thus abrogates CPT-11-induced drug resistance and inhibits tumor growth. In order to maximize the amount of NF-κB inhibitor delivered to tumors, we synthesized a novel polymeric prodrug, termed PCAPE, that releases the NF-κB inhibitor caffeic acid phenethyl ester (CAPE) as its major degradation product. Using a murine model of colitis-associated cancer[200] (CAC), we demonstrated that when administered systemically, CPT-11-loaded PCAPE-nanoparticles (CCNPs) are three times more effective than a cocktail of the free drugs at reducing both tumor multiplicity and tumor size. Given the central role played by NF-κB activation in drug resistance and inflammatory diseases, we anticipate numerous applications for CNPs.

## 5.2. Introduction

Despite access to advanced chemotherapeutics, patients in the United States suffering from CAC, have a five-year survival rate of less than 20%[77]. This extremely poor prognosis is due primarily to the poor clinical response of CAC to conventional chemotherapeutics. CPT-11 is currently considered the most effective drug for the treatment of CAC. Although CPT-11 is initially effective, most CAC tumors treated with CPT-11 develop resistance during the course of therapy[25]. Numerous studies have shown that CPT-11 activates NF-κB, which results in the expression of prosurvival genes that attenuate apoptosis, and thus abrogate the efficacy of CPT-11. For this reason, adjuvant strategies that inhibit NF-κB activation may potentiate the efficacy of CPT-11 on CAC tumors[24,26,201].

The NF-kB family of transcription factors is well established as regulators of genes that control immune and inflammatory function. Recently, activation of NF-κB has been shown to stimulate cell growth and inhibit apoptosis in a number of cancer cell lines. In its inactive form, NF-κB is sequestered in the cytoplasm by a family of NF-κB binding proteins called IκB. In response to activating stimuli, including cytokines and DNA-damaging agents, IκB is phosphorylated by the IκB kinase complex (IKK), which leads to IκB ubiquitination and subsequent degradation by the proteosome. The degradation of IκB liberates NF-κB allowing it to translocate to the nucleus, where it increases the expression of a variety of prosurvival genes, including Bcl-xL and survivin. In addition to inducing drug resistance, recent studies used a murine model of CAC to shown that NF-κB activation is necessary for tumorigenesis and tumor growth in CAC. These results are consistent with clinical data that indicate that NF-κB activation in the colons of patients suffering from colitis is an excellent predictor of CAC development.

By binding topoisomerase I to DNA, CPT-11 generates irreversible damage to DNA during cell replication, causing cell cycle arrest and touching off a chain reaction of

pro-apoptotic signaling pathways[202]. Although the exact mechanism by which the DNA damage caused by CPT-11 activates NF-κB is unknown, CPT-11-induced apoptosis results in an accumulation of reactive oxygen species (ROS), a known NF-κB activator, as well as the activation of IKK. Several studies have demonstrated the ability of various NF-κB inhibitors to potentiate CPT-11 in colon cancer cell lines and preclinical studies of CRC[22-24,201]. Although these studies achieved impressive levels of sporadic CRC tumor growth inhibition, they employed NF-κB inhibitors that either have toxicities that are likely to limit their clinical application, or have since been shown to be ineffective in human trials[203,204]. Furthermore, since CAC tumors are known to have higher levels of constitutive NF-κB activation compared to sporadic CRC tumors, CAC tumors are more difficult to treat, and thus often do not respond to the same treatment regimen used to treat sporadic CRC[69].

NF-κB inhibitors should be non-toxic, effective, and clinically viable. Numerous food-derived polyphenols are effective inhibitors of NF-κB, pharmacologically safe, and currently marketed as food supplements. Caffeic acid phenethyl ester (CAPE), a biologically active ingredient in bee's wax, is a well-known inhibitor of NF-κB that has demonstrated efficacy in numerous animal models of inflammatory diseases[106,124,128,131,140,152,205-207]. Studies have demonstrated that, as a standalone therapeutic, CAPE inhibits the proliferation of various cancer cell lines by inhibiting NF-κB, but is innocuous to normal cells. CAPE has also been shown to be tumor suppressive in preclinical studies; however, its efficacy as an adjuvant therapeutic has yet to be examined *in vivo*.

Despite CAPE's numerous beneficial properties, its relatively moderate activity coupled with its extremely poor water solubility make it difficult to achieve and maintain therapeutic concentrations in the blood compartment. Furthermore, it is likely that the combination of CAPE and CPT-11 will suffer from a universal problem plaguing all NF-

κB inhibitor/chemotherapy cocktails—the increased toxicity cause by inhibiting NF-κB in non-malignant cell types that are susceptible to chemotherapeutics.

Our goal was to develop a robust delivery platform that could overcome the above limitations by targeting therapeutic concentrations of CAPE and CPT-11 to tumors. Prior to selection of materials and delivery vehicle design, we defined performance parameters applicable to almost any solid malignancy, not just CAC. These requirements included the ability to target solid tumors, simultaneously deliver CAPE and CPT-11, resist hepatic clearance, and sustain a therapeutic concentration of the therapeutics in the tumor microenviroment between doses. Given their ability to passively accumulate in tumors[208], deliver multiple therapeutics[209], and serve as controlled release drug depots[210], polymeric nanoparticle are an attractive platform for the delivery of CAPE and CPT-11. However, the high doses of CAPE (70 - 500 $mg^{-1}$ $kg^{-1}$ $wk^{-1}$) required to inhibit NF-κB *in vivo* precluded the use of nanoparticle formulations that require an excessive amount of polymer to form a stable matrix around the drug.

In order to formulate hyper-loaded nanoparticles that can deliver the quantity of CAPE reported to be required to inhibit NF-κB, we synthesized a polymeric CAPE prodrug (PCAPE) that releases CAPE as its major degradation product. Particles formulated from PCAPE, termed CAPE nanoparticles (CNPs), are composed of 65 % CAPE and can be loaded with CPT-11 using standard protocols. In this chapter, the ability of the NF-κB inhibitor CAPE to improve the efficacy of CPT-11 on HT-29 cancer cells was examined and a mechanism for improved efficacy suggested. Polymers that incorporate the NF-κB inhibitor CAPE into their backbone were synthesized and characterized. CPT-11-loaded nanoparticles formulated from PCAPE (CCNPs) were generated and characterized. Finally, the efficacy of CCNPs versus appropriate controls was assessed in a preclinical murine model of CAC.

## 5.3. Materials and Methods:

Unless stated otherwise all chemicals were obtained from Sigma.

### 5.3.1. Synthesis of caffeic acid phenethyl ester (CAPE) (6)

To a solution of caffeic acid **(4)** (1.98 g) in 25 ml of hexamethylphosphoramide (HMPA), 2.28 ml of 25% NaOH was added. After stirring for 1 h, a solution of β – bromoethylbenzene **(5)** (5.7 ml) in 10 ml HMPA was added dropwise with a separatory funnel and the solution was stirred for 52 h at rt. The reaction mixture was then poured into ice water (50 ml), and the product was extracted with diethylether (2350 ml). The ether extract was washed successively with 1 N HCl (20 ml) and water (20 ml), dried over $MgSO_4$ (10—15 g), and evaporated under vacuum. The product dissolved in ether was chromatographed on a silica gel column (150 g), eluted with $CHCl_3$ and then with increasing proportions of ethyl acetate. The fraction eluted with 30% ethyl acetate contained the desired product.

### 5.3.2. Synthesis of (CAPE-DPA) (8):

CAPE **(6)**, pyridine, and a catalytic amount of DMAP were added to DMF (ml) and stirred at 0°C. After 1 h, penenoic anhydride **(7)** was added drop-wise to the stirred solution. The reaction mixture was allowed to come to r.t. and stirred overnight before being reduced to 25% of its original volume via rotary evaporation. The concentrated reaction mixture was then poured into a mixture of ice and sodium bicarbonate and extracted 3 X with DCM. The combined organic phases were washed with water and dried over $Na_2SO_4$. The crude product was evaporated onto silica gel and purified via flash silica gel chromatography by eluting with hexanes and then with increasing proportions of DCM. The fraction eluted with 30% DCM contained the desired product, **(8)**.

### 5.3.3. Synthesis of PCAPE (9):

CAPE-DPA **(8)** and 1st generation Grubbs Catalyst were added neat to a 15 ml flask equipped with a condenser and vacuum adapter and stirred immediately at 70°C under light vacuum. After 6 h, the reaction mixture became too viscous to stir, at which time 0.5 ml of degassed distilled toluene were added to the flask to liberate the stir bar. After the initial addition of toluene, 0.5 ml of toluene were added every 6 h to replace the toluene removed by the vacuum. After 18 h, the reaction was added to methanol and and cooled to -20°C. Once the polymer had precipitated from the mixture, the methanol, unreacted monomers, and Grubbs Catalyst were decanted and the remaining precipitated polymer was concentrated under vacuum.

### 5.3.4. CAPE nanoparticle formulation

Nanoparticle coated in the pluronic F-127 were formulated via a typical solvent displacement procedure. A solution of tetrahydrofurane (THF) containing 1.0 % CAPE and 0.15% CPT-11 (w/v) was slowly added to 20 equivalents of rapidly stirred pH 6.5 PBS via a syringe pump to form a semi-stable emulsion. After 30 min of stirring, the emulsion was then transferred to a 250 ml flask and the THF was removed via rotary evaporation under reduced pressure. Next, the flask was transferred to a stir plate and the solution containing the now hardened particles was stirred at a moderate rate while an equal volume of a 0.2% solution of F-127 in PBS (pH7.4) was slowly poured into the particle solution. The solution was allowed to stir for an hour to allow the pluronic to adsorb to the surface of the particles. The particles were then transferred to ultra centrifuge tubes (Beckman Coulter), and centrifuged at 42,000 RPM and 4°C for 30 min. The supernatant was then decanted and the particles were resuspended in PBS (pH 7.4) and re-centrifuged as before. After the second centrifugation, the particles were

resuspended in a 0.01% solution of glucose in DI water, flash frozen in liquid nitrogen, and then lyophilized overnight (Labconco). The particles were recovered from the lyophilizer as a gray powder and stored at – 20°C. Empty nanoparticles were prepared as described above with the exception of the CPT-11 in the organic phase. Particle size was measured via dynamic light scattering (Brookhaven Instruments Corporation), and morphology was assessed via SEM (Hitachi).

5.3.5. Colitis associated cancer tumor induction and treatment.

CAC was induced as previously described, with some modifications [211]. C57BL/6 Mice (Jackson Laboratories) were intraperitoneally injected with AOM (10 mg $kg^{-1}$) and maintained on regular diet and water for 7 days. The mice were then subjected to 3 cycles of DSS treatment, in which each cycle consisted of 2.5% DSS for 7 days followed by a 14-day recovery period with regular water. After the final recovery period, mice received four weekly intravenous *(iv*) tail vein injections containing 200 µl of either a 10% solution of ethanol in PBS (v/v) or a 10% solution of ethanol in PBS containing one of the following therapeutics: empty CNPs (62.8 mg $kg^{-1}$ $wk^{-1}$), unencapsulated CPT-11 (8.0 mg $kg^{-1}$ $wk^{-1}$) and unencapsulated CAPE (40.8 mg $kg^{-1}$ $wk^{-1}$), CNPs loaded with a "low" dose of CPT-11 (62.8 mg $kg^{-1}$ $wk^{-1}$ of particles containing 2.0 mg $kg^{-1}$ $wk^{-1}$ CPT-11), and CNPs loaded with a "high" dose of CPT-11 (62.8 mg $kg^{-1}$ $wk^{-1}$ of particles containing 8.0 mg $kg^{-1}$ $wk^{-1}$ CPT-11). Two weeks after the final injection, the mice were sacrificed and the colon tissues were taken for further analysis.

5.3.6. Immunofluorescence

HT-29 cells were seeded in 8-well glass chamber slides (Lab-Tek™, Thermo Scientific) at 3.0 X $10^5$ cells $ml^{-1}$ in media prepared as described above. After 48 h, cells received media containing either 80 µM CPT-11, 80 µM CPT-11 and 80 µM CAPE, or

DMSO. Cells were treated for a total of 4 h, and then washed 3 X with 0.01% Tween in TBS (0.01% TBST) and incubated with a 4% solution of paraformaldehyde in PBS for 20 min. After 20 min, the cell were washed 3 X with 0.01% TBST before being incubated in 1% TBST at 37°C for 30 min. The slides were then allowed to cool for 10 minutes before being washed 3X with 0.01% TBST and incubated in Immunohistochemistry blocking buffer (Bethyl Labs INC.) for 30 min. The blocking buffer was removed via aspiration, and anti-rabbit primary antibodies suspended in primary antibody dilution buffer (Bethyl Labs INC.) were added directly to the cells. After 1 h, the primary antibody solution was removed, and the cells were washed 3X with 0.01% TBST, before being incubated at r.t. with primary antibody dilution buffer containing a fluorescent goat anti-rabbit antibody. After 30 min, the secondary antibody solution was removed from the cells, and the cells were washed 3X with 0.01% TBST. The medium chamber was then removed from each slide and a small amount of VECTASHIELD mounting medium with DAPI (Vector Laboratories) was added to each well before a cover slip was placed over the slide and sealed with Laque Brillance Extreme (Coco Chanel). Images were acquired using an LSM 700 laser scanning confocal microscope (Carl Zeiss Micro Imaging) running Zen image acquisition software (Carl Zeiss Micro Imaging).

5.3.7. Immunohistochemistry.

5-µm paraffin-embedded tissue sections were deparaffinized in xylene, incubated in 3% hydrogen peroxide in methanol for 30 minutes, rehydrated in decreasing concentrations of ethanol (100, 95, 70%), and then treated with 10 mM sodium citrate buffer (pH 6.0) containing 0.05% Tween 20 at 120°C for 10 minutes in a pressure cooker. Sections were blocked with 2% nonfat dry milk and 0.01% Tween 20 in PBS for 1 hour at 37°C, and then incubated with anti-Ki67 (Novocastra) overnight at 4°C. After washes with PBS containing 0.01% Tween 20, sections were treated with appropriate

biotinylated secondary antibodies for 30 minutes at 37°C, and color development was performed using the Vectastain ABC kit (Vector Laboratories). Sections were then counterstained with hematoxylin, dehydrated, and coverslipped. Images were acquired using a Zeiss Axioskop 2 plus microscope (Carl Zeiss Micro Imaging) equipped with an AxioCam MRc5 CCD camera (Carl Zeiss USA).

5.3.8. Real time RT-PCR

Total RNA was extracted from mouse colons using TRIzol (Invitrogen). A reverse transcription (RT) reaction was performed on 2 µg of each sample and an oligo-dT primer, using a RETROscript® System (Ambion Inc.). Next, 10 ng of reverse-transcribed cDNA, 400 nM of gene-specific primers, and the iQ SYBR Green Suppermix (Biorad) was amplified at 50°C for 2 min and 95°C for 10 min, followed by 40 cycles of 95°C for 15 s and 60°C for 1 min. The 36B4 expression levels were used as reference, and fold-induction was calculated by the Ct method as follows: $\Delta\Delta CT=(Ct_{Target} - Ct_{36B4})_{DSS+Treatment} - (Ct_{Target} - Ct_{36B4})_{DSS+ PBS}$. Thus producing results normalized against mice receiving DSS and treated with PBS. The final data were then derived from $2^{-\Delta\Delta CT}$. The primers used were designed using the Primer Express Program (Applied Biosystems) and were as follows: TNFα sense 5'-AGG CTG CCC CGA CTA CGT-3' antisense 5'-GAC TTT CTC CTG GTA TGA GAT AGC AAA-3'; IL-1β sense 5'-TCG CTC AGG GTC ACA AGA AA-3' antisense 5'-CAT CAG AGG CAA GGA GGA AAA C-3'; IL-6 sense 5'-ACA AGT CGG AGG CTT AAT TAC ACA T-3' antisense 5'-TTG CCA TTG CAC AAC TCT TTT C-3'; IFN-γ sense 5'-CAG CAA CAG CAA GGC GAA A -3' antisense 5'-CTG GAC CTG TGG GTT GTT GAC -3'.

## 5.4. Results

### 5.4.1. CAPE potentiates the efficacy of CPT-11

In order to demonstrate the ability of CAPE to induce chemo-sensitivity in the drug resistant cell line HT-29, we treated HT-29 cells with CPT-11, CAPE, or the combined therapeutics then assayed the cells for the surface presentation of phosphatidylserine, a known marker for apoptosis, via FACS.

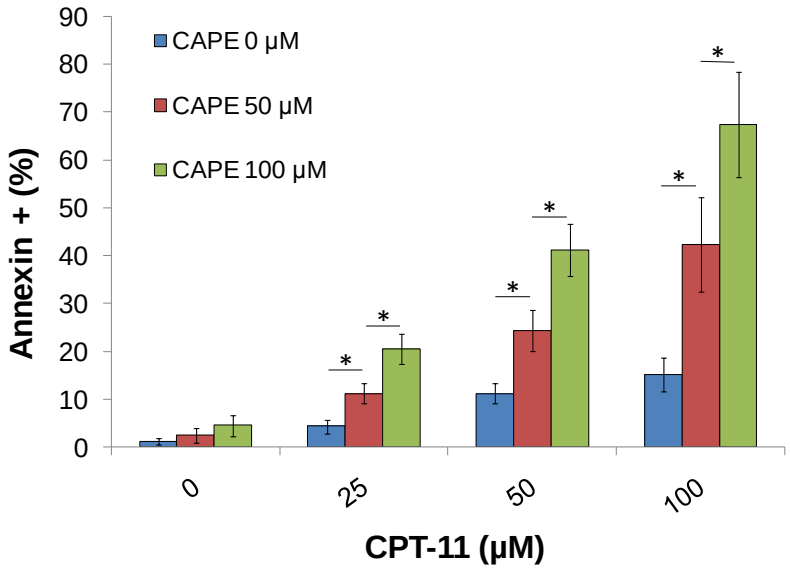


**Figure 5.1. CAPE potentiates the activity of CPT-11.** HT-29 cells were treated with various amounts of CAPE and CPT-11 for 48 h then stained with annexin V and analyzed via FACS. Results presented as median percentage of annexin V positive cells ± s.d. for n = 4 replicates per group. Statistical differences determined by one-way ANOVA using Bonferroni's post hoc test (*$p \leq 0.05$).

Quantification of apoptosis in cells treated with either CAPE or CPT-11 (Figure 5.1) showed that there was no significant difference in apoptosis between the 3 doses of CAPE, and only a moderate increase in apoptosis when the CPT-11 concentration was increased from 25 µM to 50 µM. However, further increasing the CPT-11 concentration from 50 µM to 100 µM had no significant affect on apoptosis. Importantly, at each one of the CPT-11 concentrations studied (i.e. 25, 50,100 µM), there was a significant increase

in apoptosis that correlated with CAPE concentration. For example, at 50 µM CPT-11, the addition of 50 and 100 µM CAPE resulted in a 2.2 and 3.5-fold increased in apoptosis over compared to cells treated with CPT-11 only.

Given that CPT-11 induces drug resistance by activating NF-κB, we assessed nuclear NF-κB levels in HT-29 cells treated with CPT-11, CAPE, or the combined therapeutics. Figure 5.2 shows the fold increase in nuclear NF-κB over the level of nuclear NF-κB in untreated cells. (e.g. a value of 1.0 represents no increase in NF-κB as compared to the untreated cells) Cells treated with CPT-11 at 50 and 100 µM experienced a 1.8 and 3-fold increase in nuclear NF-κB, respectively.

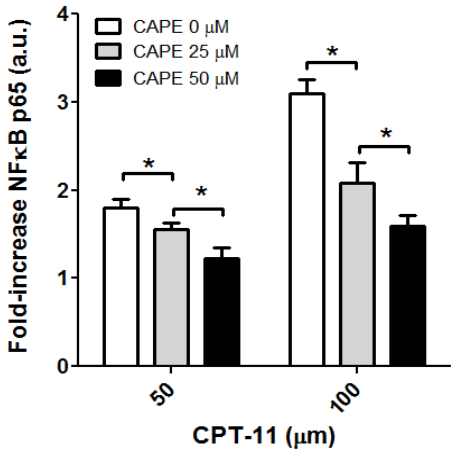


**Figure 5.2. CAPE reduces CPT-11-induced NF-κB activation in HT-29 cells.** HT-29 cells were treated with various amounts of CAPE and CPT-11 for 4 h then analyzed for nuclear NF-κB content via ELISA. Results presented as median fold increase in nuclear NF-κB over nuclear NF-κB levels of untreated cells ± s.e.m. for n = 4 replicates per group. Statistical differences determined by a one-way ANOVA using Bonferroni's post hoc test (*$p \leq 0.05$).

However, at both of the CPT-11 concentrations examined, adding CAPE to the regimen resulted in a significant decrease in the amount of nuclear NF-κB. For example, adding CAPE at a concentration of 25 and 50 µM to cells treated with CPT-11 at 100 µM, resulted in a 30% and 43% decrease in nuclear NF-κB, respectively.

In order to confirm the results obtained by ELISA, NF-κB nuclear localization was visualized in HT-29 cells that had been treated with CPT-11 alone and in combination with CAPE. In cells treated with CPT-11 (50 μM), NF-κB was localized to the nucleus as indicated by the co-localization of the signal for NF-kB (Figure 5.3, panel a & c) and nuclear DNA (Figure 5.3, panel b & c). However, HT-29 cells treated with CPT-11 (50 μM) and CAPE (100μM) showed cytoplasmic sequestration of NF-kB (Figure 5.3, panel d & f), indicative of NF-κB inhibition.

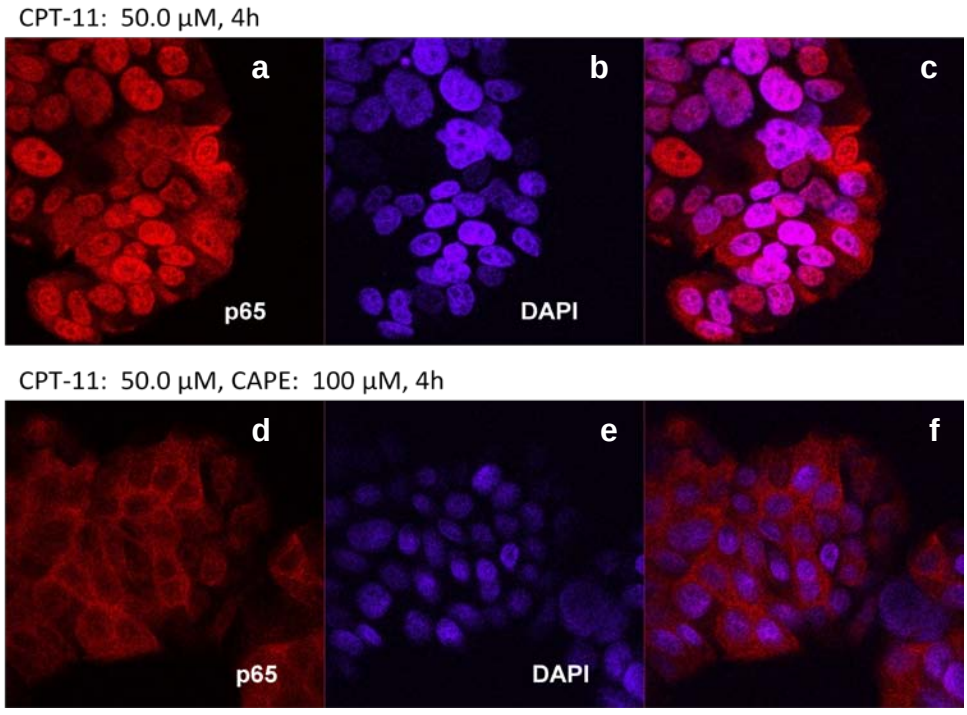


**Figure 5.3. CAPE decreases CPT-11-mediated nuclear localization of the NF-κB subunit p65:** HT-29 cells treated with CPT-11 (50μM) alone (upper panels) or in conjunction with CAPE (100 μM) (lower panels) for 4 h were immunostained for the p65 subunit of NF-κB (red) and for genomic DNA (blue) then imaged by confocal microscopy. (a – c) Confocal microscopy clearly indicates that CPT-11 initiates the nuclear localization of NF-κB. (d – f) In contrast, NF-κB remained sequestered in the cytosol of cells treated with CPT-11 and the NF-κB inhibitor CAPE.

### 5.4.2. PCAPE polymers are designed to release CAPE upon degradation

Given CAPE's relatively low activity, we decided to maximize CAPE encapsulation within nanoparticles by synthesizing a polymer that contained CAPE in its backbone. PCAPE was synthesized via the synthetic pathway shown in Figure 5.4.a

This synthetic strategy produced CAPE polymers with molecular weights $M_w$ ~ 7.5 kDa at an overall yield of 23%.

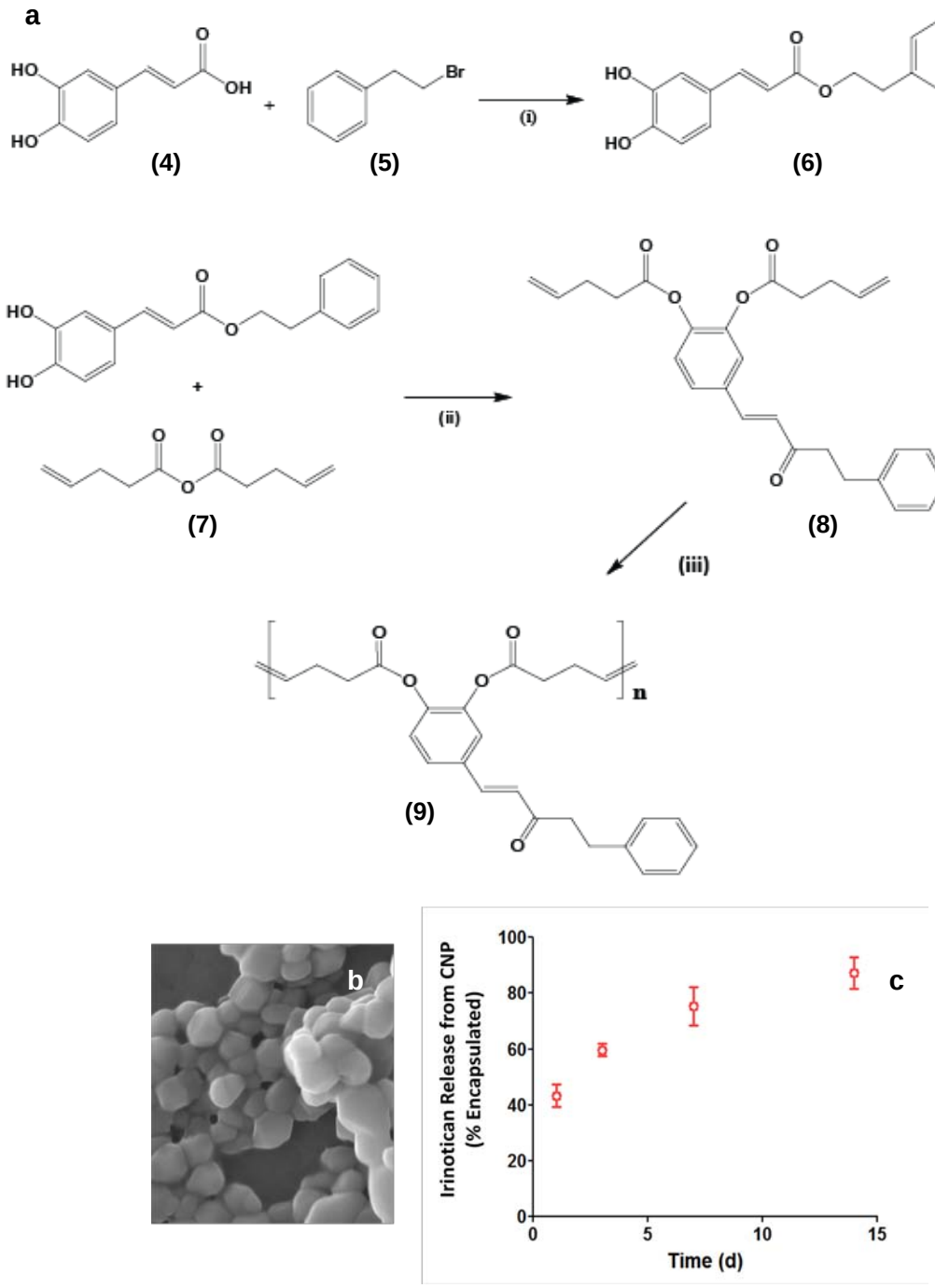


**Figure 5.4. Synthesis of PCAPE and characterization of CNPs.** (a) (i) hexamethyl-phosphoramide (HMPA), NaOH, 54 h; (ii) pyridine, DMAP, DMF 1h; (iii) Grubb's Catalyst (neat) 1h, toluene 20 h. (b) SEM image of CNPs (c) % Irinotecan (CPT-11) released from CCNPs as a function of time. Results represented as the % of encapsulated irinotecan released ± s.e.m. for n = 3 replicates.

PCAPE was used to formulate CNPs, and CCNPs via a solvent displacement method (Figure 5.4.b). In order to verify the deposition of pluronic F-127 on the surface of the particles, CNPs were made with and without F-127 and sized via DLS before lyophilization. CNPs coated with F-127 had an average diameter of ~180 nm, and CNPs without had an average diameter of 130 nm. The distribution of both particle formulation were symmetric about the mean, indicating that the increase in size was not the result of particle aggregation[212,213]. Irinotecan (CPT-11) release studies (Figure 5.4.c) performed in PBS pH 7.4 show that 12 % CCNPs (12 wt % CPT-11) release their payloads over a 14 day period, with an approximate half-life of 2.3 days.

5.4.3. CCNPs reduce tumor multiplicity and tumor size

To assess the efficacy of CCNPs we treated mice bearing AOM-induced tumors with CCNPs and appropriate controls. Prior to treatment, colon tumor formation was verified via colonoscopy as shown in Appendix B. Tumor-bearing mice received one of the following therapies via weekly tail vein injection: CNPs containing either 4 or 12 % CPT-11 as a percentage of total particle weight (4% CCNP: 3.0 mg $kg^{-1}$ $wk^{-1}$ CPT-11; or 12% CCNP: 9.0 mg $kg^{-1}$ $wk^{-1}$ CPT-11), empty CNPs (CNPs), a solution containing the free CAPE and CPT-11 (CAPE + CPT-11), or a solution of ethanol in PBS (Vehicle). It should be noted that each formulation containing CAPE in either its free or polymeric form (i.e. 4% CCNPs, 12% CCNPs, CNPs, CAPE + CPT-11) contained the same amount of CAPE. As shown in Figure 5.5, both 4% CCNPs and 12% CCNPs elicited a significant reduction in colonic tumor number and tumor load as compared to vehicle treated mice. Mice receiving 12% CCNP had less than half as many tumors as vehicle treated mice and over 40% fewer tumors than mice treated with a solution containing an equivalent amount of free CAPE and CPT-11 (i.e. CAPE + CPT-11). Although the free

drugs were able to achieve a significant reduction in tumor load compared to vehicle treated animals, the free drugs did not significantly decrease tumor multiplicity. Importantly, although mice treated with 4% CCNPs were administered 1/3 the CPT-11 contained in the free drug formulation, 4% CCNPs generated a significant reduction in both tumor load and tumor number.

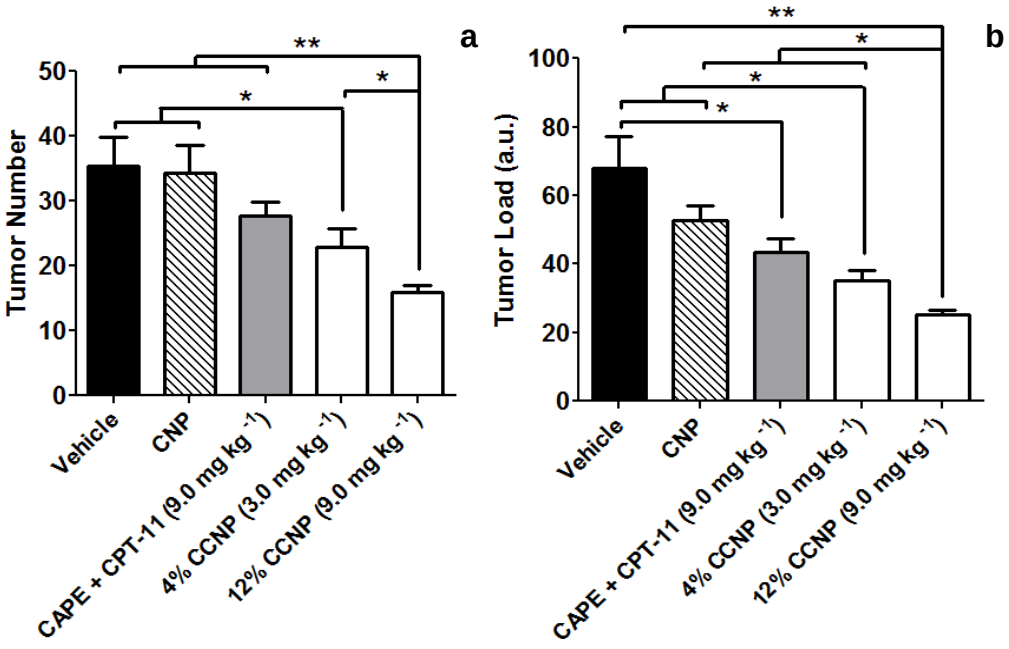


**Figure 5.5. CPT-11 loaded-CNPs reduce both the multiplicity and size of tumors in mice bearing AOM-induced colon tumors.** Mice bearing AOM-initiated colon tumors were treated with either empty CNP, a solution of free CAPE and CPT-11 (9.0 mg $kg^{-1}$ $wk^{-1}$ CPT-11), 4% CCNPs (3.0 mg $kg^{-1}$ $wk^{-1}$ CPT-11), or 12% CCNPs (9.0 mg $kg^{-1}$ $wk^{-1}$ CPT-11) via tail vein injection for 4 weeks. (a) The number of tumors present in the colons of mice bearing AOM-induced tumors after 4 weeks of treatment. Results depicted as mean tumor number per animal ± s.e.m. for n = 6 mice per treatment group. (b) Average tumor load per animal. Tumor load is calculated as the sum of the volumes of the tumors in a single animal. Results depicted as mean tumor load per animal ± s.e.m. for n = 6 mice per treatment group. Statistical differences in Figures a-d determined by a one-way ANOVA using Bonferroni's post hoc test (*$p \leq 0.05$, **$p \leq 0.01$).

Figure 5.6 displays representative photographic images of colons taken from a tumor-bearing mouse on the initial day of treatment (i.e. T-day 0) and images taken from the colons of tumor-bearing mice after receiving 4 weeks of treatment (i.e. T-day 28). As

shown in Figure 5.6.a, and in accordance with cited literature, the model of CAC used in this work generated clumps of tumors primarily in the distal and medial portions of the colon[214]. After 4 weeks, the colons of vehicle treated mice were festooned with tumors (Figure 5.6.b).

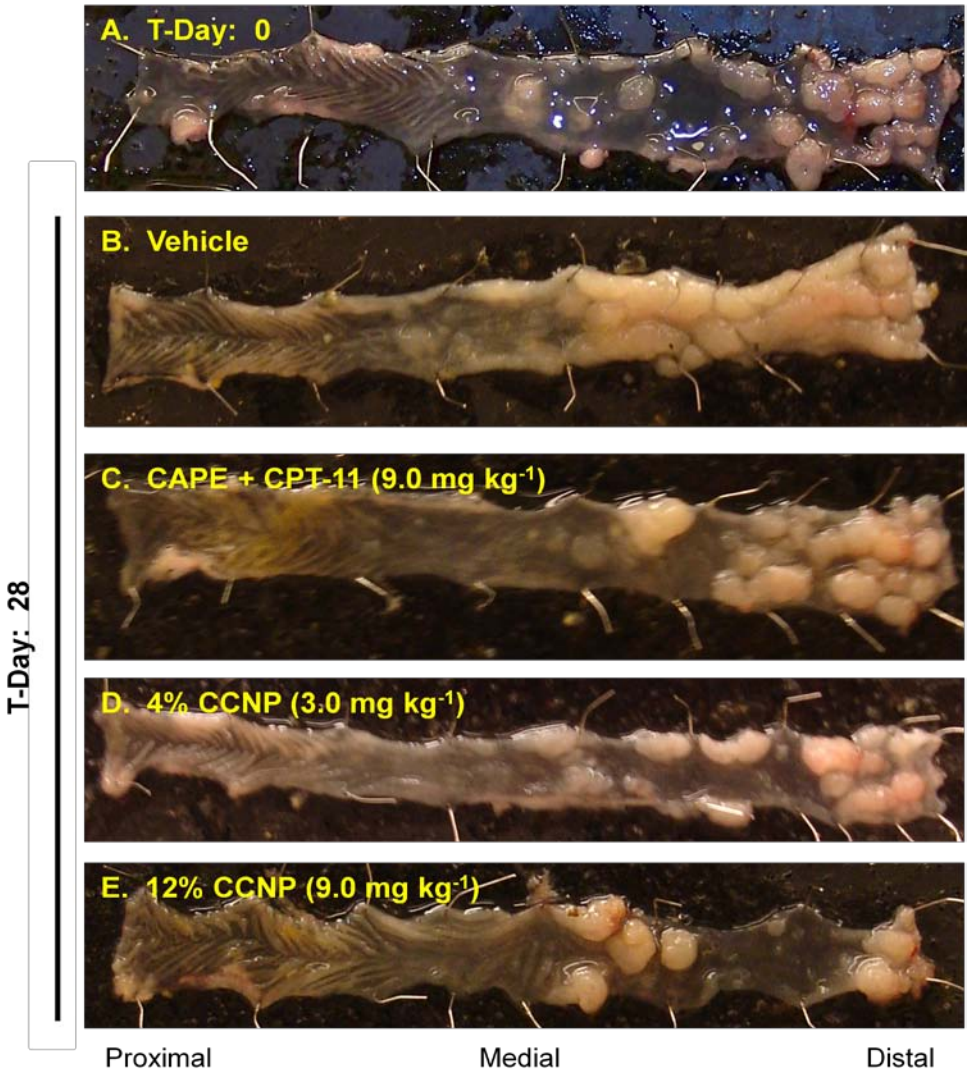


**Figure 5.6. Representative photographic images of tumor bearing colons taken from mice before and after 4 weeks of treatment.** (a) before receiving treatment; (b) vehicle treated colon after 4 weeks; (c) CNP treated colon after 4 weeks; (d) free CAPE and free CPT-11 treated colon after 4 weeks (e) 4% CCNPs treated colon after 4 weeks; (f) 12% CCNPs treated colon after 12 weeks. Colons treated with 12% CCNPs closely resembled the colons from mice receiving no therapy on the first day of treatment, (i.e.T-Day: 0) and had markedly fewer tumors than mice receiving other treatments.

However, the colons of mice treated with 12% CCNPs closely resembled the colons from mice receiving no therapy on the first day of treatment, (i.e.T-Day: 0) and had markedly fewer tumors than mice receiving other treatments.

### 5.4.5. CNPs and CCNPs inhibit NF-κB activation in tumors

In an effort to elucidate the mechanisms through which the encapsulation of CPT-11 in CNPs improves the efficacy of the combination of CAPE and CPT-11, we assessed the concentration of nuclear NF-κB in tumor samples taken from mice treated as described above. Total nuclear protein was isolated from tumor samples and assayed for NF-κB content via ELISA. Results in Figure 5.7 represent nuclear NF-κB concentration relative to the nuclear NF-κB concentration of vehicle treated mice. Tumors from animals treated with CNP, 4% CCNPs, and 12% CCNPs had significantly lower levels of nuclear NF-κB as compared to animals treated with the vehicle or the free drugs. Interestingly, animals treated with a solution of CAPE and CPT-11 had significantly higher levels of nuclear NF-κB compared to vehicle treated animals.

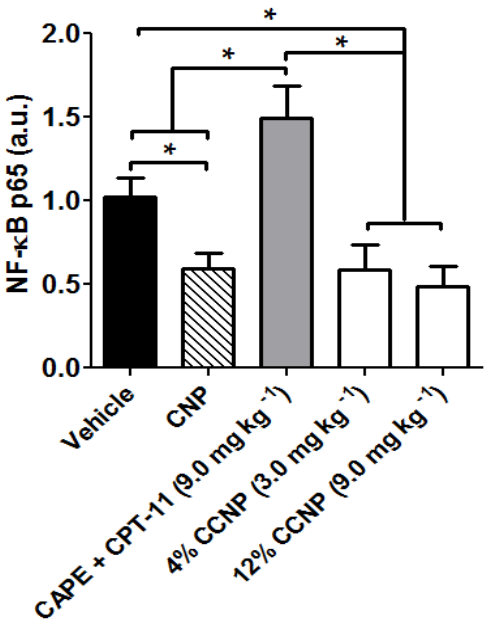


**Figure 5.7. CNPs suppress NF-κB activation in AOM-induced tumors.** Mice bearing AOM-initiated colon tumors were treated with either empty CNP, a solution of free CAPE and CPT-11 (9.0 mg $kg^{-1}$ $wk^{-1}$ CPT-11), 4% CCNPs (3.0 mg $kg^{-1}$ $wk^{-1}$ CPT-11), or 12% CCNPs (9.0 mg $kg^{-1}$ $wk^{-1}$ CPT-11) via tail vein injection. Relative nuclear concentration of the p65 subunit of NF-κB was determined via ELISA. Results depicted as the mean relative NF-κB concentration per mouse ± s.e.m. for n=6 mice. Statistical differences determined by a one-way ANOVA using Bonferroni's post hoc test (*$p \leq 0.05$).

### 5.4.6. CCNPs deplete tumorigenic and drug resistance mRNA

The nuclear localization of NF-κB results in the expression of numerous proinflammatory and prosurvival genes that induce tumor proliferation, metastasis and thwart the activity of apoptosis-inducing chemotherapeutics, including CPT-11. We performed qPCR to quantify the tumor mRNA levels of genes known to induce cancer proliferation and drug resistance. Tumors from animals treated with both 4% and 12% CCNPs had significantly lower proinflammatory mRNA levels than mice treated with the vehicle or a solution of the free drugs. The results for cytokine mRNA levels were echoed in the analysis of prosurvival mRNA levels. These results show that only formulations containing nanoparticles (i.e. CNPs, 4% CCNP, and 12% CCNP) significantly reduced both Bcl-xL and survivin mRNA compared to vehicle treated mice.

Tumor survivin mRNAs were 65% and 70 % lower in mice treated with 12% CCNPs compared to mice treated with the vehicle or the free drugs, respectively. Interestingly, the addition of free CAPE was unable to reduce the mRNA levels of these pro-tumorgenic and prosurvival genes.

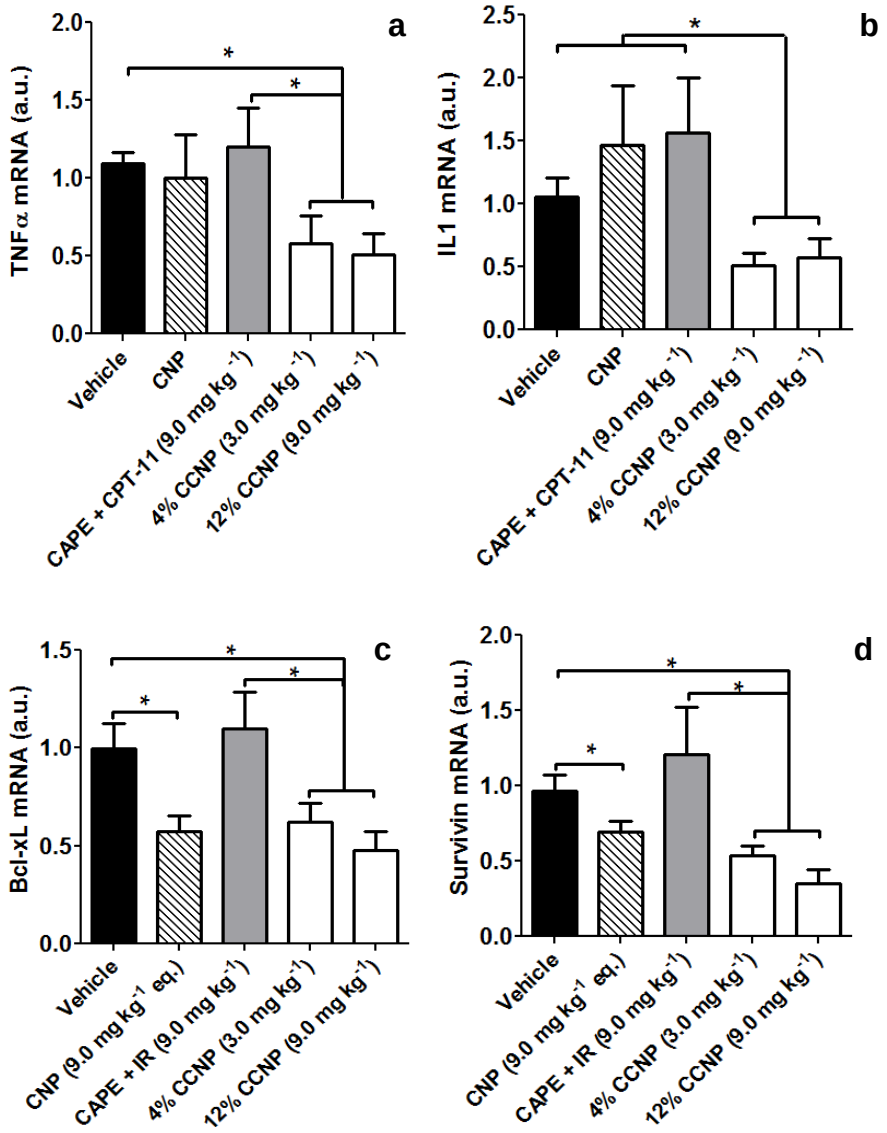


**Figure 5.8. CCNPs reduce the tumor mRNA levels of gene known to promote tumorigenesis and drug resistance.** Mice bearing AOM-initiated colon tumors were treated with either empty CNP, a solution of free CAPE and CPT-11 (9.0 mg $kg^{-1}$ $wk^{-1}$ CPT-11), 4% CCNPs (3.0 mg $kg^{-1}$ $wk^{-1}$ CPT-11), or 12% CCNPs (9.0 mg $kg^{-1}$ $wk^{-1}$ CPT-11) via tail vein injection. (a - d) Tumor mRNA levels for various genes up regulated by NF-κB activation that are known to promote tumorigenesis (i.e. TNF α and IL-1) and drug resistance (i.e. Bcl-xL and survivin). Results depicted as mean mRNA level ± s.e.m. for n = 6 mice per treatment group. Statistical differences in Figures a - d determined by a one-way ANOVA using Bonferroni's post hoc test (*$p \leq 0.05$).

### 5.4.7. CNP nanoparticles passively accumulate in AOM-induced tumors

Mice bearing AOM-induced tumors were administered CNPs loaded with the near-infrared dye IR-780 (CNP-780) or free IR-780. After 48 h, the colons of these mice were harvested and analyzed for fluorescence. Qualitative analysis of the fluorescent images taken of colons treated with CNP-780 and IR-780 shows that the colons from animals treated with CNP-780 (Figure 5.9. a, left panel) produce considerably more fluorescent signal than the colons taken from animals treated with the free dye (Figure 5.9 a, right panel). Furthermore, the colons of animals treated with CNP-780 exhibit punctuate high intensity fluorescence that is coincidental with sites of tumor development. Integration of the fluorescent intensities of the colons indicate a more than 15-fold increase in colonic fluorescence in mice treated with CNP-780 as compared to those treated with free IR-780. Analysis of the other organs typically affected by chemotherapeutics (Figure 5.9.c & d) revealed relatively low levels of fluorescent intensity in the spleen kidney heart and lungs of mice treated with CNP-780.

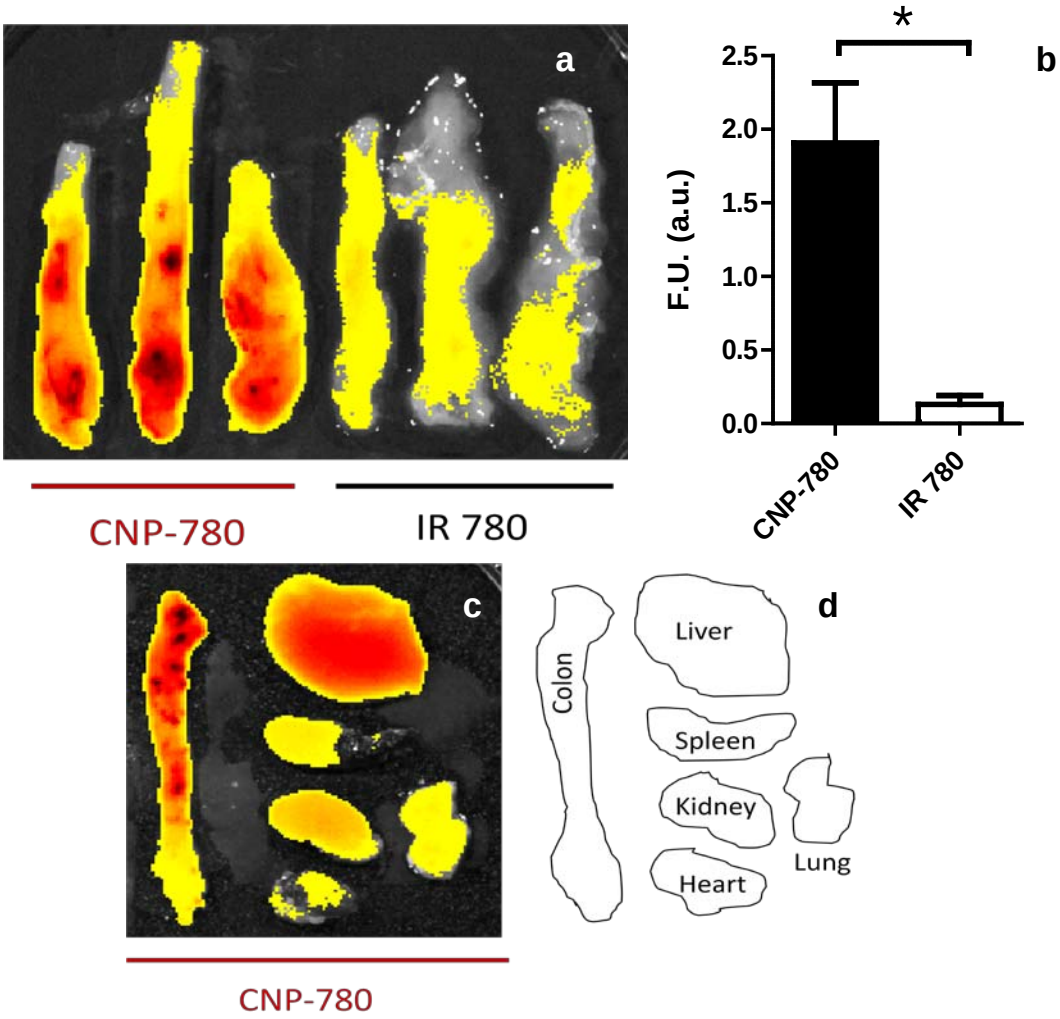


**Figure 5.9. CNPs localize the delivery of encapsulated agents to AOM-induced tumors.** Mice bearing AOM-initiated colon tumors were treated with either CNPs loaded with the near-IR dye IR-780 (CNP-780) or an equivalent amount of free IR-780. After 48 h, the colons of these animals were analyzed for fluorescence. (a) Fluorescent imaging of colons bearing AOM-induced tumors and treated with CNP-780 (left) and free IR-780 (right). (b) Integration of fluorescent intensities of the colons pictured in panel a. Colons treated with CPT-780 experienced a nearly 15-fold increase in fluorescence compared to animals treated with IR 780. Results depicted as average fluorescence ± s.e.m. for n = 3 samples. Statistical differences in panel b determined by student t-test (*$p \leq 0.01$). (c) Representative image sowing relative fluorescent intensities of various organs. (d) Organ map for panel c.

## 5.5. Discussion

NF-κB activation has been shown to be the principle mechanism for drug resistance in many different tumor cells lines and primary tumor samples[80,215]. Ironically, many anticancer agents that induce apoptosis, such as CPT-11, also activate NF-κB,

and in so doing deplete their own efficacy[22,23]. Numerous cell culture and preclinical studies have demonstrated that inhibiting NF-κB potentiates the efficacy of CPT-11. Despite the convincing evidence describing the synergy between NF-κB inhibition and CPT-11 in the treatment of CRC, there has yet to be a successful clinical trial that has used an NF-κB inhibitor in concert with CPT-11 to treat CRC.

Clinically viable NF-κB inhibitors for adjuvant therapy must walk the fine line of being safe, yet effective, a task that is made all the more difficult when administered in combination with a chemotherapeutic. Based on our desire to minimize the toxicity of the combined therapy, we selected the food-derived flavonoid CAPE because of its proven NF-κB inhibiting capability in tumors[140,216-222], low toxicity[223-227], and mechanistic synergy with CPT-11. Although the exact pathways through which CAPE inhibits NF-κB have yet to be elucidated, structure-activity studies indicated that CAPE inhibits NF-κB though the generic scavenging of ROS as well as specifically inhibiting the activation of IKK[228-232]. Studies performed on numerous cancer cell lines have demonstrated that increased ROS production and IKK activation are the pathways through which CPT-11 is known to activate NF-κB. For this reason, CAPE is mechanistically well-suited to potentiate CPT-11 .

Our results confirm that CAPE potentiates CPT-11-induced apoptosis of CPT-11 resistant colon HT-29 cancer line. For example, when used in tandem, at 50 μM each, (100 μM total), the combination of CAPE and CPT-11 induced as much apoptosis as CPT-11 at a dose of 100 μM. Thus, by incorporating CAPE in the therapeutic regimen, it is possible to dramatically reduce the concentration of CPT-11 (the more toxic compound) without any loss of efficacy. This result is surprising considering that at 50 μM CAPE has almost no discernable toxicity. Furthermore, at a CAPE concentration of 50 μM, increasing the CPT-11 concentration from 50 μM to 100 μM had no significant effect on apoptosis. Paradoxically, at 50 μM CPT-11, increasing the concentration of

CAPE from 50 μM to 100 μM resulted in a significant increase in apoptosis. Together, these results demonstrate that CAPE potentiates the activity of CPT-11. To identify the mechanism responsible for the CAPE/CPT-11 synergy, we performed immunofluorescence staining for NF-κB and measured the nuclear NF-κB levels in HT-29 cells treated with the individual drugs and multiple combinations thereof. The results of these studies confirmed our hypothesis that CAPE is capable of inhibiting CPT-11-induced NF-κB activation. Furthermore, these results suggest that CAPE's ability to potentiate apoptosis is a result of its ability to block NF-κB activation—the primary mechanism of drug resistance.

It is well-documented that sub 200nm particles can passively accumulate in the tumor microenviroment, and thus increase the efficacy of encapsulated chemotherapeutics. CNPs were formulated using a solvent displacement protocol that produced ~180 nm particles. In order to further increase their circulation time, and thus the probability that the particles accumulate in a tumor, we coated the CCNPs and CNPs with the amphiphilic pluronic F-127. F-127 has been shown to self-assemble on the surface of hydrophobic particles, thus forming a hydrophilic corona that increases particle circulation time by decreasing particle opsonization and hepatic clearance[233-236]. Indeed, 48 h after administration, CNPs dramatically increase the amount of IR-780 dye retained in AOM-induced tumors. Furthermore, CNPs delivered considerably more dye to the colon as compared to the heart, lungs, kidney, and spleen, suggesting that CNPs can reduce CPT-11-induced toxicity in these organs. Although a significant portion of the particles accumulated in the liver, integration of the fluorescent intensities of the liver revealed that the fluorescent signal concentration in the liver is an order of magnitude less than the signal concentration in the colonic tumors. Interestingly, at 1/10 to 1/5 of the doses that have been reported to inhibit NF-κB activation tumors, CAPE has been shown to attenuate chemotherapy induced hepatotoxicity and toxicity in other organs[225-

[227,237-240]. These studies attributed CAPE's hepato-protective effect to CAPE's ability to scavenge ROS and not the inhibition of NF-κB. Therefore, maintaining a low non-NF-κB-inhibiting hepatic concentration of CAPE could reduce the toxicity of CPT-11 in the liver.

In order to demonstrate the efficacy of CCNPs in a preclinical tumor model, we treated mice bearing AOM-induced tumors with CCNPs and appropriate controls. Our results demonstrate that CCNPs were able to significantly reduce tumor multiplicity and the tumor load in mice bearing AOM-induced tumors. Importantly, at a three-fold lower dose of CPT-11, 4% CCNPs were more effective than the combination of free CPT-11 and CAPE at reducing tumor multiplicity and equally effective as the free drugs at inhibiting tumor growth. Analysis of tumor NF-κB activation levels revealed that mice treated with CNPs, 4% CCNPs, and 12 % CCNPs had significantly lower levels of tumor NF-κB activation compared to mice treated with the free drugs, suggesting that the superior efficacy of the CCNPs is a result of their ability to block CPT-11-induced NF-κB activation. Quantitative PCR analysis confirmed that the level of tumor NF-κB inhibition generated by the CCNPs was sufficient to reduce the activation of the downstream prosurvival genes Bcl-xL and survivin, thus confirming that CCNPs reduce tumor size and number by blocking CPT-11 induced drug resistance. Surprisingly, the free drug cocktail, which contained the same amount of CAPE as the nanoparticle formulations, caused a significant increase in NF-κB activation and had no effect on prosurvival mRNA levels. These results demonstrate that the CCNP's unique ability to localize high concentrations of CAPE to the tumor microenvironment is an essential factor in their ability to inhibit CPT-11-induced drug resistance. This necessity to maximize the amount of CAPE in the tumor microenvironment validates our nanoparticle design and our use of PCAPE to formulate hyper-loaded nanoparticles.

To further explore the mechanism by which CCNPs reduce tumor size, we performed qPCR to quantify the tumor mRNA levels of TNFα and IL-1, which are cytokines known to promote tumor initiation, growth, and proliferation. We discovered that although both CNPs, and CCNPs were able to reduce NF-κB activation levels in the tumors, only CCNPs were able to significantly reduce the tumor mRNA levels of TNFa and IL-1. Given that both IL-1 and TNFα can be activated by soluble factors that act through NF-κB-independent pathways, we hypothesized that the increased levels of cytokine mRNAs in the tumors of mice treated with CNPs was the result of soluble proinflammatory factors that diffused into the tumor microenvironment. We further postulate that by inhibiting tumor growth and tumorigenesis CCNPs are able to fundamentally transform the extra-tumor environment of the colon, and thus reduce the expression of soluble proinflammatory mediators that might diffuse into the tumor.

Several preclinical studies have employed various NF-κB inhibitors as adjuvants to potentiate the efficacy of CPT-11 in the treatment of CRC. Inhibition of NF-κB via the intratumoral adenoviral delivery of a super repressor form of IκBα in conjunction with systemic delivery of CPT-11 (57 mg $kg^{-1}$ $wk^{-1}$) resulted in a significant decrease in LoVo xenograft tumors[94]. Although adenoviral mediated NF-κB suppression resulted in an impressive level of tumor inhibition, the challenges associated with viral mediated gene delivery are major obstacles blocking the clinical viability of this approach[241,242]. In the same tumor model, the systemic administration of the proteasome inhibitor PS-341 (Bortezomib) prior to treatment with CPT-11 (66 mg $kg^{-1}$ $wk^{-1}$) inhibited CPT-11-mediated NF-κB activation and generated an impressive decrease in tumor growth[22]. Tumors treated with PS-341 and CPT-11 were 75% smaller than tumors treated with CPT-11 alone. A subsequent phase II trial that evaluated the effects of PS-341 on tumor growth showed that PS-341 did not decrease NF-κB levels in patients suffering from advanced CRC[48]. These results call into question the clinical viability of PS-341 as an adjuvant for

CPT-11. The radical scavenger edaravone has been shown to enhance CPT-11 (47 mg $kg^{-1}$ $wk^{-1}$) mediated apoptosis, tumor regression, and metastasis in mice bearing colon26 xenograft tumors. While effective in reducing CPT-11- induced NF-kB activation and tumor growth, the toxicity of edaravone is such that it is likely to limit its clinical application[203]. A recent study[26] showed that oral administration of the NF-κB inhibitor AS602868 (100 mg $kg^{-1}$ $wk^{-1}$) in combination with systemically delivered CPT-11 (60 mg $kg^{-1}$ $wk^{-1}$) lead to considerable growth suppression of HT-29 xenograft tumors. After 10 weeks of treatment, the combination of CPT-11 and AS602868 reduced tumor growth by 75% compared to vehicle treated tumors[26]. Nevertheless, after 4 weeks of therapy, the combination of CPT-11 and AS602868 was not significantly more effective than CPT-11 alone. Here, we show that treating mice with 3.0 $mg^{-1}$ $kg^{-1}$ $wk^{-1}$ CPT-11 encapsulated in CCNPs generates a significant decrease in CAC tumor size and number. Although it is impossible to compare studies performed on xenograft animal models to this study, it should be noted that mice treated with 4% CCNPs received almost 20 times less CPT-11 per week than the lowest CPT-11 dose used in previously reported preclinical studies on CRC.

In this work, we show that particles formulated from PCAPE localize to AOM-induced tumors, inhibit tumor NF-κB activation, and thus potentiate the antitumor effects of encapsulated CPT-11 in an animal model of CAC. Although studies have utilized pharmacological agents as a prophylaxis against AOM-induced oncogenesis[243,244], to our knowledge, this is the first demonstration of a therapy that abrogates the growth of pre-existing tumors and reduces subsequent tumorigenesis. While designing CPT-11, we were careful not to incorporate features that were specific to CAC, and thus CCNP's should have the chemical and physical properties necessary to treat a variety of solid tumors.

# Chapter 6: Conclusion and Future Directions

This work presents the preclinical development of two novel drug delivery platforms for treating diseases associated with intestinal inflammation. Although these nanoparticles worked well in animal models of colitis and colitis-associated cancer, the ultimate goal is to develop these delivery vehicles into clinically viable products that can improve the quality of human life. This section provides some concluding remarks, recommends additional experiments, and discusses the road to clinical translation.

## 6.1. Thioketal Nanoparticles

In Chapter 4, we presented a new polymer that could be formulated into nanoparticles that release therapeutics in response to (ROS) reactive oxygen species produced by inflamed intestinal tissue. Given the immense potential of small interfering RNAs (siRNAs) and their demonstrated potential to treat inflammatory diseases, we chose to investigate the feasibility of targeting TNFα-siRNA to inflamed intestinal tissues as a treatment for inflammatory bowel disease (IBD), specifically ulcerative colitis. We demonstrated that TKNs effectively targeted encapsulated siRNA to sites of intestinal inflammation, and when loaded with TNFα-siRNA mitigate inflammation in an experimental form of ulcerative colitis. Although the work completed above is quite substantial and ground-breaking, questions remain about the ability of this system to treat IBD in human patients.

In the preclinical studies performed above, the method for inducing intestinal inflammation via dextran sodium sulfate (DSS) does not result in physiological changes in the colon until day 2 or 3 of the experiment. However, the mice are treated with the particles on the initial day of the experiment, then everyday thereafter. Thus, the mice receive 3 to 4 days of treatment before inflammation is fully manifested in the colon.

Most patients do not take drugs before they acquire symptoms. Accordingly, experiments should be conducted to determine if the TKNs, can rescue a mouse that is already suffering from intestinal inflammation. Since the TKNs do not release therapeutics until ROS are increased in the colon, presumably at day 3 or 4, the initial doses probably have no effect on the ultimate outcome of the experiments presented above. Therefore, we feel confident that the TKNs will be able to rescue a mouse from DSS-induced colitis.

Although a brief discussion about the biological fate of the degradation products and un-degraded particles is provided in Chapter 5, a thorough investigation of the biodistribution of all degradation products, siRNA, and un-degraded particles needs to be performed in conjunction with a toxicological study of the material and its degradation products. As discussed above, TKNs degrade into hydrophobic low molecular weight compounds, which should be cleared from the body. Furthermore, we speculate that siRNAs released into the luman are either rapidly degraded or taken up by the endothelial layer, but not transcytosed, and thus do not enter the blood compartment. The results from the targeting experiments with siRNA support this hypothesis.

We chose to use siRNA to silence TNFα expression; however, the current cost of such a therapeutic would prohibit its use for a non-life threatening disease. However, nothing in the design of TKNs prohibits them from being utilized to delivery other, more reasonably priced, therapeutics that need to be targeted to inflamed intestinal tissues due to their potential toxicity. As mentioned above in Chapter 2, currently, the most effective therapeutic for IBD are monoclonal antibodies against TNFα. Encapsulating these antibodies in TKNs, and delivering them orally would reduce their toxicity and increase patient compliance.

In this work, we synthesized PPADT from a monomer containing a benzene ring. We chose this monomer because it was commercially available and very hydrophobic,

which we hypothesized would help protect siRNA. However, due to their ability to intercalate in genetic materials, benzene rings are not the most biocompatible structure that could be used. Additionally, a more hydrophilic monomer would increase the TKN's ROS sensitivity, which would result more siRNA being released as the particles traverse the GI tract, and better targeting of low levels of inflammation. Although not shown here, we have indeed successfully synthesized polythioketals from a variety of other monomers.

### 6.2. Poly-CAPE

In Chapter 5, we presented a novel drug delivery platform capable of targeting CAPE and CPT-11 to AOM-induced tumors. Our results show that CPT-11-loaded CAPE nanoparticles (CCNPs) were capable of inhibiting CPT-11-induced drug resistance. In order to deliver a therapeutic quantity of CAPE to the tumor microenviroment, we incorporated CAPE into the backbone of a polymer via biodegradable linkages. In a head-to-head experiment with an equivalent amount of free CAPE and CPT-11, the CCNPs elicited a significant reduction in tumor NF-κB, whereas the free drugs actually increased NF-κB activation in the tumors. This result in concert with the targeting data, demonstrates that maximizing the concentration of CAPE in the tumor microenvironment is essential for potentiating the efficacy of CPT-11, and thus validates our efforts to maximize CAPE encapsulation by synthesizing PCAPE.

Given the questionable nature of passive nanoparticle accumulation in human tumors, another platform that can actively target cancer tumors will have to be selected for clinical translation. This could be accomplished by synthesizing a hyper-branched polymer that contained CAPE in its structure. CPT-11 as well as targeting molecules could then be attached to the polymer, and the polymer delivered as a single strand.

Another interesting application of the CNPs is in the treatment of inflammatory diseases. Aberrant NF-κB activation is a contributing factor to most inflammatory disorders. In their current form, CNPs could be used to treat pulmonary fibrosis, myocardial infarct, and acute liver failure.

# Appendix: A

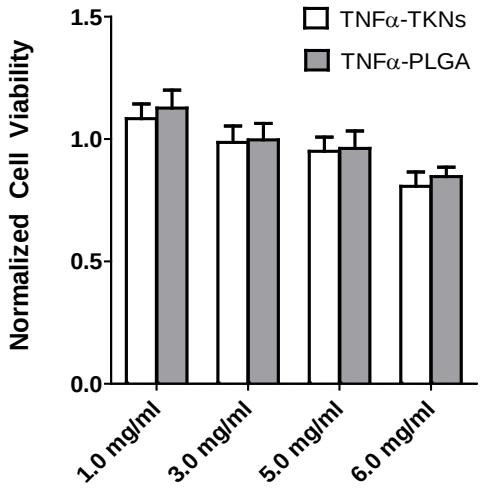


**Figure A1.1. Thioketal nanoparticles have a toxicity profile simular to PLGA.** We determined that TNFα-TKNs have no detectable toxicity up to a dose of 5.0 mg/ml and that their toxicity profile is similar to that of TNFα-siRNA-loaded nanoparticles formulated from the FDA approved material poly(lactic-co-glycolic acid) (TNFα-PLGA).

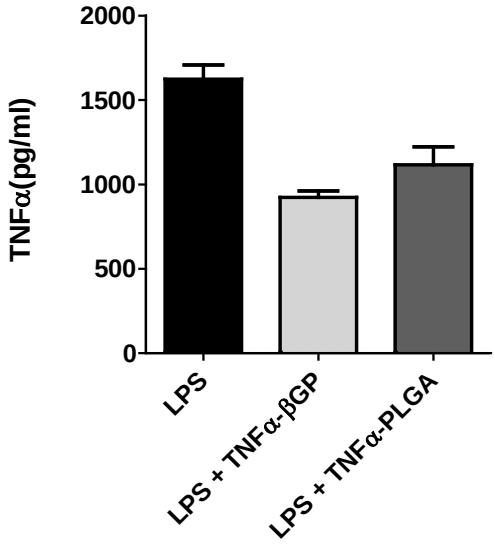


**Figure A1.2. Extracellular TNFα mRNA levels as determined by ELISA.** To demonstrate the efficacy of TNFα-βGPs and TNFα-PLGA particles, macrophages were treated with 0.1 mg/ml TNFα-siRNA contained within PLGA nanoparticles or βGPs, then activated by stimulating them with LPS. After 24 h, these results show that both TNFα-PLGA and TNFα-βGPs reduced TNFα expression by activated macrophages. Results depicted as mean pg of TNFα per ml of media ± s.e.m. for n = 3 per treatment group. Statistical significance was determined by a one-way ANOVA using Bonferroni's post hoc test (*$p \leq 0.05$).

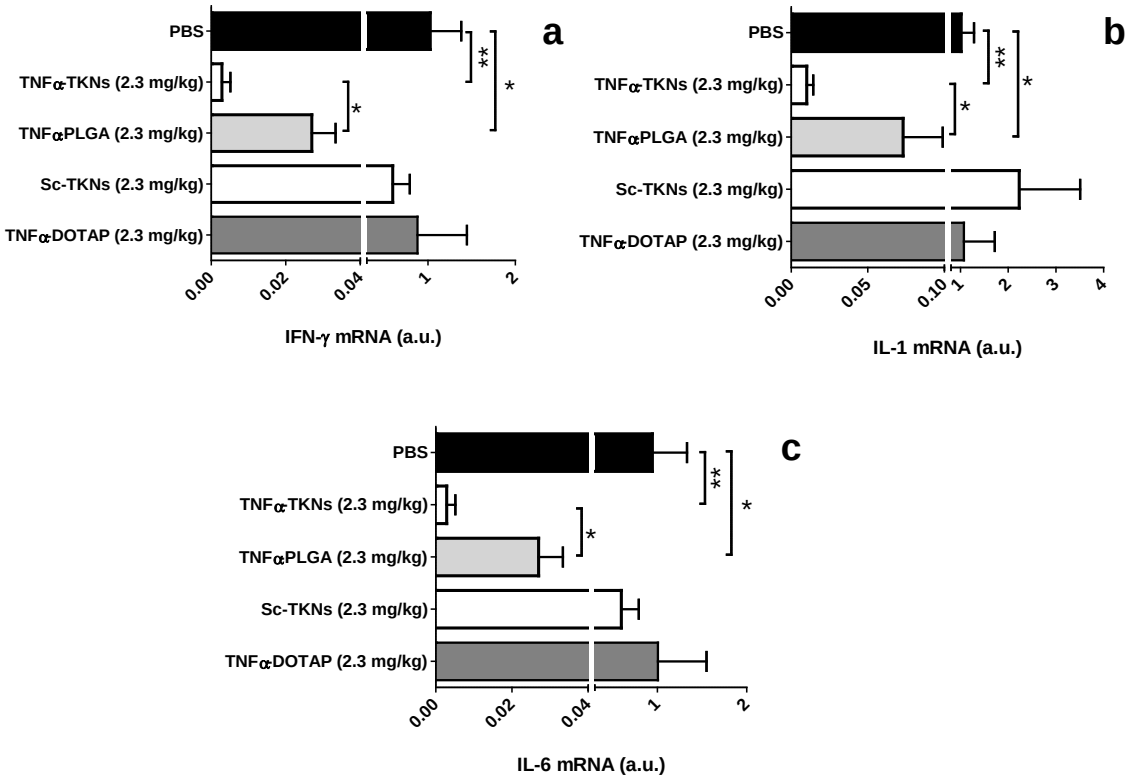


**Figure A1.3. Cytokine profile for TKNs.** (a-c) Fold increase of IFN-γ, IL-1, and IL-6 mRNA in the colons of mice receiving DSS and treated with a daily oral gavage of 2.3 mg/kg of either TNFα-siRNA or scrambled siRNA encapsulated within: TNFα-TKNs (n = 6), TNFα-PLGA (n = 5), Scram-TKNs (n = 5), siRNA-DOTAP (n = 6), or PBS (n = 6), for six days. Statistical differences determined by a one-way ANOVA using Bonferroni's post hoc test (*$p \leq 0.05$, **$p \leq 0.001$).

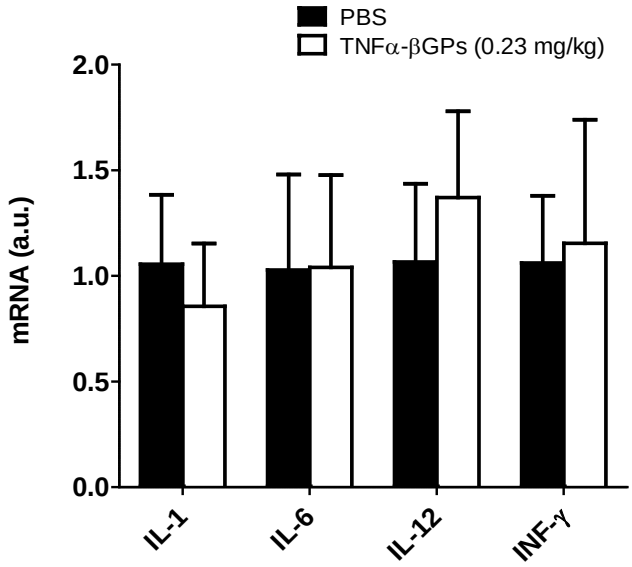


**Figure A1.4. Cytokine profile for β-glucan nanoparticles.** Colonic cytokine mRNA levels in mice receiving DSS and treated with either PBS or 0.23 mg TNFα-siRNA 0.23/kg/day via βGPs (n = 10). Statistical differences in Figures a-d determined by a one-way ANOVA using Bonferroni's post hoc test (*$p \leq 0.05$, **$p \leq 0.001$).

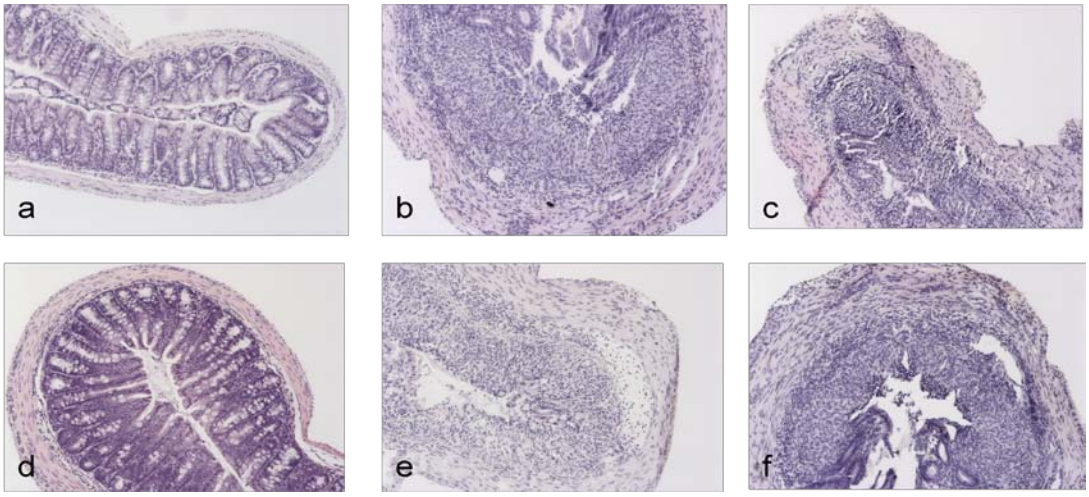


**Figure A1.5. H&E-stained colon sections.** (a) H&E-stained colon section of mice after seven days of receiving normal water and a daily oral gavage of PBS (10X). (b-f) H&E-stained colon sections for mice receiving DSS and treated with a daily oral gavage of PBS (b) or 2.3 mg/kg of either TNFα-siRNA or scrambled siRNA via: (c) TNFα-PLGA, (d) TNFα-TKNs, (e) Scram-TKNs, or (f) TNFα-DOTAP (10X).

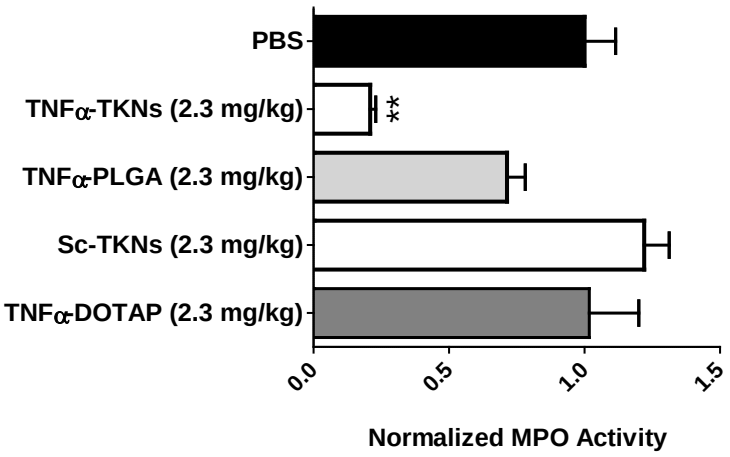


**Figure A1.6. Colonic MPO activity.** Colonic MPO activity for mice receiving DSS and treated with 2.3 mg siRNA/kg/day. Results are expressed as mUnits of MPO activity per mg protein. Results represent the mean ± s.e.m., statistical significance was calculated using a one-way ANOVA and Bonferroni's post hoc test (**$p \leq 0.001$).

# Appendix: B

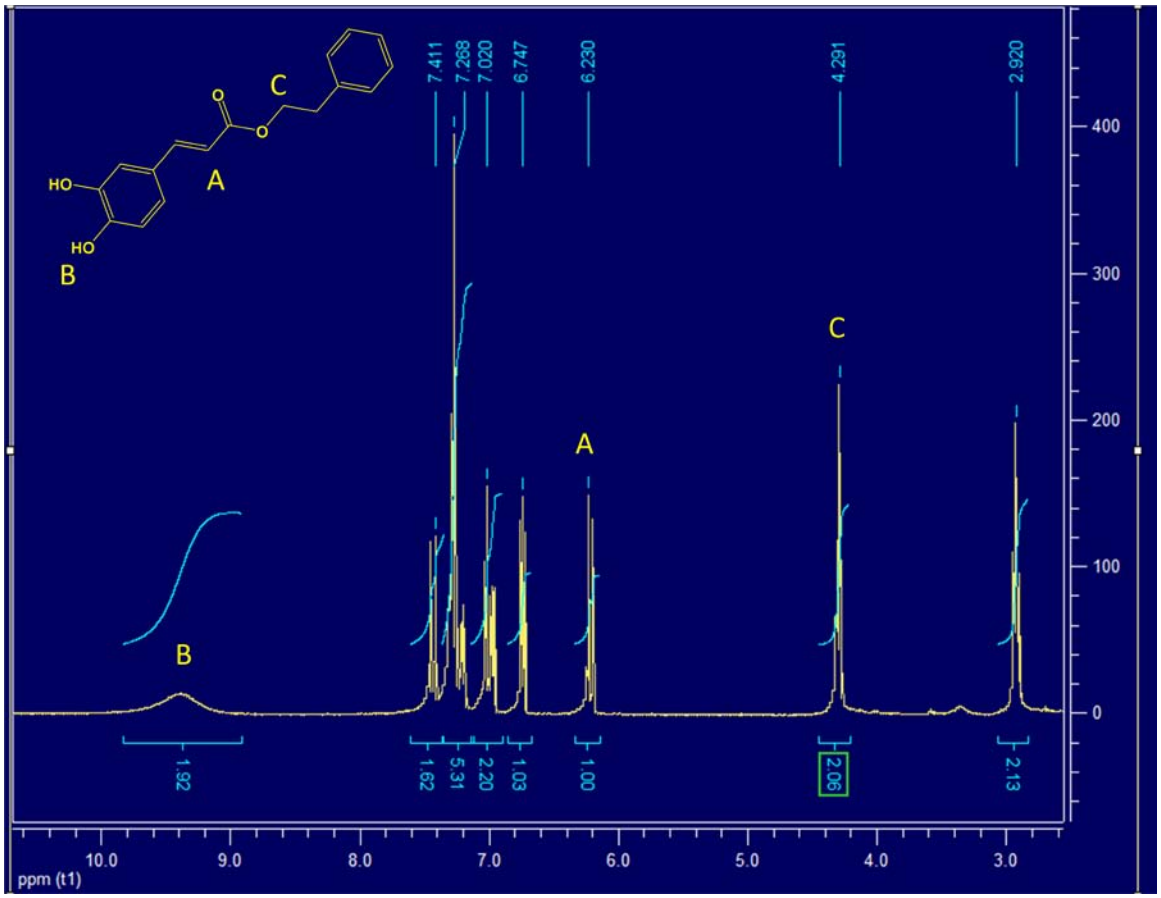


**Figure A2.1.** Proton NMR spectra for Caffeic acid phenethyl ester (CAPE)

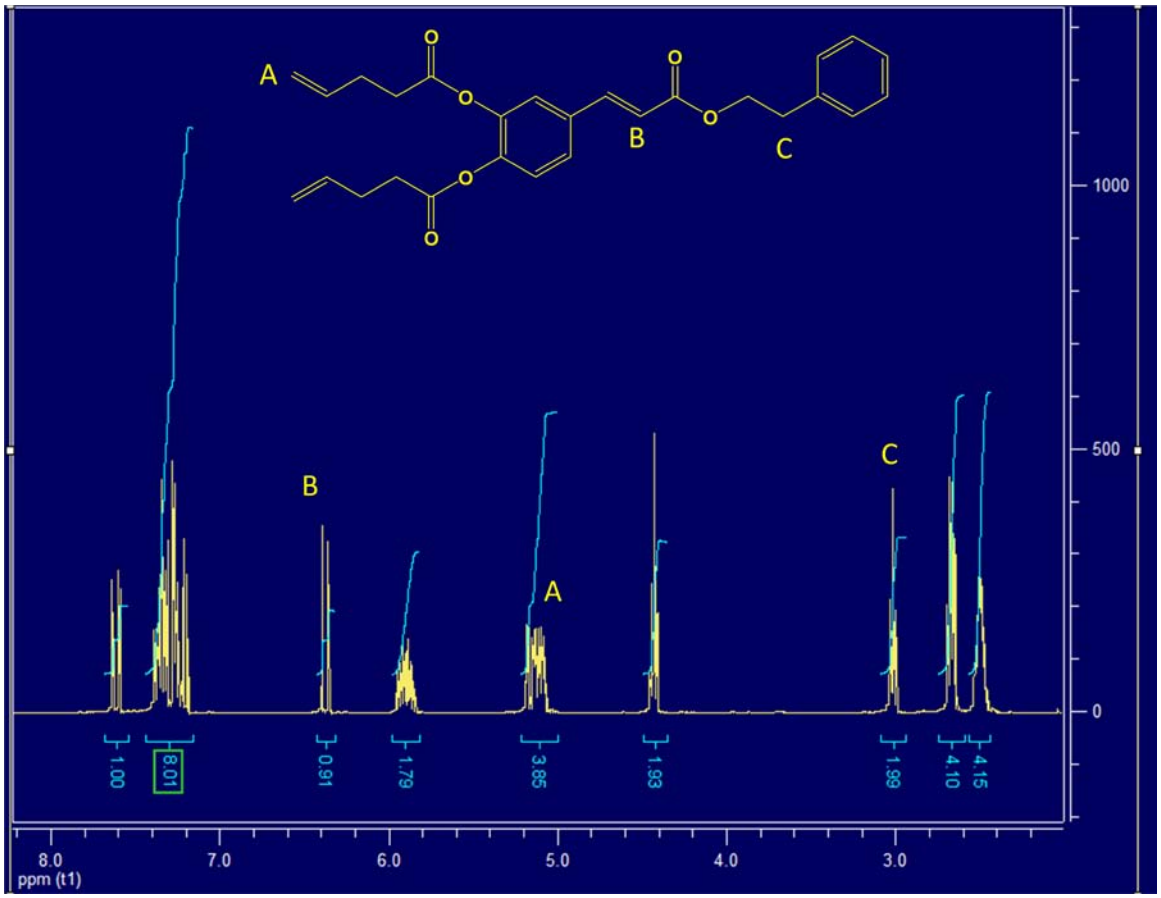


**Figure A2.2. Proton NMR spectra for Caffeic acid phenethyl ester monomer**

**Figure A2.3. Representative image of tumor verification via colonoscopy**

# References


1 Lih-Brody, L. *et al.* Increased oxidative stress and decreased antioxidant defenses in mucosa of inflammatory bowel disease. *Digestive diseases and sciences* **41**, 2078-2086 (1996).

2 Kountouras, J., Chatzopoulos, D. & Zavos, C. Reactive oxygen metabolites and upper gastrointestinal diseases. *Hepatogastroenterology* **48**, 743-751 (2001).

3 Simmonds, N. J. *et al.* Chemiluminescence assay of mucosal reactive oxygen metabolites in inflammatory bowel disease. *Gastroenterology* **103**, 186-196, doi:S0016508592002683 [pii] (1992).

4 Whitehead, K. A., Langer, R. & Anderson, D. G. Knocking down barriers: advances in siRNA delivery. *Nat Rev Drug Discov* **8**, 129-138, doi:nrd2742 [pii] 10.1038/nrd2742 (2009).

5 Nurden, A. T. Platelets, inflammation and tissue regeneration. *Thrombosis and haemostasis* **105 Suppl 1**, S13-33, doi:10.1160/THS10-11-0720 (2011).

6 Coussens, L. M. & Werb, Z. Inflammation and cancer. *Nature* **420**, 860-867, doi:10.1038/nature01322 (2002).

7 McAlindon, M. E. & Mahida, Y. R. Pro-inflammatory cytokines in inflammatory bowel disease. *Alimentary pharmacology & therapeutics* **10 Suppl 2**, 72-74 (1996).

8 Brynskov, J., Nielsen, O. H., Ahnfelt-Ronne, I. & Bendtzen, K. Cytokines in inflammatory bowel disease. *Scandinavian journal of gastroenterology* **27**, 897-906 (1992).

9 Moss, S. F. & Blaser, M. J. Mechanisms of disease: Inflammation and the origins of cancer. *Nature clinical practice. Oncology* **2**, 90-97; quiz 91 p following 113, doi:10.1038/ncponc0081 (2005).

10 Every, A. L. *et al.* Localized suppression of inflammation at sites of Helicobacter pylori colonization. *Infection and immunity*, doi:10.1128/IAI.05602-11 (2011).

11 Shacklett, B. L. Immune responses to HIV and SIV in mucosal tissues: 'location, location, location'. *Current opinion in HIV and AIDS* **5**, 128-134, doi:10.1097/COH.0b013e328335c178 (2010).

12 Roessner, A., Kuester, D., Malfertheiner, P. & Schneider-Stock, R. Oxidative stress in ulcerative colitis-associated carcinogenesis. *Pathology, research and practice* **204**, 511-524, doi:10.1016/j.prp.2008.04.011 (2008).

13 Baskol, M., Baskol, G., Kocer, D., Ozbakir, O. & Yucesoy, M. Advanced oxidation protein products: a novel marker of oxidative stress in ulcerative colitis. *Journal of clinical gastroenterology* **42**, 687-691, doi:10.1097/MCG.0b013e318074f91f (2008).

14 Seril, D. N., Liao, J., Yang, G. Y. & Yang, C. S. Oxidative stress and ulcerative colitis-associated carcinogenesis: studies in humans and animal models. *Carcinogenesis* **24**, 353-362 (2003).

15 Venturini, D. *et al.* Increased oxidative stress, decreased total antioxidant capacity, and iron overload in untreated patients with chronic hepatitis C. *Digestive diseases and sciences* **55**, 1120-1127, doi:10.1007/s10620-009-0833-1 (2010).

16 Kundu, J. K. & Surh, Y. J. Inflammation: gearing the journey to cancer. *Mutation research* **659**, 15-30, doi:10.1016/j.mrrev.2008.03.002 (2008).

17 Sethi, G., Sung, B. & Aggarwal, B. B. Nuclear factor-kappaB activation: from bench to bedside. *Exp Biol Med (Maywood)* **233**, 21-31, doi:10.3181/0707-MR-196 (2008).

18 Marie, J. C. *et al.* Linking innate and acquired immunity: divergent role of CD46 cytoplasmic domains in T cell induced inflammation. *Nature immunology* **3**, 659-666, doi:10.1038/ni810 (2002).

19 Baldwin, A. S. Control of oncogenesis and cancer therapy resistance by the transcription factor NF-kappaB. *The Journal of clinical investigation* **107**, 241-246, doi:10.1172/JCI11991 (2001).

20 de Jong, F. A. *et al.* ABCG2 pharmacogenetics: ethnic differences in allele frequency and assessment of influence on irinotecan disposition. *Clinical cancer research : an official journal of the American Association for Cancer Research* **10**, 5889-5894, doi:10.1158/1078-0432.CCR-04-0144 (2004).

21 Xu, Y. & Villalona-Calero, M. A. Irinotecan: mechanisms of tumor resistance and novel strategies for modulating its activity. *Annals of oncology : official journal of the European Society for Medical Oncology / ESMO* **13**, 1841-1851 (2002).

22 Cusack, J. C., Jr. *et al.* Enhanced chemosensitivity to CPT-11 with proteasome inhibitor PS-341: implications for systemic nuclear factor-kappaB inhibition. *Cancer research* **61**, 3535-3540 (2001).

23 Cusack, J. C., Jr., Liu, R. & Baldwin, A. S., Jr. Inducible chemoresistance to 7-ethyl-10-[4-(1-piperidino)-1-piperidino]-carbonyloxycamptothe cin (CPT-11) in colorectal cancer cells and a xenograft model is overcome by inhibition of nuclear factor-kappaB activation. *Cancer research* **60**, 2323-2330 (2000).

24 Kokura, S. *et al.* The radical scavenger edaravone enhances the anti-tumor effects of CPT-11 in murine colon cancer by increasing apoptosis via inhibition of NF-kappaB. *Cancer letters* **229**, 223-233, doi:10.1016/j.canlet.2005.06.039 (2005).

25 Scartozzi, M. *et al.* Nuclear factor-kB tumor expression predicts response and survival in irinotecan-refractory metastatic colorectal cancer treated with cetuximab-irinotecan therapy. *Journal of clinical oncology : official journal of the American Society of Clinical Oncology* **25**, 3930-3935, doi:10.1200/JCO.2007.11.5022 (2007).

26 Lagadec, P. *et al.* Pharmacological targeting of NF-kappaB potentiates the effect of the topoisomerase inhibitor CPT-11 on colon cancer cells. *British journal of cancer* **98**, 335-344, doi:10.1038/sj.bjc.6604082 (2008).

27 Lakatos, P. L. Prevalence, predictors, and clinical consequences of medical adherence in IBD: how to improve it? *World journal of gastroenterology : WJG* **15**, 4234-4239 (2009).

28 Neuman, M. G. Immune dysfunction in inflammatory bowel disease. *Translational research : the journal of laboratory and clinical medicine* **149**, 173-186, doi:10.1016/j.trsl.2006.11.009 (2007).

29 Bodger, K. Cost effectiveness of treatments for inflammatory bowel disease. *PharmacoEconomics* **29**, 387-401, doi:10.2165/11584820-000000000-00000 (2011).

30 Longobardi, T., Jacobs, P. & Bernstein, C. N. Work losses related to inflammatory bowel disease in the United States: results from the National Health Interview Survey. *The American journal of gastroenterology* **98**, 1064-1072, doi:10.1111/j.1572-0241.2003.07285.x (2003).

31 Flood, L., Innala, E., Lofberg, R. & Wikstrom, A. C. Patients with ulcerative colitis responding to steroid treatment up-regulate glucocorticoid receptor levels in

colorectal mucosa. *Journal of Crohn's & colitis* **2**, 123-130, doi:10.1016/j.crohns.2007.10.002 (2008).

32 Borigini, M. J. & Paulus, H. E. Innovative treatment approaches for rheumatoid arthritis. Combination therapy. *Bailliere's clinical rheumatology* **9**, 689-710 (1995).

33 Burger, D. & Travis, S. Conventional medical management of inflammatory bowel disease. *Gastroenterology* **140**, 1827-1837 e1822, doi:10.1053/j.gastro.2011.02.045 (2011).

34 Magro, F. & Portela, F. Management of inflammatory bowel disease with infliximab and other anti-tumor necrosis factor alpha therapies. *BioDrugs : clinical immunotherapeutics, biopharmaceuticals and gene therapy* **24 Suppl 1**, 3-14, doi:10.2165/11586290-000000000-00000 (2010).

35 Danese, S., Colombel, J. F., Reinisch, W. & Rutgeerts, P. J. Review article: infliximab for Crohn's disease treatment--shifting therapeutic strategies after 10 years of clinical experience. *Alimentary pharmacology & therapeutics* **33**, 857-869, doi:10.1111/j.1365-2036.2011.04598.x (2011).

36 Sandborn, W. J. State-of-the-art: Immunosuppression and biologic therapy. *Dig Dis* **28**, 536-542, doi:10.1159/000320413 (2010).

37 Wilson, D. S. *et al.* Orally delivered thioketal nanoparticles loaded with TNF-alpha-siRNA target inflammation and inhibit gene expression in the intestines. *Nature materials* **9**, 923-928, doi:10.1038/nmat2859 (2010).

38 Souto, E. B., Nayak, A. P. & Murthy, R. S. Lipid nanoemulsions for anti-cancer drug therapy. *Die Pharmazie* **66**, 473-478 (2011).

39 Allen, P. B., Lindsay, H. & Tham, T. C. How do patients with inflammatory bowel disease want their biological therapy administered? *BMC gastroenterology* **10**, 1, doi:10.1186/1471-230X-10-1 (2010).

40 Hagel, S., Bruns, T., Theis, B., Herrmann, A. & Stallmach, A. Subacute liver failure induced by adalimumab. *International journal of clinical pharmacology and therapeutics* **49**, 38-40 (2011).

41 Chen, J. & Huang, X. F. The signal pathways in azoxymethane-induced colon cancer and preventive implications. *Cancer biology & therapy* **8**, 1313-1317 (2009).

42 Umar, A. & Greenwald, P. Alarming colorectal cancer incidence trends: a case for early detection and prevention. *Cancer epidemiology, biomarkers & prevention : a publication of the American Association for Cancer Research, cosponsored by the American Society of Preventive Oncology* **18**, 1672-1673, doi:10.1158/1055-9965.EPI-09-0320 (2009).

43 Tenesa, A. & Dunlop, M. G. New insights into the aetiology of colorectal cancer from genome-wide association studies. *Nature reviews. Genetics* **10**, 353-358, doi:10.1038/nrg2574 (2009).

44 Lippert, T. H., Ruoff, H. J. & Volm, M. Current status of methods to assess cancer drug resistance. *International journal of medical sciences* **8**, 245-253 (2011).

45 Donnenberg, V. S. & Donnenberg, A. D. Multiple drug resistance in cancer revisited: the cancer stem cell hypothesis. *J Clin Pharmacol* **45**, 872-877, doi:45/8/872 [pii]
10.1177/0091270005276905 (2005).

46 Karin, M. & Greten, F. R. NF-kappaB: linking inflammation and immunity to cancer development and progression. *Nature reviews. Immunology* **5**, 749-759, doi:10.1038/nri1703 (2005).

47 Karin, M. Nuclear factor-kappaB in cancer development and progression. *Nature* **441**, 431-436, doi:10.1038/nature04870 (2006).

48 Mackay, H. *et al.* A phase II trial with pharmacodynamic endpoints of the proteasome inhibitor bortezomib in patients with metastatic colorectal cancer. *Clinical cancer research : an official journal of the American Association for Cancer Research* **11**, 5526-5533, doi:10.1158/1078-0432.CCR-05-0081 (2005).

49 Chauhan, D., Hideshima, T., Mitsiades, C., Richardson, P. & Anderson, K. C. Proteasome inhibitor therapy in multiple myeloma. *Molecular cancer therapeutics* **4**, 686-692, doi:10.1158/1535-7163.MCT-04-0338 (2005).

50 Karp, S. M. & Koch, T. R. Oxidative stress and antioxidants in inflammatory bowel disease. *Dis Mon* **52**, 199-207, doi:S0011-5029(06)00029-0 [pii]
10.1016/j.disamonth.2006.05.005 (2006).

51 Kruidenier, L. & Verspaget, H. W. Review article: oxidative stress as a pathogenic factor in inflammatory bowel disease--radicals or ridiculous? *Aliment Pharmacol Ther* **16**, 1997-2015, doi:1378 [pii] (2002).

52 Tuzun, A. *et al.* Oxidative stress and antioxidant capacity in patients with inflammatory bowel disease. *Clin Biochem* **35**, 569-572, doi:S0009912002003612 [pii] (2002).

53 Shukla, A. K. & Singh, K. N. Superoxide induced deprotection of 1,3-dithiolanes: A convenient method of dedithioacetalization. *Indian Journal of Chemistry-B* **43B**, 5 (2004).

54 Rakha, E. A. & Ellis, I. O. Triple-negative/basal-like breast cancer: review. *Pathology* **41**, 40-47, doi:906853315 [pii] 10.1080/00313020802563510 (2009).

55 Heffernan, M. J. & Murthy, N. Polyketal nanoparticles: a new pH-sensitive biodegradable drug delivery vehicle. *Bioconjug Chem* **16**, 1340-1342, doi:10.1021/bc050176w (2005).

56 Lee, S., Yang, S. C., Heffernan, M. J., Taylor, W. R. & Murthy, N. Polyketal microparticles: a new delivery vehicle for superoxide dismutase. *Bioconjug Chem* **18**, 4-7, doi:10.1021/bc060259s (2007).

57 Heffernan, M. J., Kasturi, S. P., Yang, S. C., Pulendran, B. & Murthy, N. The stimulation of CD8+ T cells by dendritic cells pulsed with polyketal microparticles containing ion-paired protein antigen and poly(inosinic acid)-poly(cytidylic acid). *Biomaterials* **30**, 910-918, doi:S0142-9612(08)00822-3 [pii] 10.1016/j.biomaterials.2008.10.034 (2009).

58 Yang, S. C., Bhide, M., Crispe, I. N., Pierce, R. H. & Murthy, N. Polyketal copolymers: a new acid-sensitive delivery vehicle for treating acute inflammatory diseases. *Bioconjug Chem* **19**, 1164-1169, doi:10.1021/bc700442g (2008).

59 Gongora, M. C. *et al.* Loss of extracellular superoxide dismutase leads to acute lung damage in the presence of ambient air: a potential mechanism underlying adult respiratory distress syndrome. *Am J Pathol* **173**, 915-926, doi:ajpath.2008.080119 [pii]10.2353/ajpath.2008.080119 (2008).

60 Papadakis, K. A. & Targan, S. R. Role of cytokines in the pathogenesis of inflammatory bowel disease. *Annual review of medicine* **51**, 289-298, doi:10.1146/annurev.med.51.1.289 (2000).

61 Kolachala, V. *et al.* TNF-alpha upregulates adenosine 2b (A2b) receptor expression and signaling in intestinal epithelial cells: a basis for A2bR overexpression in colitis. *Cellular and molecular life sciences : CMLS* **62**, 2647-2657, doi:10.1007/s00018-005-5328-4 (2005).

62 Funakoshi, K. *et al.* Spectrum of cytokine gene expression in intestinal mucosal lesions of Crohn's disease and ulcerative colitis. *Digestion* **59**, 73-78, doi:dig59073 [pii] (1998).

63 Masuda, H., Iwai, S., Tanaka, T. & Hayakawa, S. Expression of IL-8, TNF-alpha and IFN-gamma m-RNA in ulcerative colitis, particularly in patients with inactive phase. *J Clin Lab Immunol* **46**, 111-123 (1995).

64 Murthy, S., Flanigan, A., Coppola, D. & Buelow, R. RDP58, a locally active TNF inhibitor, is effective in the dextran sulphate mouse model of chronic colitis. *Inflamm Res* **51**, 522-531 (2002).

65 Koutroubakis, I. E. *et al.* Effects of tumor necrosis factor alpha inhibition with infliximab on lipid levels and insulin resistance in patients with inflammatory bowel disease. *Eur J Gastroenterol Hepatol* **21**, 283-288, doi:10.1097/MEG.0b013e328325d42b 00042737-200903000-00007 [pii] (2009).

66 de Vries, H. S., Van Oijen, M. G. & de Jong, D. J. Safety of infliximab in inflammatory bowel disease needs to be debated. *Clin Gastroenterol Hepatol* **7**, 603-604, doi:S1542-3565(08)01248-2 [pii] 10.1016/j.cgh.2008.12.021 (2009).

67 Motilva, V., Garcia-Maurino, S., Talero, E. & Illanes, M. New paradigms in chronic intestinal inflammation and colon cancer: role of melatonin. *Journal of pineal research* **51**, 44-60, doi:10.1111/j.1600-079X.2011.00915.x (2011).

68 Klampfer, L. Cytokines, inflammation and colon cancer. *Current cancer drug targets* **11**, 451-464 (2011).

69 Terzic, J., Grivennikov, S., Karin, E. & Karin, M. Inflammation and colon cancer. *Gastroenterology* **138**, 2101-2114 e2105, doi:10.1053/j.gastro.2010.01.058 (2010).

70 Erdman, S. E. & Poutahidis, T. Roles for inflammation and regulatory T cells in colon cancer. *Toxicologic pathology* **38**, 76-87, doi:10.1177/0192623309354110 (2010).

71 Yang, L. & Pei, Z. Bacteria, inflammation, and colon cancer. *World journal of gastroenterology : WJG* **12**, 6741-6746 (2006).

72 Danese, S. & Mantovani, A. Inflammatory bowel disease and intestinal cancer: a paradigm of the Yin-Yang interplay between inflammation and cancer. *Oncogene* **29**, 3313-3323, doi:10.1038/onc.2010.109 (2010).

73 Kraus, S. & Arber, N. Inflammation and colorectal cancer. *Current opinion in pharmacology* **9**, 405-410, doi:10.1016/j.coph.2009.06.006 (2009).

74 Greten, F. R. *et al.* IKKbeta links inflammation and tumorigenesis in a mouse model of colitis-associated cancer. *Cell* **118**, 285-296, doi:10.1016/j.cell.2004.07.013 (2004).

75 Onizawa, M. *et al.* Signaling pathway via TNF-alpha/NF-kappaB in intestinal epithelial cells may be directly involved in colitis-associated carcinogenesis. *American journal of physiology. Gastrointestinal and liver physiology* **296**, G850-859, doi:10.1152/ajpgi.00071.2008 (2009).

76 Ullman, T. A. & Itzkowitz, S. H. Intestinal inflammation and cancer. *Gastroenterology* **140**, 1807-1816, doi:10.1053/j.gastro.2011.01.057 (2011).

77 Triantafillidis, J. K., Nasioulas, G. & Kosmidis, P. A. Colorectal cancer and inflammatory bowel disease: epidemiology, risk factors, mechanisms of carcinogenesis and prevention strategies. *Anticancer research* **29**, 2727-2737 (2009).

78 Bansal, P. & Sonnenberg, A. Risk factors of colorectal cancer in inflammatory bowel disease. *The American journal of gastroenterology* **91**, 44-48 (1996).

79 Srivastava, R. K., Sasaki, C. Y., Hardwick, J. M. & Longo, D. L. Bcl-2-mediated drug resistance: inhibition of apoptosis by blocking nuclear factor of activated T lymphocytes (NFAT)-induced Fas ligand transcription. *The Journal of experimental medicine* **190**, 253-265 (1999).

80 Nakanishi, C. & Toi, M. Nuclear factor-kappaB inhibitors as sensitizers to anticancer drugs. *Nature reviews. Cancer* **5**, 297-309, doi:10.1038/nrc1588 (2005).

81 Sakamoto, K. & Maeda, S. Targeting NF-kappaB for colorectal cancer. *Expert opinion on therapeutic targets* **14**, 593-601, doi:10.1517/14728221003769903 (2010).

82 Bentires-Alj, M. *et al.* NF-kappaB transcription factor induces drug resistance through MDR1 expression in cancer cells. *Oncogene* **22**, 90-97, doi:10.1038/sj.onc.1206056 (2003).

83 Chen, W., Li, Z., Bai, L. & Lin, Y. NF-kappaB in lung cancer, a carcinogenesis mediator and a prevention and therapy target. *Frontiers in bioscience : a journal and virtual library* **16**, 1172-1185 (2011).

84 Wang, S., Liu, Z., Wang, L. & Zhang, X. NF-kappaB signaling pathway, inflammation and colorectal cancer. *Cellular & molecular immunology* **6**, 327-334, doi:10.1038/cmi.2009.43 (2009).

85 Innocenti, F. & Ratain, M. J. Pharmacogenetics of irinotecan: clinical perspectives on the utility of genotyping. *Pharmacogenomics* **7**, 1211-1221, doi:10.2217/14622416.7.8.1211 (2006).

86 Fujita, K. & Sparreboom, A. Pharmacogenetics of irinotecan disposition and toxicity: a review. *Current clinical pharmacology* **5**, 209-217 (2010).

87 Fujiwara, Y. & Minami, H. An overview of the recent progress in irinotecan pharmacogenetics. *Pharmacogenomics* **11**, 391-406, doi:10.2217/pgs.10.19 (2010).

88 Hoskins, J. M. *et al.* Irinotecan pharmacogenetics: influence of pharmacodynamic genes. *Clinical cancer research : an official journal of the American Association for Cancer Research* **14**, 1788-1796, doi:10.1158/1078-0432.CCR-07-1472 (2008).

89 Gallo, R. C., Whang-Peng, J. & Adamson, R. H. Studies on the antitumor activity, mechanism of action, and cell cycle effects of camptothecin. *Journal of the National Cancer Institute* **46**, 789-795 (1971).

90 Liu, L. F. *et al.* Mechanism of action of camptothecin. *Annals of the New York Academy of Sciences* **922**, 1-10 (2000).

91 Yang, X. X. *et al.* Pharmacokinetic mechanisms for reduced toxicity of irinotecan by coadministered thalidomide. *Current drug metabolism* **7**, 431-455 (2006).

92 Nemunaitis, J., Cox, J., Meyer, W., Courtney, A. & Mues, G. Irinotecan hydrochloride (CPT-11) resistance identified by K-ras mutation in patients with progressive colon cancer after treatment with 5-fluorouracil (5-FU). *American journal of clinical oncology* **20**, 527-529 (1997).

93 Russo, S. M. *et al.* Enhancement of radiosensitivity by proteasome inhibition: implications for a role of NF-kappaB. *International journal of radiation oncology, biology, physics* **50**, 183-193 (2001).

94 Wang, C. Y., Cusack, J. C., Jr., Liu, R. & Baldwin, A. S., Jr. Control of inducible chemoresistance: enhanced anti-tumor therapy through increased apoptosis by inhibition of NF-kappaB. *Nature medicine* **5**, 412-417, doi:10.1038/7410 (1999).

95 Borner, M. M. *et al.* A randomized phase II trial of capecitabine and two different schedules of irinotecan in first-line treatment of metastatic colorectal cancer: efficacy, quality-of-life and toxicity. *Annals of oncology : official journal of the European Society for Medical Oncology / ESMO* **16**, 282-288, doi:10.1093/annonc/mdi047 (2005).

96 Kacar, S. *et al.* The toxicity rates of two different regimens of irinotecan. *Hepato-gastroenterology* **50 Suppl 2**, ccxxii-ccxxiv (2003).

97 Ratain, M. J. Irinotecan dosing: does the CPT in CPT-11 stand for "Can't Predict Toxicity"? *Journal of clinical oncology : official journal of the American Society of Clinical Oncology* **20**, 7-8 (2002).

98 Ong, S. Y., Clarke, S. J., Bishop, J., Dodds, H. M. & Rivory, L. P. Toxicity of irinotecan (CPT-11) and hepato-renal dysfunction. *Anti-cancer drugs* **12**, 619-625 (2001).

99 Sevilla Garcia, I., Rueda, A. & Alba, E. Irinotecan-induced central nervous system toxicity: a case report. *Journal of the National Cancer Institute* **91**, 647 (1999).

100 Rothenberg, M. L. Efficacy and toxicity of irinotecan in patients with colorectal cancer. *Seminars in oncology* **25**, 39-46 (1998).

101 Hecht, J. R. Gastrointestinal toxicity or irinotecan. *Oncology (Williston Park)* **12**, 72-78 (1998).

102 Callemien, D. & Collin, S. Involvement of flavanoids in beer color instability during storage. *Journal of agricultural and food chemistry* **55**, 9066-9073, doi:10.1021/jf0716230 (2007).

103 Natarajan, K., Singh, S., Burke, T. R., Jr., Grunberger, D. & Aggarwal, B. B. Caffeic acid phenethyl ester is a potent and specific inhibitor of activation of

nuclear transcription factor NF-kappa B. *Proceedings of the National Academy of Sciences of the United States of America* **93**, 9090-9095 (1996).

104 Caffeic Acid inhibits colitis in a mouse model--is a drug-metabolizing gene crucial? *Exp Biol Med (Maywood)* **234**, vi (2009).

105 Ye, Z. *et al.* Increased CYP4B1 mRNA is associated with the inhibition of dextran sulfate sodium-induced colitis by caffeic acid in mice. *Exp Biol Med (Maywood)* **234**, 605-616, doi:10.3181/0901-RM-1 (2009).

106 Ek, R. O. *et al.* The effects of caffeic acid phenethyl ester (CAPE) on TNBS-induced colitis in ovariectomized rats. *Digestive diseases and sciences* **53**, 1609-1617, doi:10.1007/s10620-007-0056-2 (2008).

107 Fitzpatrick, L. R., Wang, J. & Le, T. Caffeic acid phenethyl ester, an inhibitor of nuclear factor-kappaB, attenuates bacterial peptidoglycan polysaccharide-induced colitis in rats. *The Journal of pharmacology and experimental therapeutics* **299**, 915-920 (2001).

108 Shi, Y. *et al.* Protective effects of caffeic acid phenethyl ester on retinal ischemia/reperfusion injury in rats. *Current eye research* **35**, 930-937, doi:10.3109/02713683.2010.494820 (2010).

109 Kart, A., Cigremis, Y., Ozen, H. & Dogan, O. Caffeic acid phenethyl ester prevents ovary ischemia/reperfusion injury in rabbits. *Food and chemical toxicology : an international journal published for the British Industrial Biological Research Association* **47**, 1980-1984, doi:10.1016/j.fct.2009.05.012 (2009).

110 Namazi, H. Decreasing the expression of LFA-1 and ICAM-1 as the major mechanism for the protective effect of caffeic acid phenethyl ester on ischemia-reperfusion injury. *Journal of plastic, reconstructive & aesthetic surgery : JPRAS* **62**, 550, doi:10.1016/j.bjps.2008.01.029 (2009).

111 Yildiz, Y. *et al.* Protective effects of caffeic acid phenethyl ester on intestinal ischemia-reperfusion injury. *Digestive diseases and sciences* **54**, 738-744, doi:10.1007/s10620-008-0405-9 (2009).

112 Altug, M. E. *et al.* Caffeic acid phenethyl ester protects rabbit brains against permanent focal ischemia by antioxidant action: a biochemical and planimetric study. *Brain research* **1201**, 135-142, doi:10.1016/j.brainres.2008.01.053 (2008).

113 Ozyurt, H., Ozyurt, B., Koca, K. & Ozgocmen, S. Caffeic acid phenethyl ester (CAPE) protects rat skeletal muscle against ischemia-reperfusion-induced oxidative stress. *Vascular pharmacology* **47**, 108-112, doi:10.1016/j.vph.2007.04.008 (2007).

114 Khan, M., Elango, C., Ansari, M. A., Singh, I. & Singh, A. K. Caffeic acid phenethyl ester reduces neurovascular inflammation and protects rat brain following transient focal cerebral ischemia. *Journal of neurochemistry* **102**, 365-377, doi:10.1111/j.1471-4159.2007.04526.x (2007).

115 Cengiz, N. *et al.* Effects of caffeic acid phenethyl ester on cerebral cortex: structural changes resulting from middle cerebral artery ischemia reperfusion. *Clinical neuropathology* **26**, 80-84 (2007).

116 Zhou, Y. *et al.* Caffeic acid ameliorates early and delayed brain injuries after focal cerebral ischemia in rats. *Acta pharmacologica Sinica* **27**, 1103-1110, doi:10.1111/j.1745-7254.2006.00406.x (2006).

117 Atik, E., Gorur, S. & Kiper, A. N. The effect of caffeic acid phenethyl ester (CAPE) on histopathological changes in testicular ischemia-reperfusion injury. *Pharmacological research : the official journal of the Italian Pharmacological Society* **54**, 293-297, doi:10.1016/j.phrs.2006.06.005 (2006).

118 Ozyurt, B., Iraz, M., Koca, K., Ozyurt, H. & Sahin, S. Protective effects of caffeic acid phenethyl ester on skeletal muscle ischemia-reperfusion injury in rats. *Molecular and cellular biochemistry* **292**, 197-203, doi:10.1007/s11010-006-9232-5 (2006).

119 Ince, H., Kandemir, E., Bagci, C., Gulec, M. & Akyol, O. The effect of caffeic acid phenethyl ester on short-term acute myocardial ischemia. *Medical science monitor : international medical journal of experimental and clinical research* **12**, BR187-193 (2006).

120 Tsai, S. K. *et al.* Caffeic acid phenethyl ester ameliorates cerebral infarction in rats subjected to focal cerebral ischemia. *Life sciences* **78**, 2758-2762, doi:10.1016/j.lfs.2005.10.017 (2006).

121 Cagli, K. *et al.* In vivo effects of caffeic acid phenethyl ester on myocardial ischemia-reperfusion injury and apoptotic changes in rats. *Annals of clinical and laboratory science* **35**, 440-448 (2005).

122 Tan, J. *et al.* Caffeic acid phenethyl ester possesses potent cardioprotective effects in a rabbit model of acute myocardial ischemia-reperfusion injury.

*American journal of physiology. Heart and circulatory physiology* **289**, H2265-2271, doi:10.1152/ajpheart.01106.2004 (2005).

123 Huang, S. S. *et al.* Antiarrhythmic effect of caffeic acid phenethyl ester (CAPE) on myocardial ischemia/reperfusion injury in rats. *Clinical biochemistry* **38**, 943-947, doi:10.1016/j.clinbiochem.2005.07.003 (2005).

124 Ozer, M. K. *et al.* Ischemia-reperfusion leads to depletion of glutathione content and augmentation of malondialdehyde production in the rat heart from overproduction of oxidants: can caffeic acid phenethyl ester (CAPE) protect the heart? *Molecular and cellular biochemistry* **273**, 169-175 (2005).

125 Ozer, M. K. *et al.* Myocardial ischemia/reperfusion-induced oxidative renal damage in rats: protection by caffeic acid phenethyl ester (CAPE). *Shock* **24**, 97-100 (2005).

126 Esrefoglu, M., Gul, M., Parlakpinar, H. & Acet, A. Effects of melatonin and caffeic acid phenethyl ester on testicular injury induced by myocardial ischemia/reperfusion in rats. *Fundamental & clinical pharmacology* **19**, 365-372, doi:10.1111/j.1472-8206.2005.00331.x (2005).

127 Ozeren, M. *et al.* Caffeic acid phenethyl ester (CAPE) supplemented St. Thomas' hospital cardioplegic solution improves the antioxidant defense system of rat myocardium during ischemia-reperfusion injury. *Pharmacological research : the official journal of the Italian Pharmacological Society* **52**, 258-263, doi:10.1016/j.phrs.2005.04.002 (2005).

128 Parlakpinar, H., Sahna, E., Acet, A., Mizrak, B. & Polat, A. Protective effect of caffeic acid phenethyl ester (CAPE) on myocardial ischemia-reperfusion-induced apoptotic cell death. *Toxicology* **209**, 1-14, doi:10.1016/j.tox.2004.10.017 (2005).

129 Celik, O. *et al.* The protective effect of caffeic acid phenethyl ester on ischemia-reperfusion injury in rat ovary. *European journal of obstetrics, gynecology, and reproductive biology* **117**, 183-188, doi:10.1016/j.ejogrb.2004.05.007 (2004).

130 Calikoglu, M. *et al.* [The nitrosative effect of peripheral ischemia-reperfusion on lung and preventive of caffeic acid phenethyl ester]. *Tuberkuloz ve toraks* **52**, 218-223 (2004).

131 Ozer, M. K., Parlakpinar, H. & Acet, A. Reduction of ischemia--reperfusion induced myocardial infarct size in rats by caffeic acid phenethyl ester (CAPE). *Clinical biochemistry* **37**, 702-705, doi:10.1016/j.clinbiochem.2004.01.012 (2004).

132 Gurel, A. *et al.* Protective role of alpha-tocopherol and caffeic acid phenethyl ester on ischemia-reperfusion injury via nitric oxide and myeloperoxidase in rat kidneys. *Clinica chimica acta; international journal of clinical chemistry* **339**, 33-41 (2004).

133 Calikoglu, M. *et al.* The effects of caffeic acid phenethyl ester on tissue damage in lung after hindlimb ischemia-reperfusion. *Pharmacological research : the official journal of the Italian Pharmacological Society* **48**, 397-403 (2003).

134 Irmak, M. K. *et al.* The effect of caffeic acid phenethyl ester on ischemia-reperfusion injury in comparison with alpha-tocopherol in rat kidneys. *Urological research* **29**, 190-193 (2001).

135 Ilhan, A. *et al.* The effects of caffeic acid phenethyl ester (CAPE) on spinal cord ischemia/reperfusion injury in rabbits. *European journal of cardio-thoracic surgery : official journal of the European Association for Cardio-thoracic Surgery* **16**, 458-463 (1999).

136 Ozyurt, H. *et al.* Inhibitory effect of caffeic acid phenethyl ester on bleomycine-induced lung fibrosis in rats. *Clinica chimica acta; international journal of clinical chemistry* **339**, 65-75 (2004).

137 Liao, H. F. *et al.* Inhibitory effect of caffeic acid phenethyl ester on angiogenesis, tumor invasion, and metastasis. *Journal of agricultural and food chemistry* **51**, 7907-7912, doi:10.1021/jf034729d (2003).

138 Watabe, M., Hishikawa, K., Takayanagi, A., Shimizu, N. & Nakaki, T. Caffeic acid phenethyl ester induces apoptosis by inhibition of NFkappaB and activation of Fas in human breast cancer MCF-7 cells. *The Journal of biological chemistry* **279**, 6017-6026, doi:10.1074/jbc.M306040200 (2004).

139 Dong, A. *et al.* Caffeic acid 3,4-dihydroxy-phenethyl ester (CADPE) induces cancer cell senescence by suppressing Twist expression. *The Journal of pharmacology and experimental therapeutics*, doi:10.1124/jpet.111.181081 (2011).

140 Wu, J. *et al.* Caffeic acid phenethyl ester (CAPE), derived from a honeybee product propolis, exhibits a diversity of anti-tumor effects in pre-clinical models of human breast cancer. *Cancer letters* **308**, 43-53, doi:10.1016/j.canlet.2011.04.012 (2011).

141 Omene, C. O., Wu, J. & Frenkel, K. Caffeic Acid Phenethyl Ester (CAPE) derived from propolis, a honeybee product, inhibits growth of breast cancer stem cells. *Investigational new drugs*, doi:10.1007/s10637-011-9667-8 (2011).

142 Serafim, T. L. *et al.* Lipophilic caffeic and ferulic acid derivatives presenting cytotoxicity against human breast cancer cells. *Chemical research in toxicology* **24**, 763-774, doi:10.1021/tx200126r (2011).

143 Chang, W. C. *et al.* Caffeic acid induces apoptosis in human cervical cancer cells through the mitochondrial pathway. *Taiwanese journal of obstetrics & gynecology* **49**, 419-424, doi:10.1016/S1028-4559(10)60092-7 (2010).

144 Rajendra Prasad, N., Karthikeyan, A., Karthikeyan, S. & Reddy, B. V. Inhibitory effect of caffeic acid on cancer cell proliferation by oxidative mechanism in human HT-1080 fibrosarcoma cell line. *Molecular and cellular biochemistry* **349**, 11-19, doi:10.1007/s11010-010-0655-7 (2011).

145 Ye, J. C. *et al.* Analysis of caffeic acid extraction from Ocimum gratissimum Linn. by high performance liquid chromatography and its effects on a cervical cancer cell line. *Taiwanese journal of obstetrics & gynecology* **49**, 266-271, doi:10.1016/S1028-4559(10)60059-9 (2010).

146 Chen, M. J. *et al.* Caffeic acid phenethyl ester induces apoptosis of human pancreatic cancer cells involving caspase and mitochondrial dysfunction. *Pancreatology* **8**, 566-576, doi:10.1159/000159843 (2008).

147 Wu, C. S., Chen, M. F., Lee, I. L. & Tung, S. Y. Predictive role of nuclear factor-kappaB activity in gastric cancer: a promising adjuvant approach with caffeic acid phenethyl ester. *Journal of clinical gastroenterology* **41**, 894-900, doi:10.1097/MCG.0b013e31804c707c (2007).

148 Ribeiro, U., Jr. & Safatle-Ribeiro, A. V. Caffeic acid phenethyl ester (CAPE) may be a promising adjuvant treatment in gastric cancer. *Journal of clinical gastroenterology* **41**, 871-873, doi:10.1097/MCG.0b013e31806b5938 (2007).

149 Xiang, D. *et al.* Caffeic acid phenethyl ester induces growth arrest and apoptosis of colon cancer cells via the beta-catenin/T-cell factor signaling. *Anti-cancer drugs* **17**, 753-762, doi:10.1097/01.cad.0000224441.01082.bb (2006).

150 Hwang, H. J. *et al.* Inhibitory effects of caffeic acid phenethyl ester on cancer cell metastasis mediated by the down-regulation of matrix metalloproteinase expression in human HT1080 fibrosarcoma cells. *The Journal of nutritional biochemistry* **17**, 356-362, doi:10.1016/j.jnutbio.2005.08.009 (2006).

151 Wang, D. *et al.* Effect of caffeic acid phenethyl ester on proliferation and apoptosis of colorectal cancer cells in vitro. *World journal of gastroenterology : WJG* **11**, 4008-4012 (2005).

152 Chen, M. F., Wu, C. T., Chen, Y. J., Keng, P. C. & Chen, W. C. Cell killing and radiosensitization by caffeic acid phenethyl ester (CAPE) in lung cancer cells. *Journal of radiation research* **45**, 253-260 (2004).

153 Hung, M. W., Shiao, M. S., Tsai, L. C., Chang, G. G. & Chang, T. C. Apoptotic effect of caffeic acid phenethyl ester and its ester and amide analogues in human cervical cancer ME180 cells. *Anticancer research* **23**, 4773-4780 (2003).

154 Lee, Y. J., Liao, P. H., Chen, W. K. & Yang, C. Y. Preferential cytotoxicity of caffeic acid phenethyl ester analogues on oral cancer cells. *Cancer letters* **153**, 51-56 (2000).

155 Choi, D. *et al.* Caffeic acid phenethyl ester is a potent inhibitor of HIF prolyl hydroxylase: structural analysis and pharmacological implication. *The Journal of nutritional biochemistry* **21**, 809-817, doi:10.1016/j.jnutbio.2009.06.002 (2010).

156 McEleny, K., Coffey, R., Morrissey, C., Fitzpatrick, J. M. & Watson, R. W. Caffeic acid phenethyl ester-induced PC-3 cell apoptosis is caspase-dependent and mediated through the loss of inhibitors of apoptosis proteins. *BJU international* **94**, 402-406, doi:10.1111/j.1464-410X.2004.04936.x (2004).

157 Choi, K., Han, Y. H. & Choi, C. N-acetyl cysteine and caffeic acid phenethyl ester sensitize astrocytoma cells to Fas-mediated cell death in a redox-dependent manner. *Cancer letters* **257**, 79-86, doi:10.1016/j.canlet.2007.07.006 (2007).

158 Jin, U. H. *et al.* Caffeic acid phenethyl ester induces mitochondria-mediated apoptosis in human myeloid leukemia U937 cells. *Molecular and cellular biochemistry* **310**, 43-48, doi:10.1007/s11010-007-9663-7 (2008).

159 Berger, N., Ben Bassat, H., Klein, B. Y. & Laskov, R. Cytotoxicity of NF-kappaB inhibitors Bay 11-7085 and caffeic acid phenethyl ester to Ramos and other human B-lymphoma cell lines. *Experimental hematology* **35**, 1495-1509, doi:10.1016/j.exphem.2007.07.006 (2007).

160 Nagaoka, T. *et al.* Inhibitory effects of caffeic acid phenethyl ester analogues on experimental lung metastasis of murine colon 26-L5 carcinoma cells. *Biological & pharmaceutical bulletin* **26**, 638-641 (2003).

161 Nagaoka, T., Banskota, A. H., Tezuka, Y., Saiki, I. & Kadota, S. Selective antiproliferative activity of caffeic acid phenethyl ester analogues on highly liver-metastatic murine colon 26-L5 carcinoma cell line. *Bioorganic & medicinal chemistry* **10**, 3351-3359 (2002).

162 Kuo, H. C. *et al.* Inhibitory effect of caffeic acid phenethyl ester on the growth of C6 glioma cells in vitro and in vivo. *Cancer letters* **234**, 199-208, doi:10.1016/j.canlet.2005.03.046 (2006).

163 Onori, P. *et al.* Caffeic acid phenethyl ester decreases cholangiocarcinoma growth by inhibition of NF-kappaB and induction of apoptosis. *International journal of cancer. Journal international du cancer* **125**, 565-576, doi:10.1002/ijc.24271 (2009).

164 Dandekar, S. Pathogenesis of HIV in the gastrointestinal tract. *Curr HIV/AIDS Rep* **4**, 10-15 (2007).

165 Fantini, M. C. & Pallone, F. Cytokines: from gut inflammation to colorectal cancer. *Current drug targets* **9**, 375-380 (2008).

166 Abraham, C. & Cho, J. H. Inflammatory bowel disease. *N Engl J Med* **361**, 2066-2078, doi:361/21/2066 [pii]
10.1056/NEJMra0804647 (2009).

167 Peer, D., Park, E. J., Morishita, Y., Carman, C. V. & Shimaoka, M. Systemic leukocyte-directed siRNA delivery revealing cyclin D1 as an anti-inflammatory target. *Science* **319**, 627-630, doi:319/5863/627 [pii]
10.1126/science.1149859 (2008).

168 Wolfe, F., Michaud, K., Anderson, J. & Urbansky, K. Tuberculosis infection in patients with rheumatoid arthritis and the effect of infliximab therapy. *Arthritis Rheum* **50**, 372-379, doi:10.1002/art.20009 (2004).

169 Reddy, J. G. & Loftus, E. V., Jr. Safety of infliximab and other biologic agents in the inflammatory bowel diseases. *Gastroenterol Clin North Am* **35**, 837-855, doi:S0889-8553(06)00084-7 [pii]
10.1016/j.gtc.2006.09.008 (2006).

170 Heraganahally, S. S. *et al.* Pulmonary toxicity associated with infliximab therapy for ulcerative colitis. *Intern Med J* **39**, 629-630, doi:IMJ1999 [pii]
10.1111/j.1445-5994.2009.001999.x (2009).

171 Aouadi, M. *et al.* Orally delivered siRNA targeting macrophage Map4k4 suppresses systemic inflammation. *Nature* **458**, 1180-1184, doi:nature07774 [pii] 10.1038/nature07774 (2009).

172 Pertuit, D. *et al.* 5-amino salicylic acid bound nanoparticles for the therapy of inflammatory bowel disease. *J Control Release* **123**, 211-218, doi:S0168-3659(07)00418-X [pii] 10.1016/j.jconrel.2007.08.008 (2007).

173 Yamanaka, Y. J. & Leong, K. W. Engineering strategies to enhance nanoparticle-mediated oral delivery. *J Biomater Sci Polym Ed* **19**, 1549-1570, doi:10.1163/156856208786440479 (2008).

174 Sedghi, S. *et al.* Increased production of luminol enhanced chemiluminescence by the inflamed colonic mucosa in patients with ulcerative colitis. *Gut* **34**, 1191-1197 (1993).

175 Peng, Y. C. *et al.* Chemiluminescence assay of mucosal reactive oxygen species in gastric cancer, ulcer and antral mucosa. *Hepatogastroenterology* **55**, 770-773 (2008).

176 Shukla, A. K., Verma, M. & Singh, K. N. Superoxide induced deprotection of 1,3-dithiolanes: A convenient method of dedithioacetalization. *Indian J Chem B* **43**, 1748-1752 (2004).

177 Colonna, S., Gaggero, N., Carrea, G. & Pasta, P. Enantio and diastereoselectivity of cyclohexanone monooxygenase catalyzed oxidation of 1,3-dithioacetals. *Tetrahedron-Asymmetr* **7**, 565-570 (1996).

178 Mahida, Y. R., Wu, K. C. & Jewell, D. P. Respiratory Burst Activity of Intestinal Macrophages in Normal and Inflammatory Bowel-Disease. *Gut* **30**, 1362-1370 (1989).

179 Wirtz, S., Neufert, C., Weigmann, B. & Neurath, M. F. Chemically induced mouse models of intestinal inflammation. *Nat Protoc* **2**, 541-546, doi:nprot.2007.41 [pii] 10.1038/nprot.2007.41 (2007).

180 Kontoyiannis, D., Pasparakis, M., Pizarro, T. T., Cominelli, F. & Kollias, G. Impaired on/off regulation of TNF biosynthesis in mice lacking TNF AU-rich elements: implications for joint and gut-associated immunopathologies. *Immunity* **10**, 387-398, doi:S1074-7613(00)80038-2 [pii] (1999).

181 Sorensen, D. R., Leirdal, M. & Sioud, M. Gene silencing by systemic delivery of synthetic siRNAs in adult mice. *J Mol Biol* **327**, 761-766, doi:S0022283603001815 [pii] (2003).

182 Lamprecht, A. IBD: selective nanoparticle adhesion can enhance colitis therapy. *Nature reviews. Gastroenterology & hepatology* **7**, 311-312, doi:10.1038/nrgastro.2010.66 (2010).

183 Knight, P. T., Kirk, J. T., Anderson, J. M. & Mather, P. T. In vivo kinetic degradation analysis and biocompatibility of aliphatic polyester polyurethanes. *Journal of biomedical materials research. Part A* **94**, 333-343 (2010).

184 Marois, Y. *et al.* In vivo biocompatibility and degradation studies of polyhydroxyoctanoate in the rat: a new sealant for the polyester arterial prosthesis. *Tissue engineering* **5**, 369-386 (1999).

185 Ben Slimane, S. *et al.* Polyester arterial grafts impregnated with cross-linked albumin: the rate of degradation of the coating in vivo. *European surgical research. Europaische chirurgische Forschung. Recherches chirurgicales europeennes* **20**, 12-17 (1988).

186 Segui, J. *et al.* Superoxide dismutase ameliorates TNBS-induced colitis by reducing oxidative stress, adhesion molecule expression, and leukocyte recruitment into the inflamed intestine. *Journal of leukocyte biology* **76**, 537-544, doi:10.1189/jlb.0304196 (2004).

187 Leirdal, M. & Sioud, M. Gene silencing in mammalian cells by preformed small RNA duplexes. *Biochem Biophys Res Commun* **295**, 744-748, doi:S0006-291X(02)00736-2 [pii] (2002).

188 Murata, N., Takashima, Y., Toyoshima, K., Yamamoto, M. & Okada, H. Anti-tumor effects of anti-VEGF siRNA encapsulated with PLGA microspheres in mice. *J Control Release* **126**, 246-254, doi:S0168-3659(07)00651-7 [pii] 10.1016/j.jconrel.2007.11.017 (2008).

189 Palliser, D. *et al.* An siRNA-based microbicide protects mice from lethal herpes simplex virus 2 infection. *Nature* **439**, 89-94, doi:nature04263 [pii] 10.1038/nature04263 (2006).

190 Akhtar, S. & Benter, I. F. Nonviral delivery of synthetic siRNAs in vivo. *J Clin Invest* **117**, 3623-3632, doi:10.1172/JCI33494 (2007).

191 Zhang, S., Zhao, B., Jiang, H., Wang, B. & Ma, B. Cationic lipids and polymers mediated vectors for delivery of siRNA. *J Control Release* **123**, 1-10, doi:S0168-3659(07)00391-4 [pii]
10.1016/j.jconrel.2007.07.016 (2007).

192 Behrens, I., Pena, A. I., Alonso, M. J. & Kissel, T. Comparative uptake studies of bioadhesive and non-bioadhesive nanoparticles in human intestinal cell lines and rats: the effect of mucus on particle adsorption and transport. *Pharmaceutical research* **19**, 1185-1193 (2002).

193 Desai, M. P., Labhasetwar, V., Amidon, G. L. & Levy, R. J. Gastrointestinal uptake of biodegradable microparticles: effect of particle size. *Pharm Res* **13**, 1838-1845 (1996).

194 Lamprecht, A., Schafer, U. & Lehr, C. M. Size-dependent bioadhesion of micro- and nanoparticulate carriers to the inflamed colonic mucosa. *Pharm Res* **18**, 788-793 (2001).

195 Thiele, L. *et al.* Evaluation of particle uptake in human blood monocyte-derived cells in vitro. Does phagocytosis activity of dendritic cells measure up with macrophages? *J Control Release* **76**, 59-71, doi:S0168365901004126 [pii] (2001).

196 Yan, Y. *et al.* Temporal and spatial analysis of clinical and molecular parameters in dextran sodium sulfate induced colitis. *PloS one* **4**, e6073, doi:10.1371/journal.pone.0006073 (2009).

197 Hariharan, S. *et al.* Design of estradiol loaded PLGA nanoparticulate formulations: a potential oral delivery system for hormone therapy. *Pharm Res* **23**, 184-195, doi:10.1007/s11095-005-8418-y (2006).

198 Barnhart, R. L., Busch, S. J. & Jackson, R. L. Concentration-dependent antioxidant activity of probucol in low density lipoproteins in vitro: probucol degradation precedes lipoprotein oxidation. *Journal of lipid research* **30**, 1703-1710 (1989).

199 Akhtar, S. Oral delivery of siRNA and antisense oligonucleotides. *Journal of drug targeting* **17**, 491-495, doi:10.1080/10611860903057674 (2009).

200 Nguyen, H., Dalmasso, G., Merlin, D. & Sitaraman, S. V. You see UC: an animal model of ulcerative colitis. *Gastroenterology* **135**, 2149-2150, doi:10.1053/j.gastro.2008.10.062 (2008).

201 Saigi, E. *et al.* Phase II study of irinotecan (CPT-11) administered every 2 weeks as treatment for patients with colorectal cancer resistant to previous treatment with 5-fluorouracil-based therapies: comparison of two different dose schedules (250 and 200 mg/m2) according to toxicity prognostic factors. *Anti-cancer drugs* **15**, 835-841 (2004).

202 Ando, Y. & Hasegawa, Y. Clinical pharmacogenetics of irinotecan (CPT-11). *Drug metabolism reviews* **37**, 565-574, doi:10.1080/03602530500316254 (2005).

203 Suzuki, K. *et al.* Experimental study on the protective effects of edaravone against ischemic spinal cord injury. *The Journal of thoracic and cardiovascular surgery* **130**, 1586-1592, doi:10.1016/j.jtcvs.2005.08.049 (2005).

204 Ghobrial, I. M. *et al.* Phase II trial of weekly bortezomib in combination with rituximab in relapsed or relapsed and refractory Waldenstrom macroglobulinemia. *Journal of clinical oncology : official journal of the American Society of Clinical Oncology* **28**, 1422-1428, doi:10.1200/JCO.2009.25.3237 (2010).

205 Uz, E. *et al.* The protective role of caffeic acid phenethyl ester (CAPE) on testicular tissue after testicular torsion and detorsion. *World journal of urology* **20**, 264-270, doi:10.1007/s00345-002-0259-2 (2002).

206 Guney, M., Oral, B., Karahan, N. & Mungan, T. Protective effect of caffeic acid phenethyl ester (CAPE) on fluoride-induced oxidative stress and apoptosis in rat endometrium. *Environmental toxicology and pharmacology* **24**, 86-91, doi:10.1016/j.etap.2007.01.005 (2007).

207 Ozguner, F. *et al.* Comparative analysis of the protective effects of melatonin and caffeic acid phenethyl ester (CAPE) on mobile phone-induced renal impairment in rat. *Molecular and cellular biochemistry* **276**, 31-37, doi:10.1007/s11010-005-2734-8 (2005).

208 Acharya, S. & Sahoo, S. K. PLGA nanoparticles containing various anticancer agents and tumour delivery by EPR effect. *Advanced drug delivery reviews* **63**, 170-183, doi:10.1016/j.addr.2010.10.008 (2011).

209 Song, X. *et al.* Dual agents loaded PLGA nanoparticles: systematic study of particle size and drug entrapment efficiency. *European journal of pharmaceutics and biopharmaceutics : official journal of Arbeitsgemeinschaft fur Pharmazeutische Verfahrenstechnik e.V* **69**, 445-453, doi:10.1016/j.ejpb.2008.01.013 (2008).

210 Parajo, Y. *et al.* PLGA:poloxamer blend micro- and nanoparticles as controlled release systems for synthetic proangiogenic factors. *European journal of pharmaceutical sciences : official journal of the European Federation for Pharmaceutical Sciences* **41**, 644-649, doi:10.1016/j.ejps.2010.09.008 (2010).

211 Neufert, C., Becker, C. & Neurath, M. F. An inducible mouse model of colon carcinogenesis for the analysis of sporadic and inflammation-driven tumor progression. *Nature protocols* **2**, 1998-2004, doi:10.1038/nprot.2007.279 (2007).

212 Lin, J. J. *et al.* Folic acid-Pluronic F127 magnetic nanoparticle clusters for combined targeting, diagnosis, and therapy applications. *Biomaterials* **30**, 5114-5124, doi:10.1016/j.biomaterials.2009.06.004 (2009).

213 Mei, L. *et al.* A Novel Docetaxel-Loaded Poly (epsilon-Caprolactone)/Pluronic F68 Nanoparticle Overcoming Multidrug Resistance for Breast Cancer Treatment. *Nanoscale research letters* **4**, 1530-1539, doi:10.1007/s11671-009-9431-6 (2009).

214 Nguyen, H. T. *et al.* CD98 expression modulates intestinal homeostasis, inflammation, and colitis-associated cancer in mice. *The Journal of clinical investigation* **121**, 1733-1747, doi:10.1172/JCI44631 (2011).

215 Barkett, M. & Gilmore, T. D. Control of apoptosis by Rel/NF-kappaB transcription factors. *Oncogene* **18**, 6910-6924, doi:10.1038/sj.onc.1203238 (1999).

216 El-Refaei, M. F. & El-Naa, M. M. Inhibitory effect of caffeic acid phenethyl ester on mice bearing tumor involving angiostatic and apoptotic activities. *Chemico-biological interactions* **186**, 152-156, doi:10.1016/j.cbi.2010.04.019 (2010).

217 Kudugunti, S. K., Vad, N. M., Ekogbo, E. & Moridani, M. Y. Efficacy of caffeic acid phenethyl ester (CAPE) in skin B16-F0 melanoma tumor bearing C57BL/6 mice. *Investigational new drugs* **29**, 52-62, doi:10.1007/s10637-009-9334-5 (2011).

218 Demestre, M. *et al.* CAPE (caffeic acid phenethyl ester)-based propolis extract (Bio 30) suppresses the growth of human neurofibromatosis (NF) tumor xenografts in mice. *Phytotherapy research : PTR* **23**, 226-230, doi:10.1002/ptr.2594 (2009).

219 Jung, J. E. *et al.* Caffeic acid and its synthetic derivative CADPE suppress tumor angiogenesis by blocking STAT3-mediated VEGF expression in human renal carcinoma cells. *Carcinogenesis* **28**, 1780-1787, doi:10.1093/carcin/bgm130 (2007).

220 Lee, Y. J. *et al.* Involvement of tumor suppressor protein p53 and p38 MAPK in caffeic acid phenethyl ester-induced apoptosis of C6 glioma cells. *Biochemical pharmacology* **66**, 2281-2289 (2003).

221 Huang, M. T. *et al.* Inhibitory effects of caffeic acid phenethyl ester (CAPE) on 12-O-tetradecanoylphorbol-13-acetate-induced tumor promotion in mouse skin and the synthesis of DNA, RNA and protein in HeLa cells. *Carcinogenesis* **17**, 761-765 (1996).

222 Grunberger, D. *et al.* Preferential cytotoxicity on tumor cells by caffeic acid phenethyl ester isolated from propolis. *Experientia* **44**, 230-232 (1988).

223 Yagmurca, M. *et al.* Caffeic acid phenethyl ester as a protective agent against doxorubicin nephrotoxicity in rats. *Clinica chimica acta; international journal of clinical chemistry* **348**, 27-34, doi:10.1016/j.cccn.2004.03.035 (2004).

224 Rezzani, R., Giugno, L., Buffoli, B., Bonomini, F. & Bianchi, R. The protective effect of caffeic acid phenethyl ester against cyclosporine A-induced cardiotoxicity in rats. *Toxicology* **212**, 155-164, doi:10.1016/j.tox.2005.04.020 (2005).

225 Kus, I. *et al.* Protective effects of caffeic acid phenethyl ester (CAPE) on carbon tetrachloride-induced hepatotoxicity in rats. *Acta histochemica* **106**, 289-297, doi:10.1016/j.acthis.2004.05.002 (2004).

226 Janbaz, K. H., Saeed, S. A. & Gilani, A. H. Studies on the protective effects of caffeic acid and quercetin on chemical-induced hepatotoxicity in rodents. *Phytomedicine : international journal of phytotherapy and phytopharmacology* **11**, 424-430 (2004).

227 Fadillioglu, E. *et al.* Protective effects of caffeic acid phenethyl ester on doxorubicin-induced cardiotoxicity in rats. *Journal of applied toxicology : JAT* **24**, 47-52, doi:10.1002/jat.945 (2004).

228 Fu, J., Cheng, K., Zhang, Z. M., Fang, R. Q. & Zhu, H. L. Synthesis, structure and structure-activity relationship analysis of caffeic acid amides as potential antimicrobials. *European journal of medicinal chemistry* **45**, 2638-2643, doi:10.1016/j.ejmech.2010.01.066 (2010).

229 Zou, H. *et al.* Synthesis, biological evaluation, and structure-activity relationship study of novel cytotoxic aza-caffeic acid derivatives. *Bioorganic & medicinal chemistry* **18**, 6351-6359, doi:10.1016/j.bmc.2010.07.016 (2010).

230 Wang, X., Stavchansky, S., Kerwin, S. M. & Bowman, P. D. Structure-activity relationships in the cytoprotective effect of caffeic acid phenethyl ester (CAPE) and fluorinated derivatives: effects on heme oxygenase-1 induction and antioxidant activities. *European journal of pharmacology* **635**, 16-22, doi:10.1016/j.ejphar.2010.02.034 (2010).

231 Lin, M. W., Yang, S. R., Huang, M. H. & Wu, S. N. Stimulatory actions of caffeic acid phenethyl ester, a known inhibitor of NF-kappaB activation, on Ca2+-activated K+ current in pituitary GH3 cells. *The Journal of biological chemistry* **279**, 26885-26892, doi:10.1074/jbc.M400356200 (2004).

232 Chen, J. H., Shao, Y., Huang, M. T., Chin, C. K. & Ho, C. T. Inhibitory effect of caffeic acid phenethyl ester on human leukemia HL-60 cells. *Cancer letters* **108**, 211-214 (1996).

233 Lai, J. *et al.* Glyceryl monooleate/poloxamer 407 cubic nanoparticles as oral drug delivery systems: I. In vitro evaluation and enhanced oral bioavailability of the poorly water-soluble drug simvastatin. *AAPS PharmSciTech* **10**, 960-966, doi:10.1208/s12249-009-9292-4 (2009).

234 d'Angelo, I. *et al.* Improved delivery of angiogenesis inhibitors from PLGA:poloxamer blend micro- and nanoparticles. *Journal of microencapsulation* **27**, 57-66, doi:10.3109/02652040902954729 (2010).

235 Csaba, N., Caamano, P., Sanchez, A., Dominguez, F. & Alonso, M. J. PLGA:poloxamer and PLGA:poloxamine blend nanoparticles: new carriers for gene delivery. *Biomacromolecules* **6**, 271-278, doi:10.1021/bm049577p (2005).

236 Muller, R. H., Maassen, S., Weyhers, H. & Mehnert, W. Phagocytic uptake and cytotoxicity of solid lipid nanoparticles (SLN) sterically stabilized with poloxamine 908 and poloxamer 407. *Journal of drug targeting* **4**, 161-170, doi:10.3109/10611869609015973 (1996).

237 Yildiz, O. G., Soyuer, S., Saraymen, R. & Eroglu, C. Protective effects of caffeic acid phenethyl ester on radiation induced lung injury in rats. *Clinical and investigative medicine. Medecine clinique et experimentale* **31**, E242-247 (2008).

238 Lee, K. J., Choi, J. H., Hwang, Y. P., Chung, Y. C. & Jeong, H. G. Protective effect of caffeic acid phenethyl ester on tert-butyl hydroperoxide-induced oxidative hepatotoxicity and DNA damage. *Food and chemical toxicology : an international journal published for the British Industrial Biological Research Association* **46**, 2445-2450, doi:10.1016/j.fct.2008.03.032 (2008).

239 Gokcimen, A. *et al.* Protective effect of N-acetylcysteine, caffeic acid and vitamin E on doxorubicin hepatotoxicity. *Human & experimental toxicology* **26**, 519-525, doi:10.1177/0960327107076885 (2007).

240 Uz, E., Oktem, F., Yilmaz, H. R., Uzar, E. & Ozguner, F. The activities of purine-catabolizing enzymes and the level of nitric oxide in rat kidneys subjected to methotrexate: protective effect of caffeic acid phenethyl ester. *Molecular and cellular biochemistry* **277**, 165-170, doi:10.1007/s11010-005-5875-x (2005).

241 Zheng, C. *et al.* Toxicity and biodistribution of a first-generation recombinant adenoviral vector, encoding aquaporin-1, after retroductal delivery to a single rat submandibular gland. *Human gene therapy* **17**, 1122-1133, doi:10.1089/hum.2006.17.1122 (2006).

242 Rojas-Martinez, A. *et al.* Distribution, persistency, toxicity, and lack of replication of an E1A-deficient adenoviral vector after intracardiac delivery in the cotton rat. *Cancer gene therapy* **5**, 365-370 (1998).

243 Yasui, Y., Hosokawa, M., Mikami, N., Miyashita, K. & Tanaka, T. Dietary astaxanthin inhibits colitis and colitis-associated colon carcinogenesis in mice via modulation of the inflammatory cytokines. *Chemico-biological interactions* **193**, 79-87, doi:10.1016/j.cbi.2011.05.006 (2011).

244 De Robertis, M. *et al.* The AOM/DSS murine model for the study of colon carcinogenesis: From pathways to diagnosis and therapy studies. *Journal of carcinogenesis* **10**, 9, doi:10.4103/1477-3163.78279 (2011).